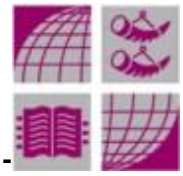

Short Distance Telemetry for Piston Monitoring

Design and Development of Short Distance Telemetry for Engine Condition Monitoring

A Lewalski, BSc (Hons), MPhil

Submitted for Degree of Doctor of Philosophy

School of Engineering, Design and Technology

University of Bradford

2011

ABSTRACT

Piston telemetry research involves monitoring the temperatures at specific internal location points within a combustion engine piston. The temperatures are detected with type K thermocouples as voltages and processed to convert them into temperatures using cold junction compensation methods.

The present system uses a specific sensor designed to operate in the high temperature environment within the piston, reading multiple thermocouples. Because of the reciprocating motion of the piston, power generation is intermittent and available only when the piston reaches near bottom dead centre, using inductive coupling to power the sensors and transmit data to an evaluation unit for data processing.

The planned system involves designing and building a prototype telemetry unit using 'off the shelf' components that integrate the reading of thermocouple outputs, signal processing and cold junction compensation. Wireless telemetry is adopted for data transmission with an integrated Bluetooth and microcontroller module. The data acquisition module can be adapted for other sensors by adapting the firmware uploaded to the microcontroller. The hardware electronics are envisaged to be encased in thermal insulation to enable operation in high temperature environments.

The considered system requires a power supply for the integrated components in the form of a power generator and that it should meet two criteria: to be located within confined spaces and to be permanently available, without having to dismantle systems to change batteries. The selected method is an induction generator constructed from a coil stator connected to the piston connection rod big end and a permanent magnet rotor connected to the crankshaft.

The suggested mechatronic system is validated against the present system by comparing both systems to determine whether wireless telemetry can perform within acceptable tolerances and limits for the specified task. Then, for acceptable performances, reduce costs and include flexibility to operate in multiple environments.

Bench testing shows that the power generator is capable of driving the sensors and the Bluetooth integrated DAQ system.

Keywords: **Telemetry, Bluetooth, Data Acquisition, Power Generator, Mechatronics, Short Distance Telemetry**

Acknowledgements

I would first and foremost wish to acknowledge Professor M.K. Ebrahimi for giving me the opportunity to study for this PhD, and together with Professor Alastair Wood for their invaluable guidance, supervision and support that led me through the research with confidence.

I would also wish to give my grateful acknowledgement to EPSRC and University of Bradford for the funding that enabled the research and to Ford U.K.

My heartfelt gratitude for not only academic support, but for their invaluable friendship during my studies. Prof. M.K. Ebrahimi, Dr. Alaa Abdul-Ameer, Dr. Hussni Al-Hajjar, Dr H. Amirian, Mr. Zahir Jamil.

I would also wish to thank the Hyper-C research group for their support, encouragement and friendship. Dr. Antonios Pezouvanis, Dr. Shalabi el-shalabi, Dr. Byron Mason, Mr. Martin Gargett, and also technicians and administration staff.

Contents

List of Figures

List of Tables

Glossary

3D	Three Dimensional
8DPSK	Differential Phase-Shift Keying
π/4 DQPSK	Differential Quadrature Phase-Shift Keying
AC	Alternating Current
ADC	Analogue to Digital Converter
ANSI	American National Standards Institute
API	Application Programming Interface
ASICs	Application Specific Integrated Circuits
AWG	American Wire Gauge
BDC	Bottom Dead Centre
CDMA	Code division multiple access
CFD	Computational fluid dynamics
CJC	Cold Junction Compensation
COTS	Commercial Off The Shelf
CS	Chip Select
CSV	Comma Separated values
DAC	Digital to Analogue Converter
DARC	Data Acquisition Remote Control
DAQ	Data Acquisition
DC	Direct Current
DIL	Dual In Line
DSC	Digital Signal Controller
DSSS	Direct Sequence Spread Spectrum
EDR	Enhanced Data Rate
EMF	Electro Motive Force

FEA	Finite Element Analysis
FHSS	Frequency Hopping Spread Spectrum
FM	Frequency Modulation
FSK	Frequency Shift Keying
GFSK	Gaussian Frequency Shift Keying
GHz	Giga Hertz
GOEP	Generic Object Exchange Profile
GPRS	General Packet Radio Service
GPS	Geostationary Positioning System
GSM	Global System for Mobile Communications
HCI	Host Controller Interface
HF	High Frequency
HTML	Hyper Text Markup Language
Hz	Frequency
IC	Internal Combustion
IC	Integrated Circuit
ID	Identification
IDE	Integrated Development Environment
IEEE	Institute of Electrical and Electronics Engineers
ISM	Industrial Scientific Medical
IO	Input Output
IR	Infra Red
IrDA	Infra Red Data Connect
JABWT	Java API Bluetooth Wireless Technology
K	Kelvin
Kbaud	Kilo Baud

Kbps	Kilo bits per second
LAN	Local Area Network
LED	Light Emitting Diode
LSB	Least Significant Byte
L2CAP	Logical Link Control and Adaptation protocol
mA	milli Amp
mV	milli Volts
mW	milli Watt
Mb	Mega bits
MEMS	Micro Electro Mechanical
MHz	Mega Hertz
MSB	Most Significant Byte
M2M	Machine To Machine
NdFeB	Neodymium Ferrite Boron
NIST	National Institute of Standards and Technology
nF	nano Farad
OBEX	Object Exchange
PC	Personal Computer
PCB	Printed Circuit Board
PDA	Personal Digital Assistant
PIN	Personal Identification Number
RF	Radio Frequency
RFCOMM	Radio Frequency Communication
RFID	Radio Frequency Identification
RPM	Revolutions Per Minute
RS-232	Recommended Standard 232

SDAP	Service Discovery Application Profile
SIG	Specialist Interest Group
SOIC	Small Order Integrated Circuit
SPP	Serial Port Protocol
SPI	Serial Peripheral Interface
TDC	Top Dead Center
TCP/IP	Transport Control Protocol / Internet Protocol
TDD	Time Division Duplexing
µA	microAmp
µF	microFarad
µs	microsecond
µV	microVolt
µW	microWatt
UART	Universal Asynchronous Receiver Transmitter
ULP	Ultra Low Power
USB	Universal Serial Bus
V	Volt
Vdd	Positive Voltage Pin
Vss	Negative Voltage Pin
WAP	Wireless Application Protocol
WBXML	Wireless Binary XML
WLAN	Wireless Local Area Network
WPAN	Wireless Personal Area Network
wUSB	wireless USB
XML	eXtensible Markup Language

1 Introduction

In 1820 Hans Christian Ørsted discovered the relationship between electricity and magnetism in a simple experiment by demonstrating that a wire carrying a current was able to deflect a magnetized compass needle. In 1831 Michael Faraday conducted a series of experiments whereby he discovered electromagnetic induction. The relation was mathematically modelled by Faraday's law, which subsequently became one of the four Maxwell equations.

Faraday explained that electric and magnetic effects result from lines of force that surround conductors and magnets. Building on Faraday's ideas, James Clerk Maxwell derived equations by drawing an analogy between the behaviour of these lines of force and the flow of a liquid, and in 1861, developed a model for a hypothetical medium consisting of a fluid which could carry electric and magnetic effects, and considered what would happen if the fluid became elastic and a charge was applied to it. A disturbance in the fluid would produce waves that would travel through the medium, and the German physicists Friedrich Kohlrausch and Wilhelm Weber calculated that these waves would travel at the speed of light.

Maxwell's ideas were confirmed in 1888 when German physicist Heinrich Hertz discovered electromagnetic radiation called radio waves. He devised a transmitting oscillator, which

radiated radio waves, and detected them using a metal loop with a gap at one side. When the loop was placed within the transmitter's electromagnetic field, sparks were produced across the gap, proving that electromagnetic waves could be sent out into space and be remotely detected, detecting them across the length of his laboratory.

In 1893 Nikola Tesla described the principles of radio communication in detail and gave a public demonstration of "wireless" radio communication.

Guglielmo Marconi, fascinated by Hertz's discovery, realised that if radio waves could be transmitted and detected over long distances, wireless telegraphy could be developed. In 1894, he experimented with rough aerials on opposite sides of the family garden, receiving signals over a distance of 100 metres, and by the end of 1895 had extended the distance to over a mile, increasing to 8 miles in 1896 with demonstrations in England. He also developed tuned circuits for wireless transmission, tuned to a particular frequency to remove all other transmissions except the one of interest. In December 1901, Marconi and his associates succeeded in transmitting a signal across the Atlantic Ocean.

The term telemetry, (from Greek roots *tele*, remote, and *metron*, measure), did not come into use until some medium of transmission had been invented, with the earliest telemetry system based on electrical wires, following the invention of the telegraph and later the telephone. The first system was installed in Chicago in 1912 and used telephone lines for transmitting data from electric power plants to a central office, and was termed supervisory because of the monitoring capabilities [1].

Telemetry typically refers to wireless communications, but can refer to data transfer over any media. A basic telemetry system consists of a measuring instrument or detector, a

medium for sending the transmission, a receiver, and an output device that records and displays data [2].

Many of today's telemetry systems are built from commercial-off-the-shelf (COTS) products with many common elements, but uniquely configured to meet specific application requirements. A transducer obtains the monitored signal and converts the value into an electrical impulse ready for transmission. But telemetry applications which support large numbers of measurands are too costly and impractical to use separate transmission channels for each measured quantity (such as pressure, speed, and temperature). Individual measurements are formatted or multiplexed, using either time division or frequency division multiplexing, and transmitted as a single data stream. At the receiver, the data stream is separated into the original measurement components for analysis [3].

Simple forms of telemetry use wire links, whilst radio is the preferred medium for use over long distances, with light or sonic signals for specialized applications. Telemetry technology has been extended to the point where astronomical information can be obtain from the farthest planet, or biological data from within a person's body via micro-miniature transmitters.

1.1 Engine Condition Monitoring

A major application in the automotive industry is piston telemetry where manufacturers endeavour to develop more efficient engines with higher power and reduced emissions. In order to achieve these goals, certain piston parameters such as temperature, forces, and pressure need to be monitored, sampled, and accurately analyzed. Manufacturers of engine components, lubricants, and fuels also need the information to assess the performance of

their products under varying conditions of engine load and to refine the software models used in engine development. As piston design, and to a lesser extent, lubricants, affect emissions, their optimisation is vital, necessitating the use of simulation software.

Finite Element Analysis (FEA) is used for both the creation of a new piston design, as well as identifying the causes of a failure during actual use and makes it possible to evaluate a detailed and complex structure, in a computer, during the planning of the structure. Modelling the thermal and mechanical behaviour of a piston is crucial, as it allows for the prediction of piston characteristics such as dynamics, friction and high stress areas which directly affect the efficiency of an internal combustion engine. It is important to calculate the piston temperature distribution in order to control the thermal stresses and deformations within acceptable levels. The temperature distribution enables the optimization of the thermal aspects of the piston design at lower cost, before the first prototype is constructed and reducing the number of prototypes built.

The analysis of heat dissipation plays a major role in designing pistons. Piston skirt design is one of the most important features for control of friction performance. Substantially reducing the overall piston skirt area by 40 per cent reduces frictional drag. This redesign of the piston reduces fuel consumption and lowers emissions. A uniform oil spreading pattern is also very important in reducing piston skirt friction. And analysis of ring design and position can reduce the amount of trapped hydrocarbons during operation by placing piston top ring closer to the top of the piston crown [4].

With less expensive and less effective additives, carbon deposits can build up and decrease fuel efficiency by affecting the air/fuel mixture in the fuel injector, absorbing fuel in the intake valve during engine warm-up, or auto-ignite the air/fuel mixture in the combustion

chamber. Fuel quality is also very important and the engine and fuel system design and after treatment devices are the primary routes to emission improvements. Lubricant quality is significant in diesel engines where it may provide more than half of the total contribution to diesel particulates. With this exception, lubrication makes a very small contribution to emissions relative to fuel, as a percentage. This percentage is likely to become less as engine designs are improved to reduce lubricant consumption. For gasoline engines, viscosity, volatility and additive chemistry of low emission lubricants are important variables, and although it has been demonstrated that physical and chemical properties can affect emissions, there are no general lubricant formulation to reduce exhaust emissions. The phosphor, silicon and sulphur levels in lubricants have a detrimental effect on catalytic converters, on the deterioration of de-NOx catalysts and particulate traps [5].

1.1.1 Piston Telemetry

Information cannot be obtained directly from the piston. With non wireless systems, there must be a physical link with the piston crank. Some telemetry systems are inflexible, in that they detect specific parameters and changing the system parameters could mean dismantling the engine [6].

The measurement of piston temperature in a reciprocating engine aims to measure temperature inside the cylinder at the piston head surface, piston ring grooves and pin holes. Pistons are especially challenging to measure because they are constantly in motion and temperature measurement in the inherently harsh operating environments of internal combustion engines and automotive transmissions has historically been a difficult, time-consuming and expensive process.

A number of sensors are used to measure the rapid change of high temperatures and uneven distribution of heat at different positions or areas of the piston. Measurement equipment must be protected against several conditions in the engine, with acceleration forces near 2000g occurring at Top Dead Centre (TDC) at rated speed. Operating temperatures inside the crankcase can reach 200°C. Also, to allow complete mapping of piston temperature, several measuring locations are required in the piston and data must be obtained under various engine operating conditions. In addition, adopting wireless technology requires a power supply that does not need regular access to the piston, which would be the case with battery technology.

1.2 Short Distance Telemetry

Short distance telemetry, where short distance is taken to be up to 2 cm in range, is a telemetry method designed for the substitution of slip rings in a rotating system.

To eliminate the requirement of cabling and through these, power transfer, short distance telemetry is employed between data acquisition system and host receiver. But such a system requires a source of power to drive the circuit components. The power source can be in the form of a battery or power generator.

A power generator employs a coil stator and rotating permanent magnets, AC-DC conversion circuitry and voltage regulation circuitry to provide a constant voltage to drive the telemetry circuit.

1.2.1 Slip Rings

A slip ring is a method of making an electrical connection through a rotating assembly. An alternating current slip ring consists of a conductive band mounted on a shaft and insulated from it. Sliding electrical connections from the rotating part of the system, such as the rotor of a generator, are made to the ring through fixed brush contacts run, transferring electrical power or signals to the exterior, static part of the system.

The slip ring is usually made of copper or copper alloy and the brush made of carbon, usually graphite, electro-graphite or metal-graphite. A brush holder holds the brush that conveys current to an external device. A carbon film forms between the brush and slip ring, which must be deposited uniformly to ensure satisfactory operation and whose lubricating properties prevent wear and seizure. Ring surface conditions, with different currents flowing, are more important than brush conditions.

A slip ring consists of a conductive band mounted on, and insulated from, a shaft and is used where electrical power or signals need to be transferred to a rotating device [7]. Electrical connections from the rotating part of a system are made to the ring. Fixed contacts or brushes run in contact with the ring, transferring electrical power or signals to static exterior systems. The disadvantages of slip rings are; brush wear and ring wear, arcing of worn brushes, the requirement of transferring power through the rings and cabling of the system. Also, voltage surges and spikes can cause slip rings to fail [8].

Many variables have to be considered in the specification and configuration of slip rings. Considerations may include: Basic design: separate or integrated brush and ring, permanent mounting, mounted on bearings; System interface: electrical connections, mounting

method, rotational speed, component routing; Electrical interface: data rate, signal frequency, maximum current; Environment: operating temperatures, vibration, harsh environments, integral seals [9].

Through monitoring and maintenance, utmost care must be taken to avoid or remedy faults that occur with slip ring use. Brush wear appears as broken pads and pad edges; Uneven wear by cross section or length and inherent roughness which limits the contact surface; Brush holder vibration appears as brush bounce and shorting, due to the brush lifting; Ring wear appears as groove formation, pitting (chemical attack), corrosion or ring surface etching. A smooth, glazed surface appearance or uneven carbon film formation are also a symptoms of problematic performance.

The fault symptoms of slip rings are inter-related and are diagnosed holistically, not individually. The mechanical problems manifest themselves as Arching, when brush is not in contact with the ring; Flash over between two rings; Flat spots caused by brush vibration or partial seating of the brush; Chattering, caused by the brush rocking in the holder and Polarity effect. Particles or gases in the atmosphere can interfere with oxidization after de-filming and greatly increase friction, where threading, discolouration and burning on the rings are symptoms of these faults. The carbon film is a semi-insulating film that is required to be of even thickness around the ring. Too thin and the film wear is rapid causing brush friction wear and over heating. Too thick a film makes too good an insulation, prohibiting brush and ring contact and thus current transfer. Two other important conditions are that the rotor must run true with respect to concentricity and without wobble, and that machine unbalance causes vibration. These two conditions must be eliminated as completely as possible for satisfactory operation.

1.2.2 Wireless Technology

Wireless sensor technology was once impracticable due to cost and design complexity, but is now a viable option for data logging and measurement from remote locations. Wireless communication uses electromagnetic radiation instead of wire cables and can be included in any existing network.

Common reasons for adopting a wireless system are: The bulk and cost of cabling between sensors; the practicalities of applying a system within a confined space and the convenience of distributing wireless sensors in remote locations. The considerations are the range, data rate, power requirements and security of a wireless system compared to the costs of cabling for a wired system.

Table 1.1 Comparison of four wireless technologies.

Standard	**Technology**	**Power consumption**	**Data Rate**
IEEE 802.11	WiFi	Very High	High
-	Wireless USB	Medium	Medium
IEEE 802.15.1	Bluetooth	Low	Low
IEEE 802.15.4	ZigBee	Low	Low

The four common wireless technologies, as listed in Table 1.1, show a comparison of power consumption versus data rate. IEEE 802.11 WiFi has the highest data rate, but with the penalty of very high power consumption, whilst IEEE 802.15.4 ZigBee uses the least power, but achieves this with long periods of sleep mode. The more measurements that are taken, the more power will be used.

1.3 Bluetooth Technology

Bluetooth is a cable replacement technology between low power devices operating in the 2.4 GHz range providing connectivity to a PC, handheld device, or machine to machine communication. Figure 1.1 indicates Bluetooth's low power compared to ZigBee lower power via sleep mode, enabling new measurement applications in sensor reading and data acquisition. With Wifi & wUSB at one end and Bluetooth & ZigBee at other end, these four technologies each target different niche applications [2].

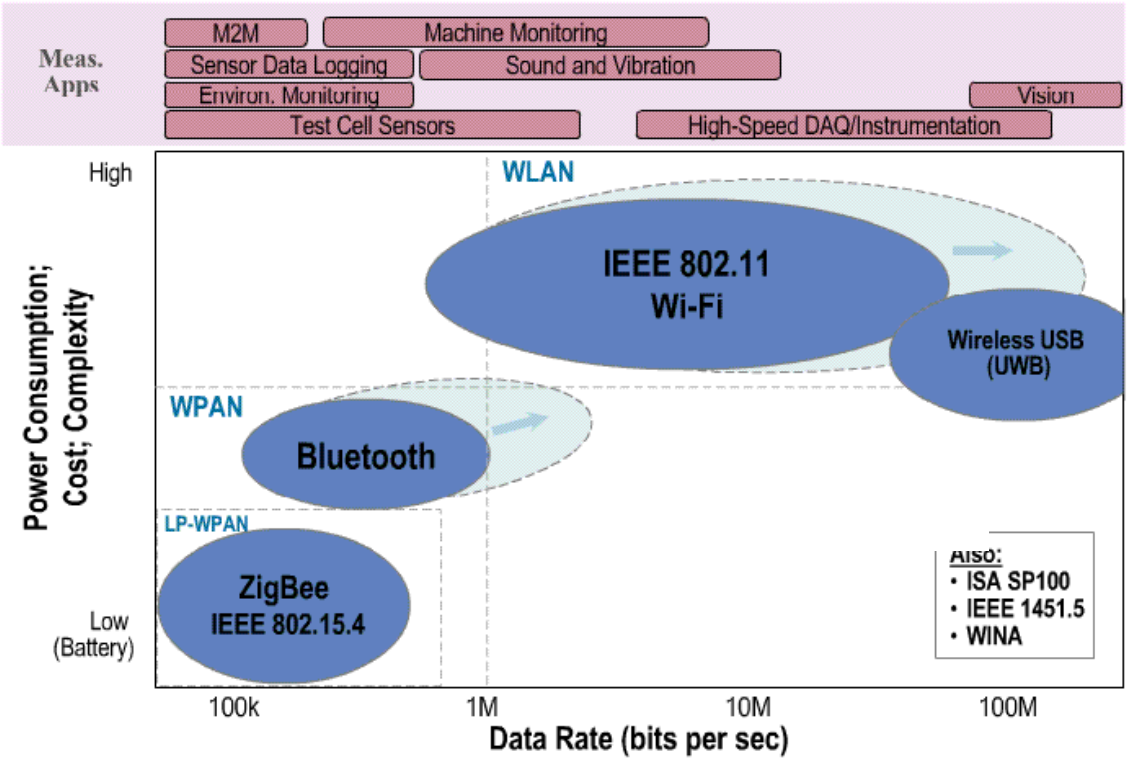

Figure 1.1 Comparison of Wireless Standards [2].

1.4 Statement of Problem

Temperatures at various points on the piston crown indicate the performance of the piston, and hence provide data to enable the design of more efficient piston heads to meet efficiency standards. Early methods to obtain temperature data from temperature sensors

located in limited / confined space or hazardous locations inside the piston cylinder, relied on physical links or contacts. The problem is to extend the limited contact time of such methods and eliminate the cabling required to transfer data to an external a host.

1.5 Aims and Objectives of the work

The aims of this work are to develop a system that incorporates:

- A Wireless mechatronic telemetry system.
- An Independent Power Generator.

The objectives for the overall system are:

- Design and construct an induction power generator comprising of magnets, coils and an electronic circuit to rectify induced AC voltage to DC to drive a data acquisition module at a variable rpm range.
- Select a technology for wireless telemetry that is suitable for cable and slip ring replacement and provides a low power, robust, digital transmission over a short range with sufficient data transfer rates for data acquisition, and eliminates interference from other devices.
- Construct a data acquisition module that connects the output signal from temperature sensors or transducers, performs signal conditioning and through firmware, transmits data to a host.
- Develop software (firmware) using publicly available software tools for the components used in the data acquisition module.
- Develop a test rig utilising a variable speed motor that spins the rotor and induces voltage into the stator coils, powers the data acquisition electronics to test

thermocouples and transmit data over the Bluetooth link to display voltage values on a PC host user interface. Using the software tools, simulate devices and test the firmware source code.

1.6 Contribution

In this work, the requirement is for more precise control of voltage and temperature measurements, and piston telemetry can help achieve this with a system that is robust and reliable and a more cost effective method than existing systems or techniques available at the moment.

The most important module of the work is a permanent magnet axial flux power generator that replaces slip rings. It is a compact design that allows it to be attached to reciprocating devices such as pistons or rotating components such as shafts, providing power for the full rotational cycle.

The system is a modular mechatronic Bluetooth data acquisition system incorporating a wireless telemetry system that replaces cabling, with voltage and temperature acquisition and signal processing performed at the data acquisition side of the system.

1.7 Structure of the Thesis

Chapter 2 The literature review describes methods used for data acquisition with various telemetry techniques, the problems and effects of the piston environment, and emerging technology for independent power generation.

Chapter 3 Describes an existing telemetry system and explains the techniques employed by a specific induction telemetry system and the issues present in that system that are required to be overcome by an alternative wireless system. Also described are the processes

involved for creating a piston ready for instrumentation. These processes are the development of a CAD drawing, CNC machine code and the machining process for creating a prototype piston and the importance of finite element analysis in simulating and predicting temperature distribution.

Chapter 4 The proposed system is an explanation of the theory and techniques used by Bluetooth transmission and the attributes of thermocouple transducers and the methods used to install them within the harsh environments of pistons and piston crowns, followed by the reasons that these characteristics are desirable in this system.

Chapter 5 Describes the design of an axial flux power generator to supply power to the components of the wireless telemetry system.

Chapter 6 Describes the prototype Bluetooth telemetry system, explaining the hardware and software employed to build a generic mechatronic system for wireless telemetry.

Chapter 7 Describes the creation of test rig and the results obtained when using the test rig to drive the power generator and the resultant output to drive the telemetry electronics.

Chapter 8 Discusses the issues encountered in obtaining temperature data from within internal combustion engine pistons and the design of a generic mechatronic wireless telemetry system. Also future work in adapting the prototype system to incorporate emerging technology as it becomes available.

2 Literature Review

This chapter explains the background importance as to why the temperature readings inside engine piston chambers and crankshaft casings are required and then reviews the literature for piston temperature acquisition, the methods used with regards to the electronics and methods of short distance telemetry and applications that employ these methods.

2.1 Background

The piston is one of the most complex automotive components and considered the most important part of an engine. Damage occurs mainly due to wear, temperature, and thermal and mechanical fatigue over a wide temperature range at the crown, ring grooves, pin holes and skirt [10]. Heat transfer affects the performance, efficiency and emissions, as well as life of the engine components, such as piston, rings and valves. The local value of heat transfer coefficient varies considerably in different parts of the cylinder, but they have equivalent trend with crank angle. Therefore it is necessary to analyse the variation of local heat transfer in order to study thermal stress problems [11]. Heat is transferred from the hot gases to the piston top surface, conducted to the under side of the piston, then transferred to the other parts of the engine from the piston components such as ring land, skirt, under side and pin, leading to thermal deformations and thermal stresses. Therefore it is important to calculate this temperature distribution and keep them to acceptable levels [12].

Understanding the sensitivity of chamber thermal conditions allows more precise control of the load range and thermal transient management. Temperatures are measured with thermocouples inserted through holes drilled below the piston head to accurately measure instantaneous temperature and heat flux.

Example temperatures are gas temperature of 1000 °C affecting the piston head, water temperature of 85 °C affecting the piston skirt and oil temperature of 70 °C affecting the bottom of piston [13].

The temperature prediction of pistons is very important for recent high power engines to maintain reliability under higher thermal load as the increase in temperature will have a very serious effect on the lubricating oil, as at elevated temperatures, the oil will have greatly reduced viscosity. Therefore, it is essential to bring the temperature down by having a proper cooling arrangement for the piston system [14].

The specific power and overall efficiency of the engine are strongly dependent on heat loss. The more heat that is transferred through the engine parts, the less work is transferred to the engine shaft through the piston and piston rod. Also, if temperatures are too low, then compression loss between the cylinder liner and the piston parts may result, increasing leakage through the crankcase, emissions, loss in power, decrease in viscosity of lubricating oil and loss in overall efficiency. All these requirements need a careful design of the critical parts, indicating the importance of keeping the temperature of the engine parts within a certain range for all operational conditions [15].

Conventional engine materials, such as iron, steel, and aluminium, may not be able to handle the increased thermal loading required of certain engine parts, such as pistons, rings,

bearings, and exhaust ports. Advanced materials such as ceramics, aluminium alloys, powdered metals, and coatings handle thermal stress better and thereby extend engine life [16]. The many stresses and strains exerted on a piston during its use all cause some form of distortion. Piston designers attempt to predict this distortion and manufacture the piston to allow for these effects.

As pressure, heat and kinetic energy influence the piston performance, the piston must be designed for optimum performance under these forms of energy. To achieve this optimisation, calculation of the thermal and temperature distribution on the piston is predicted by Finite Element Analysis (FEA).

FEA may be real or theoretical (simulation). Real analysis requires initial temperature measurements from various points in the piston and heat flow coefficients at various locations as input to the FEA model. Theoretical analysis uses assumed or defined initial temperature values for various piston points in the FEA model.

Inside the engine, moving valves and pistons, complicated piston shapes, complex spray and combustion processes can be modelled or simulated for a variety of situations. To create the model, the dimensions and 3D structure of the piston body, boundary conditions and the properties of thermal conductivity, heat transfer coefficients, material density and thermal expansion are required. FEA software packages simulate the model or perform the complex equations required to solve the analysis. FEA employs a meshing technique to define the elements, and the higher the number of elements, the higher the precision of the model analysis, but longer computational time. Figure 2.1 [17] shows the thermal gradients of a modelled piston, from the high temperatures at the piston crown to the cooler temperatures at the piston skirt.

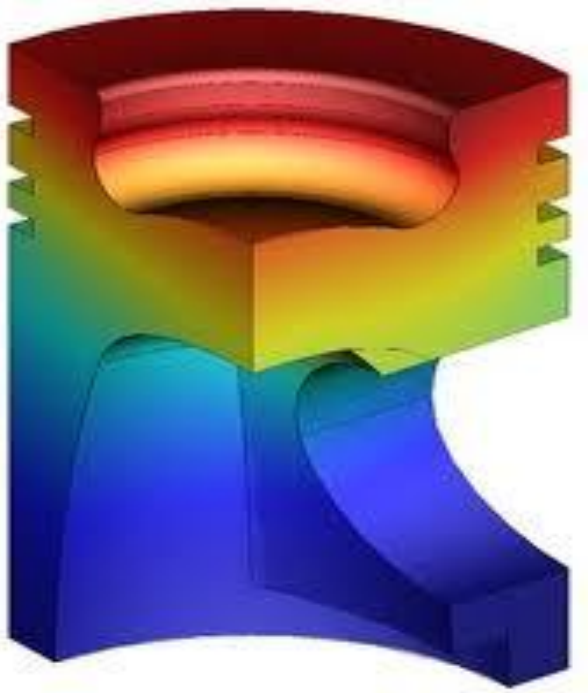

Figure 2.1 Example Temperature Distribution on a Piston [17].

As much as 60% of the total engine mechanical power loss is generated by piston ring assembly [12], therefore, cooling of the piston is one of the determining factors in a successful engine design, and the accurate prediction of the piston temperature [18] is as important as taking temperature measurements from within the piston and the instantaneous temperature on the combustion chamber wall surfaces [19]. The heat transfer coefficient in the cooling gallery has great effect on the piston temperature, but is hard to predict with sufficient accuracy because it is influenced by various factors, including oil flow, engine speed and oil hole diameter [18] and have been determined empirically by past experience [20] or by a variety of measurement methods such as link, contact-point, telemeter, electromagnetic induction and wire take-out [20].

The measurement of piston temperature in reciprocating engines has historically been a time consuming and expensive process, and measurement equipment must be protected

against acceleration of near 2000g at Top Dead Centre and operating temperatures inside the crankcase can reach near 150°C. To allow complete mapping of piston temperature, several measuring locations are required in the piston and data must be obtained at various engine operating conditions [21].

Piston temperature data has been acquired using many types of devices ranging from simple temperature plugs to sophisticated electronic methods. The greatest difficulty with electronic methods is getting the data from the reciprocating piston to a stationary component such as the cylinder block [21].

An early and widely used electrical technique is to use long sensor leads from the piston along a linkage arrangement to the engine block then to an external DAQ (Data Acquisition) equipment outside the engine [21, 22], but is difficult to install within the crankcase and alterations to the engine crankcase are sometimes required. This method has a short life expectancy with failures due to lead wire fatigue. A later method is to use two induction coils, one of which is attached to the piston and the other to the crankcase and relies on careful alignment of the coils. Data is obtained and transmitted once per engine revolution, near bottom dead centre when the two coils become close-coupled, which is sufficient for most temperature measurements [21]. Modern techniques concentrate on wireless technology for data transmission.

2.2 Literature Review

The literature review begins with piston temperature prediction, measurement and telemetry, followed by a review of telemetry methods, an overview of telemetry applications, then a review of wind energy technology, Bluetooth and Zigbee technology.

2.2.1 Piston Temperature Prediction

The highest temperature at any point in the piston must not exceed 66% of the melting point of the piston alloy (1000°K (728°C), maximum, approximately 640°K (368°C)), therefore it is important to calculate the piston temperature distribution in order to control the thermal stresses and deformations within acceptable levels [12].

Case studies describe fatigue damage to the piston elements of crown, ring grooves, pin hole and skirt, caused by thermal and mechanical fatigue. High temperature mechanical fatigue is described where temperatures can reach 382°C at piston bowl rim, 225°C at the pin hole and 209°C at the top groove, depending on piston geometry. Piston cooling is also described where temperatures can be reduced by as much as 30°C – 50°C at piston top groove [23].

Temperature measurements are taken in the cylinder head, liner and piston, using type K thermocouples, ranging from 140°C to 280°C at engine speeds between 1430 rpm and 4000 rpm. Models of heat transfer and thermal behaviour of piston temperature distribution are investigated by Esfahanian et al. [12] and predicting cylinder wall temperature by Torregrosa et al. [10] with the aim of controlling thermal stresses and deformations.

A new approach to piston temperature prediction is the use of CFD tools [11, 18] to calculate the coefficient of heat transfer [18] and analyse heat transfer and combustion in a combustion chamber, piston and intake / exhaust outlets [11] in order to improve predictions compared to temperature estimation based on past experience as better predictions contribute to better engine design.

2.2.2 Piston Temperature Measurement

Yamada et al. and Uchimi et al, [19, 24] investigated the effects of particle matter (soot) adhering to the chamber wall surfaces on heat loss in the piston. Measurements were taken at seven points using type J thin film thermocouples with the engine running at 1200 rpm. High order polynomials were applied to convert the average of 256 readings to temperature values.

Thermistor sensors, at six points, were measured by an enhanced ‘contact point’ method where each contact point is a separate channel located at bottom dead centre from where data is transmitted at engine speed between 9,000 rpm and 12,000 rpm [20].

2.2.3 Piston Telemetry

Furuhama and Enomoto [25] developed a linkage mechanism that carried up to 15 pairs of thermocouple wires from the piston to outside the crankcase. The wires were fastened to plates and through coil springs in order to minimise twisting of the wires, but eventually lead to fatigue failure. Temperatures were measured at various pints by drilling holes in the piston to position the thermocouples as close as possible to the piston crown. The experiments were an investigation into ‘knocking’ and the temperatures at many points in the engine were also measured.

Wu and Chiu [26] investigated of piston temperature at various engine torques, as one part of a whole engine energy system, and also used a linkage mechanism to guide thermocouple wires away from the piston.

Barna et al. [27] developed a telemetry system employing infra red technology. Temperature data is transmitted as modulated IR pulses. A photo-detector mounted on the

crankcase picks up the signals and transfers them via wire to an external receiver. The transmitter system is mounted on the underside of the piston and powered by lithium batteries. Type E thermocouples or thermistors are read with voltage to frequency conversion and calibration performed before infra red LEDs transmit the data as pulses. The line of sight photo-transistor receiver passes the data to a frequency to voltage converter and calibration unit before passing the data to an external voltage readout. The piston temperatures were in the range of 100°C to 400°C at engine speeds up to 5000 rpm and 2100g. The operating temperatures of the telemetry system were between 90°C and 150°C.

Burrahm et al. [21] developed a telemetry based system that is attached to the underside of the piston with data transmitted to an antenna located in the engine crankcase. The power generator utilises the reciprocating motion of the piston and induces inertial forces on a metal slug, producing a magnetic flux that induces a voltage in a generator coil, allowing the transmitter to be self powered. The transmitter oscillator frequency is controlled by the capacitor, where a change in temperature change causes a change in capacitance, thus changing the output frequency, which is proportional to the change in temperature. An eight turn 22 AWG wire loop antenna receiver, formed around the oil pan, connects to a coaxial cable and computer. The receiver signal is amplified and filtered before the frequency to voltage conversion is sampled by a computer that also applies a conversion algorithm using a comparison table.

During testing, temperatures of 250°C in the engine, up to 152°C in the pistons and 104°C in the oil sump were reached. The transmitter failed when the temperature reached a higher than expected 150°C. The highest g forces encountered were 2300g at 5500rpm. The

generator produced up to 40V, but the signal circuitry required a voltage range between 0 – 10V and transmitter circuitry required both positive and negative voltages.

Wiczynski et al. [22] developed a two module telemetry system to measure temperature and strain on a spherical piston joint, withstanding high inertia and high temperature environments of up to 130°C. The transmission module contained signal conditioning, multiplexing and FM radio data transmission. The antenna was mounted on the engine oil pan and connected via cabling to an external receiver / demodulator. A linear power generator relies on the motion of the piston to convert thermal and mechanical energy into electrical energy to power the telemetry system. A coil is wound around a permanent magnet whose pole pieces extend to a modified cylinder wall of alternating ferromagnetic and non-ferromagnetic bands. As the piston and magnet travel past the bands, changes in the magnetic flux generate an EMF in the coil. The output from the coil is rectified and regulated to provide the required 15 mA, 9V DC voltage.

Varo and Archuleta [28] developed a similar power generator in that crescent shaped grooves are machined into the cylinder lining and whose depth alters the air gap between magnet and cylinder. As the piston reciprocates past the cylinder lining and grooves, this fluctuating air gap causes a fluctuating flux through the coil, thus inducing a voltage, which powers transducers and the telemetry system. Operation of this system occurs only at sufficient engine speed as the generated voltage is DC rectified and regulated and optimised to provide a voltage at low idling speed. A mechanical link carries the wires of the telemetry unit to a stationary antenna receiver located in the crankcase. Data transmission is an RF signal which is demodulated by the receiver.

Horler and Picken [29] explain how previous telemetry systems are unidirectional, from transmitter to receiver with fixed sampling rate, and proposes a bi-directional system enabling alternative modes of operation at selectable sampling rates.

The piston system transceiver is housed in a high temperature plastic housing powered by a 6V battery consuming 29mA. The antenna is attached to the crankcase wall. The crankcase system transceiver and microcontroller are embedded on an aluminium plate which covers an aperture machined into the crankcase wall and connected to a PC via a RS232 channel, and powered by regulated 9V from mains supply, consuming 500mA. Measurements were taken at engine speeds of 2200 rpm and temperatures of 182°C in the engine, although at 300°C during testing.

Horler [30] also developed a wireless piston telemetry unit in which the telemetry system and sensor circuits are powered by a magnet situated on the connection rod little end that moves relative to a solenoid coil (with inner soft magnetic material) as the piston reciprocates. An RFID device is controlled externally by a separate radio frequency signal to remotely switch the power supply on and off. An external processing unit feeds a RF carrier signal to a primary coil located within the crankcase, which is picked up by a secondary coil located in the skirt of piston. By rectification, smoothing and filtering, the sensor unit derives DC power and generates a clock signal from the inductively coupled carrier signal. A microcontroller modulates the signal from a number of sensors. Horler explains a problem with RF transmission in that frequency drift of the carrier signal occurs as the engine temperature rises resulting in a loss of communication if the processing unit can no longer detect the carrier signal conveying the sensor data. His solution is to modify the carrier signal by an amount depending on engine temperature.

Temperature data is modulated onto the carrier signal and wirelessly transmitted to the base station where it is demodulated to extract the temperature data. This is done in two stages with lookup tables. The first lookup table is used to calibrate the frequency drift of the carrier signal by comparing the carrier frequency to a lookup table of temperature values and the second lookup table is used for CJC for the sensor temperature values.

Kato et al. [31] measured temperatures of up to 400°C in a piston using electromagnetic induction at engine speeds of up to 6000 rpm. Transmitter and receiver coils are installed in the lower part of the cylinder bore, and a resonator coil is wired to a thermistor embedded in the piston at the point of the measurement. Alternating current applied to the transmission coil generates a current of the same frequency in the receiver coil and current is induced in the resonator coil as it passes the receiver coil near Bottom Dead Centre, resulting in lower current flowing through the receiver coil. Since the thermistor resistance drops as the temperature rises, then the higher the piston temperature, the larger the resonator induction, and thus a lower current in the receiver coil.

Suster et al. [32] developed a prototype MEMS (Micro Electro Mechanical) sensor and telemetry system using a tunnel diode oscillator transmitter with an onboard optical power converter. A MEMS capacitive pressure sensor performs pressure to frequency conversion and a spiral loop serves as an inductor and transmitting antenna. A photodiode converts an incoming laser beam to dc power, for powering the prototype design. The system achieves a telemetry performance of up to 250°C temperature measurements over a distance of 1.5 m with a transmitter power consumption of approximately 60 μW.

MEMS capacitive pressure sensor converts environmental pressure to capacitance, resulting in variation of the oscillator output frequency. This frequency change is detected by an

external spectrum analyzer receiver through a wireless link. The frequency modulation achieves reliable data transmission compared to amplitude modulation techniques.

Lee et al. [33] explain that temperature measurements are required when investigating the thermal problems induced in modern automobile engines and a piston telemetry system is developed using a Bluetooth wireless network. The system comprises of a piston part and a data acquisition part measuring temperatures in an engine environment of 6000 rpm, exceeding 2000g and piston temperatures over 300°C. The telemetry system is installed at the big end of the connecting rod to avoid the high thermal loads encountered in the piston.

For the temperature sensors, type K thermocouple wires are extended and connected via a bracket arrangement in order to prevent damage. The telemetry node consists of three circuits – a sensor board, a Bluetooth board and a power board. The sensor board reads the thermocouple outputs and performs signal conditioning in the form of amplification and analogue to digital conversion by a microcontroller. The microcontroller acts as a Bluetooth host and passes the digital data to the Bluetooth board for transmission. The sampling rate of the ADC is limited by the data rate of the Bluetooth module and the number of channels measured. The power board uses bridge diodes, capacitors and a linear regulator to transform the induced AC voltage from the generator into a 3.3V DC supply to the sensor and Bluetooth boards. This AC generator must also produce more than the 3.3V supply to allow for the voltage drop across a linear regulator. The generator consists of five 22 mm diameter NdFeB permanent magnets and a coil. The magnets are arranged in an arc, centred on the crank pin, and made of high flux density neodymium. The 20 mm thick coil is positioned on the connecting rod. When the crank rotates, the coil moves linearly over the magnets for 150°, producing a sinusoidal flux density for a short duration, with a large value capacitor is used for voltage storage. The Bluetooth module transmits data to a

Bluetooth antenna (Bluetooth adapter) located inside the engine case and connected to an external PC via a USB cable.

2.2.4 Telemetry Reviews

A representative selection of reviews of telemetry follows covering energy transfer, sensor technologies and industrial applications.

2.2.4.1 Wireless Energy Transfer

The 2001 review by Van Devoorde and Puers [34], describes the difference between low and high power inductive links, comparing the wireless energy transfer of high and low power applications employing induction, focusing on high power inductive links and methods of integrating them into standalone systems.

High power systems employ closed loop link drivers, without constraints on coil size, and produce power of several watts, whereas low power systems use magnetically coupled coils for power and data transmission but have constraints on size, position or distance, producing power of a few milliwatts.

Low power magnetic links are characterised by either large coil separation or small coil diameter, where the coupling factor can be as low as 1%. High power magnetic links are characterised by closely coupled large coil diameters producing 30% - 96% depending on coil dimensions and placing more importance on the rectifier and regulator. Full bridge rectifiers are used in high power links, but not in low power links, to compensate for the forward conduction losses and high frequency losses encountered by the switching time of the diodes.

2.2.4.2 Wireless Sensor Technologies

The review of wireless sensor technologies by Wang et al. [35] described how wireless technologies have been under rapid development, from simple IrDA for short-range, point-to-point communications, Bluetooth and ZigBee wireless personal area network (WPAN) for short range, point-to multi-point communications, to mid-range, multi-hop wireless local area network (WLAN), and long range cellular phone systems, such as GSM/GPRS and CDMA.

Various wireless standards exist that are used for measurement and automation applications using the 2.400–2.4835 GHz ISM radio bands, i.e. Wireless LAN (IEEE 802.11), "WiFi" (IEEE 802.11b), Bluetooth (IEEE 802.15.1) and ZigBee (IEEE 802.15.4).

A wide variety of wireless sensors are available including accelerometers, barometric pressure, light, temperature, humidity, acoustic sensors; soil moisture, soil temperature, wind speed, rainfall meters, seismic and solar radiation sensors; magnetic RPM sensors, magnetometers, IR detectors, GPS modules.

"Smart transducers" are sensors or actuators equipped with microcontrollers to provide local intelligence, networking capability and signal processing functions that interface with ADC, DAC, digital IO, analogue IO and network modules. A new standard, 1451.1, aims to integrate smart sensors with wireless communications such as WiFi, Bluetooth and ZigBee.

Although cellular phones have become ubiquitous, the greater potential is for applications and development of wireless sensor networks for environmental monitoring, data collection, machine to machine (M2M) process control, building automation and traceability systems (RFID).

2.2.5 Telemetry Applications

Telemetry has been, and continues to be, applied to many traditional and emerging disciplines, including: Defence Systems, where without telemetry critical system data would be unavailable; Space Exploration; Geological Exploration Systems such as oil rigs and chemical plants; Motor sport, to interpret data collected during a test or race; Medicine (biotelemetry) for physiological measurement or remote diagnosis via telemetry; Wildlife Study and Management; Retail Businesses that make use of RFID tags. Instruments range from simple RFID tags to GPS transceivers to provide position and other information [36].

A large quantity of telemetry research is applied to medical applications, animal research and power generation. Medical applications that have telemetry aspects are mainly prosthetic implants [37-39] and endoscopic devices [40-43] with some biological data [44, 45] from incubators [46, 47] or neural signals [48]. Sensors are used as part of the system in the majority of cases [37, 38], but some telemetry boards incorporate microcontrollers with digital conversion [49] or Serial Peripheral Interface (SPI) [45]. The main method of data transmission is through inductive links that also transfer power [37-39, 41, 42, 48, 50]. Other methods are transceiver ICs or ASICS [40, 49], radio waves [46], Bluetooth [51], ZigBee [45], ibutton [44], web server [45]. Host processing is designed with LabVIEW [46] or SyncML [51] software. Firmware is created with MPLAB [49] or nesC [45].

Animal research telemetry focuses mainly on implanted probes or sensors to acquire physiological or environmental data. The majority of data is collected by microcontrollers [52-54], NI 6008 DAQ module [55], a FlexiPanel Pixie module board [56], iButton [53], or a custom built head pack [57]. A variety of transmission techniques are employed, RF [52, 53], FSK [58], FM [59], ISM band [54], ZigBee [56] and Bluetooth [57], with none being

more popular than others. Transmitted data is either collected by a host PC [58], PDA [57], a microcontroller post processed by LabVIEW software [56], [55] or over the internet [53].

For power generation, the technique of inducing power from a primary coil to one secondary coil is employed in many applications, with novel techniques being explored such as a primary coil coupled to implanted secondary coil(s) [39] and on-chip planar coils coupled to an external antenna [60], with similar techniques also using miniaturised micro coils [61].

2.2.6 MEMS Technology

MicroElectroMechanical techniques use IC fabrication methods and miniaturisation methods to manufacture power generation devices that are designed to drive integrated sensors and embedded modules.

Wise [62] described in his review how the 1960s saw mechanical systems, with the addition of signal processing, microfabricated into silicon, the 1980's witnessed the emergence of new fabrication techniques, the 1990's experienced an emphasis on systems and the 2000's realized an increased integration of sensors with embedded computing and wireless technology, providing complete application solutions. He also stated that the automotive industry was a leader in these efforts as it attempted to meet fuel economy and emissions requirements using electronic engine control.

Energy sources for MEMS energy conversion fall into five broad categories; MicroFuel cells consisting of alchohols, hydrocarbons or methanol [63]; turbines, coupled to a generator that require fuel [64] or air to drive blades at 1000s of rpm. Microbatteries employing thin film technology [65]; Thermoelectric generators that generate electricity when placed across a temperature gradient from the environment or a fuel cell producing

heat [66]. Energy harvesting or scavenging that utilises the movement and vibration of mechanical energy to provide electrical energy. The main physical principles for vibration-to-electrical energy conversion are piezoelectric (stress) and electromagnetic (inductive) [67]. Raisigel et al, [68] developed a micro turbogenerator consisting of a permanent magnet (NdFeB) disc rotor and a stator with electroplated planar coils. With speeds up to 380,000 rpm, at 50,000 rpm, the generator produced 5v at 1mA. Kim et al, [69] developed a similar generator technique for vibration scavenging, producing 198 mV at 6 Hz. Lee K. et al, [70] developed a micro system where an electroplated stator acted upon permanent magnets attached to a flywheel, to store energy. The disadvantage of MEMS devices are the increased complexity required to interface the multiple components that make up the system. Although MEMS generators provide the power to drive 'systems on a chip', they do not produce sufficient power to drive discrete components.

2.2.7 Wind Energy Technology

Although axial flux research occurred soon after the discovery of electromagnetism, popularity eventually elapsed because magnet strength was weak and unable to produce the desired output. It was with the Japanese development of Neodymium Ferrite Boron magnets in the 1980's that a resurgence of research into axial flux generators has occurred. In the literature, there are no comparisons of Axial Flux Permanent Magnet machines and Radial Flux Permanent Magnet machines, as there are a large number of technical solutions that require experience in parameter selection. Experience is still limited for novel prototype machines [71].

It is the wind energy industry that is at the forefront in axial flux generator technology and development. Wind energy technology for small machines is described in many papers,

whilst other papers describe the same technology applied on a larger scale to direct drive wind turbines, and yet other papers describe the technology as applied to MEMS applications.

A three phase generator usually has overlapping coils wound on a slotted stator. The generator is then subject to cogging and lower efficiency through iron losses and eddy current losses. Cogging is reduced by having a magnet to coil ratio other than 1:1, with a ratio of 4:3 or 3:2 being most common. Other ratios reported are 16:12, 8:6, 8:16, 8:12, 12:6. Eddy current losses are greatly reduced by using a laminated core instead of a solid core. Iron losses are still an issue as the slots are in the flux path of the magnets and will still produce losses if the magnet size were increased.

By selecting a single phase machine, in which cogging does not occur, and using an air core to eliminate iron losses and eddy current losses, the weight of the machine is greatly reduced, adapts itself to modular design and construction and gives greater freedom of coil windings. The rotors on large single phase machines with large magnets can be subject to high centrifugal force such that the rotor construction has to restrain the magnets. This is achieved by constructing the rotor from mild steel or aluminium alloys and adding a back plate, thereby also adding weight to the machine. By reducing the size of the rotor (and magnets) and stator, much weight and centrifugal force is reduced to the extent that the rotor and stator can be constructed from plastics. For 3 phase machines, a back plate of either steel, non ferrous material, aluminium alloy or plastic composites are used, but are not required in small single phase machines.

Although much of the research in wind energy technology is still applied to 3 phase machines, there is a growing trend into novel single phase axial flux air core machines with

a flat geometry and compact construction. A multi-disc generator is the most common configuration in the literature. A single stator and double rotor has most research activity [72-75], with dual stator and dual or triple rotor also attracting interest [76], as magnets either side of a coil forms a flux path. A single stator and single rotor has been investigated [77], but is deemed to have the disadvantage of the magnets on the rotor producing attracting forces on the stator. By using small diameters for rotor, stator and magnet sizes, these attractive forces can be discarded.

In slotless and ironless machines, the air gap between magnet and coil is an important parameter. As the air gap is increased, a higher flux density is required to cross the gap, which entails a larger magnet. In a single stator single rotor machine, the air gap is as small as possible, allowing the magnet size to be reduced, thereby allowing a more compact construction of the generator.

The magnets used in all of the generator designs are NdFeB and either embedded within, or glued to the rotor [72, 73, 78]. The shape of the magnets utilised are varied, with the most common being a circular magnet. Other shapes are Rectangle, Bar, Trapezoid, Ring segments, Disc segments, Quadrants and Halbach arrays.

The shape of the coil windings are commonly Circle or Trapezoid, with U shaped, Wedge and PCBs (planar windings) also used. The circular or trapezoid coils are arranged as either overlapping, grouped or concentrated, in 3 phase machines and as concentrated coils for single phase machines. Concentrated coils have the same efficiency as overlapping coils, but use less copper. The coils are glued to the stator [72, 73, 79] using epoxy resin [73]. Generally, the coil does not have to be the same shape as the magnet, except, that a

trapezoid magnet is used with a trapezoid coil to achieve the best efficiency with this configuration.

The wire used for the coils are mostly single core copper wire or Litz wire. Single core wire with small diameter has a higher resistance than larger diameter wire (0.4mm (26 guage)). Litz wire is multi strand enamelled copper wire, used in high frequency applications (> 20 MHz) that would be subject to the skin effect when inducing a voltage. When calculating the cross sectional area of the wire, Litz wire requires approximately a 14% larger diameter to compensate for the multiple strands.

The magnets (rotor) and coils (stator) are arranged circumferentially [73, 75], with the magnets arranged with alternate North and South polarity and the coils wound alternately clockwise and counter-clockwise so that change of flux adds to the induced voltage.

2.2.8 Bluetooth

The research into the technical aspects of Bluetooth reported in the literature focuses mainly on optimising Bluetooth piconet and scatternet networks or optimising data transmission with regard to interference from other ISM band devices. The application of Bluetooth telemetry is mainly in medical and animal research, whilst automotive applications have been in infotainment, with only limited research into engine telemetry.

In order to reduce the size of devices the antenna is also required to be miniaturised. Research into replacing the dipole antenna with a microstrip on the PCB was undertaken by Luand and Coetzee [80], Vermeeren et al. [81] and Dou and Chia [82], with Jan and Kuo [83] improving the radiation pattern and bandwidth.

Bluetooth employs GFSK (Gaussian Frequency Shift Keying) signal transmission, whose optimisation was investigated by Tibenderana and Weiss [84] and Seshadri and Valenti [85] Feng et al. [86] explored the impact of interference from other devices on piconets.

Interference affects the transmission of data packets. Lindholm [87] analysed data packets over the transport link, Golmie et al. [88] employed packet scheduling, whilst Shih et al. [89] used adaptive packet selection (now called adaptive frequency hopping) to reduce the effects of interference.

The main reason for the use of Bluetooth in industry is to replace cables, but the main applications of Bluetooth is in the research areas of medical monitoring or remote monitoring of animals (Nagl et al. [90], Warren et al. [91]).

The Bluetooth standard evolves as technology progresses and this is illustrated by Wibree, consuming a small fraction of the battery power of Bluetooth 1.0 with a data rate of up to 1 Mbps. The Wibree standard has been renamed Bluetooth low power technology [92] with the aim of deploying this technology on a stand-alone chip.

2.2.9 ZigBee

Another class of wireless telemetry module operating in the ISM band is ZigBee, that sends small data packets at 250 Kbps [93] and is designed for low power to extend battery life for months or even years. Zigbee sensors can be configured in networks consisting of a few ‘motes’ to thousands of ‘motes’, employed in homes, buildings or industrial environments, Alves and Tovar [94]. Zigbee is also used in medical research or animal monitoring, Milenkovic et al. [45], Golmie and Matta [95], Valdastri et al. [56], Hsu et al. [96], Van Helleputte et al. [97] and Susilo et al. [98]. Other research investigated sensor networks,

Bellis et al. [99], and energy harvesting, Akyildiz et al. [100], as a feasible method to eliminate batteries .

2.2.10 Web Access

Metrilog developed a service for SCADA installations. The telemetry system uses wireless GPS, satellite, WAP or SMS connectivity to collect data from sensors. Data is sent as a WBXML file (Wireless Binary XML) using XML data transfer protocol and transmitted to a dedicated customer gateway on the Metrilog server, which is then made available over the internet via web application servers. With the wide spread use of Wi-Fi based devices, mobile telephony and internet in the form of smart phones and PDAs, data can be accessed from remote locations. Users outsource telemetry requirements to Metrilog which has the responsibility to keep servers running, thus the costs of the data centre, redundant servers, internet connection, maintenance and backup, etc. are covered amongst a large number of customers [101].

2.3 Summary

The use of thermocouples to obtain actual temperature from important locations in the piston and software to calculate coefficients of heat transfer enables better prediction of temperatures that contribute to better engine design compared to estimations based on past experience. Separate channels of thermocouple or thermistor data from various points in the piston are transferred at bottom dead centre of the rotational cycle, using polynomials for voltage to temperature conversion.

Various mechanical methods of telemetry from within the piston have been reported in the form of linkage, contact and inductance mechanisms. Wireless techniques have been in the

form of Infra Red (IR) and various radio frequencies. IR requires line of sight between a led and photo detector frequency to voltage and voltage to frequency conversion and calibration. RF carrier oscillator frequencies are changed by a change in capacitance by direct change in temperature, the pressure on a capacitive sensor, the resistance of a thermister changing capacitance or through resistance changing the current through a coil. The generated clock signal from induced carrier signal requires temperature drift compensation with the use of two lookup tables (one for cold junction compensation and one for temperature drift conversion). Electromagnetic methods have taken the form of machining the cylinder wall to accommodate alternating ferromagnetic and non ferromagnetic bands, machining slots that fluctuates the air gap between magnet and coil, or mounting a magnet inside the piston and a coil on the connection rod. Multiplexed - demultiplexed signals are transmitted to antenna coils located at oil pan. Wireless energy transfer compares the difference between energy transfer of high and low power applications employing inductive links.

Some wireless technologies are not suited for short distance telemetry such as wifi, wirelessLAN or GPS, but suitable technologies have focused on simple IR, Bluetooth or ZigBee. Telemetry is applied to many traditional and emerging disciplines as well as novel applications, with a large amount of short distance telemetry research into medical, animal, power generation. Most reported power transfer methods are via inductive links, but with Bluetooth, ZigBee, FSK, ICs, Asics and RF-FM coming to the fore as these technologies evolve. Power generation is between a primary coil to a secondary coil, a primary coil to an implanted secondary coil, on chip planar coil to external antenna or employing micro coils.

Mems research is into energy sources: microfuels, turbines, microbatteries, generators, energy harvesting and scavenging (thermal or vibration), and as MEMS becomes

established, an increase in complexity, multiple components, or ‘systems on a chip’ are researched. But these devices provide insufficient power to drive discrete components

Wind technology is at the forefront of axial flux research and eliminates the issues regarding three phase machines. With the use of single phase, a modular design and construction and flexibility on windings and magnets, a flat geometry of compact construction with minimum air gap, Nedfe magnets and concentrated coils, a circumferential arrangement adopted for the power generator.

Bluetooth technology is an established wireless cable replacement technology conforming to defined standards operating in the licence free 2.4 Ghz ISM band, utilising adaptive frequency hopping to eliminate interference from other devices, silicon oscillators to eliminate EMI and ceramic antennae to reduce size and costs. Networking research is mainly optimising piconets and scatternets. ZigBee is a low power, low data rate technology spending the majority of time in sleep mode. It can be configured in small or large networks and used mainly in medical or animal research, but not harsh environments.

Transmission problems encountered in the research include temperature dependant sensors or components that drive an oscillator or change the current through a coil. The temperature induced change in capacitance varies oscillator frequency, whereas temperature changes thermistor resistance, and thus the current through a coil. A RF receiver is required to detect these frequencies that represent temperature data values. An RF signal that generates a clock signal from carrier signal must also compensate for temperature drift of carrier signal and then use two lookup tables – one for carrier signal and one for temperature values. Infra red light pulses have to be aligned with ‘line of sight’ and require calibration of frequency to voltage and voltage to frequency conversions.

To overcome these problems, digital transmission is the preferred option. For short distance wireless telemetry that replaces cables and slip rings, Bluetooth is a robust digital data transfer method that has low power consumption, has continuous transmission and eliminates signal interference and EMI when used with a silicon oscillator.

ZigBee appears to be preferable because of lower power consumption, but if is switched on for the same amount of time as Bluetooth, then it would use the same amount of power, but still have a lower data transfer rate.

Traditional methods of telemetry in the research require post processing cold junction compensation processing on host, on host transmitted by RF signals that require calibration and conversion of data to temperature. For the proposed system thermocouples are connected to amplifier sensors that incorporate CJC to provide voltage values. The Bluetooth module then digitises the voltage values for wireless transmission by a Bluetooth radio to a host where they are displayed on a user interface. All the signal conditioning is performed on the sensors and requires no further calibration or conversion processing. The Bluetooth module is flexible and can be adapted to different applications by changing firmware. The firmware is uploaded wirelessly to the microcontroller so that engine parts do not need to be removed in order to update the unit.

Power generators in the research involve machining engine components, attaching magnets to pistons, aligning magnets and coils, use of mains supply or employ MEMs devices. One method is to machine the cylinder wall to create alternating ferromagnetic and non-ferromagnetic bands or machine grooves in the cylinder wall in order to fluctuate the air gap and attach magnets to the piston skirt base to sweep past the bands or grooves and induce a voltage. Another method is to embed magnets in the crankshaft counterweight and

attaching a coil bobbin to the connection rod arm. The size of the bobbin has depth in order to align to the magnets with sufficiently small air gap to induce required voltage. Other methods use the momentum of the piston to move an attached magnet relative to a coil, with some methods requiring 0 – 10v signal range plus positive and negative circuit supplies. All of these techniques have limited contact time and therefore a limited transmission time to transfer data to a receiver or host. For the methods that use the mains supply to drive the primary coils, there is a requirement to separate the high power supply from the system, more complex power regulation and loss of mobility. It is possible to use MEMS devices to generate a few mA of current, but at present, they cannot produce the power required for data transmission using the Toothpick module [102]. These voltage and high current demands make an alternative power source necessary, which takes the form of a power generator.

The proposed Power generator overcomes the preceding issues, using magnets, coils and flexibility in alignment with a compact unit attached to piston big end without component machining. Power is induced for whole of the rotational cycle, providing a continuous supply at variable rpm. The AC voltage is rectified to a low voltage DC output to meet the system 5v requirement.

3 Existing System

The existing Manner Sensortelemtrie system is investigated as a comparative system in order to understand the type of signal and signal levels produced. The existing telemetry system comprises of a bespoke thermocouple sensor that can multiplex multiple signals onto a RF carrier signal which is then transferred to a receiver via primary and secondary induction coils. The precisely located secondary coil transmits data to a de-multiplexor unit via a coaxial cable where it is converted to a voltage and then transferred to a host for conversion to temperatures using look up tables. Piston instrumentation explains why thermal distribution is important and the methods developed to produce a piston that can be tested with the proposed wireless telemetry system. The procedures are dimensional analysis to enable modelling of a piston, development of a machining process to position thermocouples and FEA to model a piston and determine the effects of temperature distribution and predict piston behaviour before a prototype is built.

3.1 Inductive telemetry system

A widely used induction telemetry system is developed by Manner Sensortelemtrie of Germany. A high voltage power supply (90V to 230V) transfers power and data through induction coils. The induction coil is attached to the piston and aligns with the stator coil at bottom dead centre, producing a small time window to transmit both power and FM

modulated data. The thermocouple data and control data signals are multiplexed for transmission by the sensor unit and de-multiplexed to individual 0 - 10V signals in an evaluation unit, which are then post processed for cold junction compensation on a PC host.

3.1.1 Thermocouple Telemetry Module

The existing telemetry system is an implementation of a Manner Sensortelemetrie 16 channel radio telemetry system which is specially developed for working in heavy or harsh environment conditions. It consists of a radio transmitter and miniaturized Sensor Signal Amplifier. Strain gauges, thermocouples and Resistive Thermal Devices can be directly interfaced with the Sensor Signal Amplifier. The signal from the transducer is digitized to a resolution of 12 bits for thermocouples or 16 bits for strain gauges. The digital data is FM-modulated on the RF carrier of 433/868 MHz, guaranteeing wireless transmitting over approximately 50 meters in free space. The system is available in single or multi channel versions of 2, 4, 8 or 16 channels. Every channel has a separate power supply, amplifier, analogue to digital converter and digital to analogue converter, with no crosstalk between channels. Figure 3.1 shows the energy and data flow between the sensor signal amplifier and receiver via the induction loop [103].

3.1.1.1 Signal acquisition

Up to twelve type K thermocouples are connected to the sensor input channels. The thermocouple signals, plus reference signals and internal chip temperature signals are also included in the signal acquisition. The sensor signals are fed through a multiplexor to a signal amplifier before being input to an analogue to digital converter [103].

3.1.1.2 Signal telemetry

Power is transmitted to the sensor amplifiers through the inductive coupler rotor and stator coil, and at the same time data is transmitted to the evaluation unit in the opposite direction. The multiplexed signals are transmitted to the evaluation unit by a single coaxial cable (Figure 3.2). The evaluation unit performs digital to analogue conversion before feeding the signal through the corresponding de-multiplexor where the individual signals are then made available on the appropriate output channel (Figure 3.2).

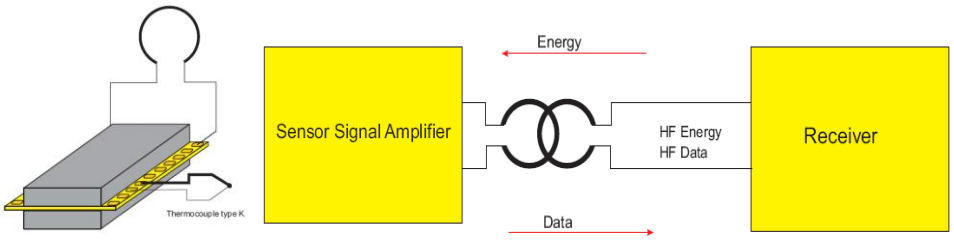

Figure 3.1 Energy and Data Transmission [103].

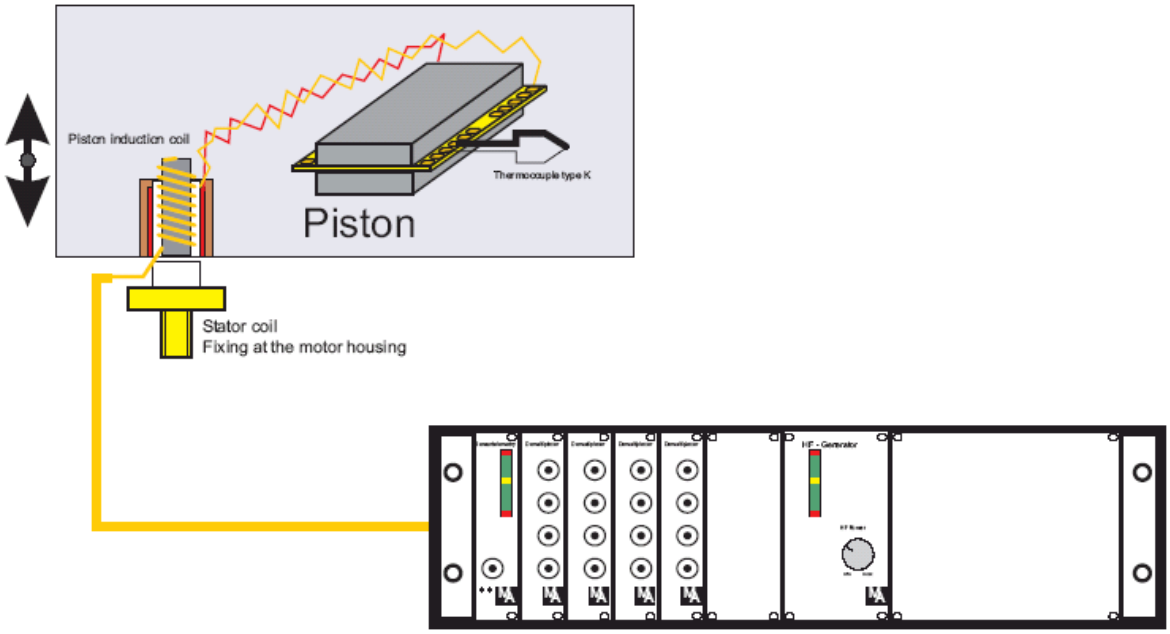

Figure 3.2 Measurement Configuration of the Manner Telemetry System [103].

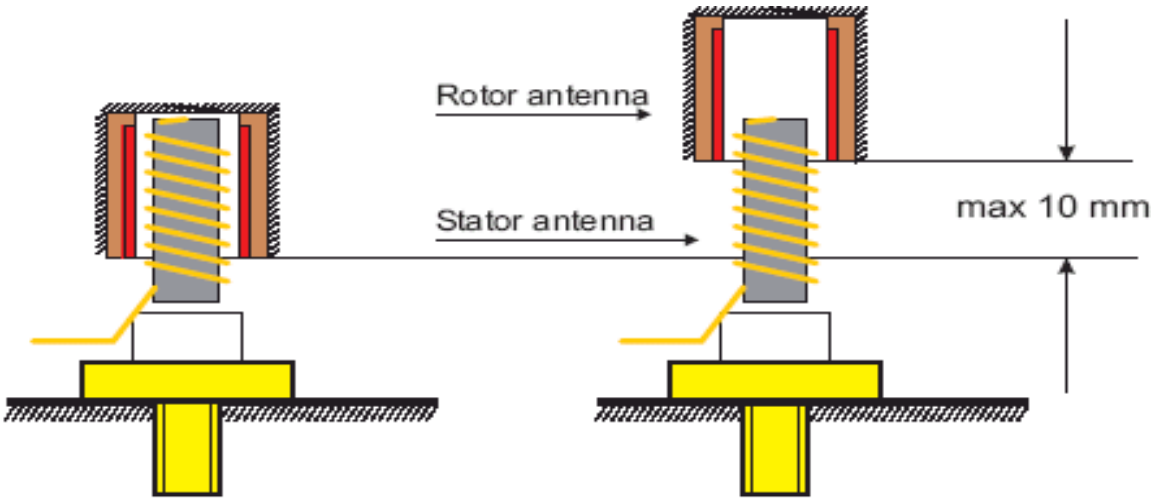

Figure 3.3 Contact Range of HF Coupling Area [103].

3.1.2 Sensors

Figure 3.3 shows the range of travel for the inductive coupling. The stator is stationary at a location below BDC of the piston, with the rotor travelling vertically from TDC to BDC. The range of vertical travel is 10 mm and care must be taken not to exceed this distance, as doing so may cause destruction of the coupling [103].

3.1.3 Evaluation Unit

The evaluation unit is a modular unit consisting of the telemetry receiver, four four-channel de-multiplexor units, a high frequency power generator and a high frequency power regulator. The output power of the high frequency generator can be adjusted to different voltage requirements and is set up as recommended by the setup procedure in order to achieve coupling at optimal level.

3.1.3.1 Signal Output

The telemetry signal can be checked at the 'Test Output' by connecting the signal sum output to an oscilloscope where a single phase signal, either positive or negative (Figure 3.4) of nearly constant amplitude should be observed. An example signal output is shown in Figure 3.5, and an example data output is shown in Figure 3.6.

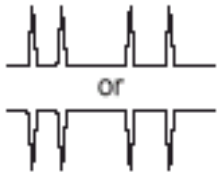

Figure 3.4 Test Output Signal at Evaluation Unit [103].

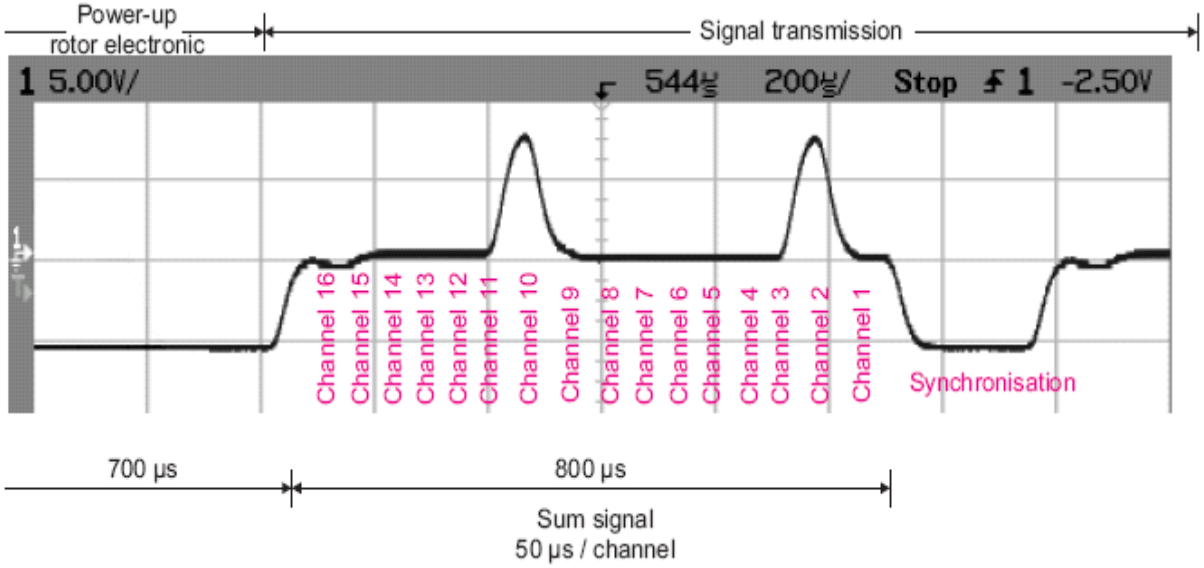

Figure 3.5 Adjustment to check the transmission [103].

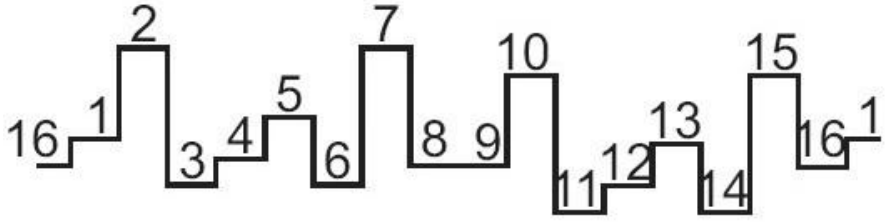

Figure 3.6 Example Data Output [103].

3.1.3.2 Thermocouple Positioning

The length of the thermocouple sheath for each hole should be approximately 75mm. The thermocouple tails are trimmed to suit the position of the allocated channel on the sensor, connect as per manual and soldered using high temperature solder and that the thermocouple wires be connected to the correct terminals, as permanent damage will occur if incorrectly connected (Figure 3.7).

Figure 3.7 Thermocouple Locations [13].

3.1.3.3 Sensor Chip Location

The sensor has a maximum functional ambient temperature of 180°C and should be positioned on the piston where the temperature is the lowest. Usually the best location for automotive applications is on the pin boss. Care must be taken to ensure that the crankshaft does not impede on the sensor, and to this end, the piston is machined on the lower face of the bosses to increase the clearance between the sensor and the rotating components (Figure

3.8). The sensor is attached to the piston by a bracket and adhesive, and allowing for a thin vibration isolating layer, is held in place with fixing screws [104].

3.1.3.4 Rotor and Stator Antenna Location

The stator (male) coil is mounted on a rigid bracket attached to the engine block and the rotor (female) coil is attached to the piston and should mate with the stator male coil at bottom dead centre (Figure 3.9) and located in the engine where it is not necessary to modify the crankshaft.

Figure 3.8 Location of components [104].

It is important that the overlap of the two coils is sufficient to enable power and data transmission for all channels to take place. Calculations are taken from the manual [104].

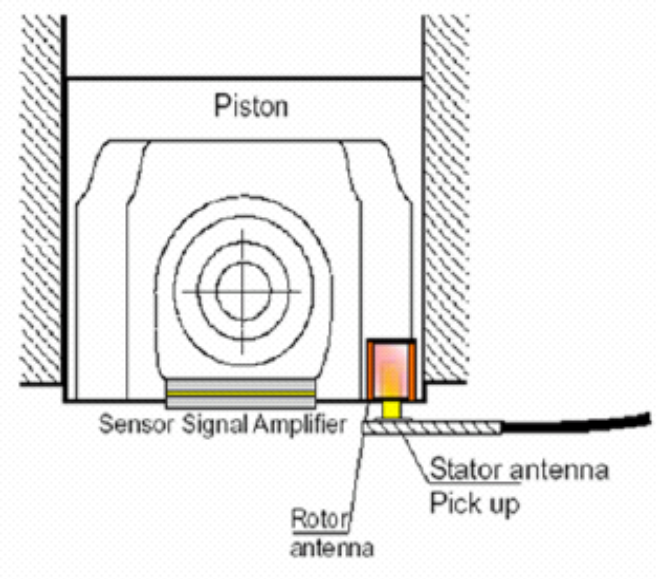

Figure 3.9 Moving Coil Induction [104].

3.1.4 Signal Transmission Time

Signal transmission time does not occur for the full rotation cycle of the piston. The calculation of signal transmission time for a 10 mm antenna and maximum rotational speed for transmission of all acquired data is shown in figure 3.10.

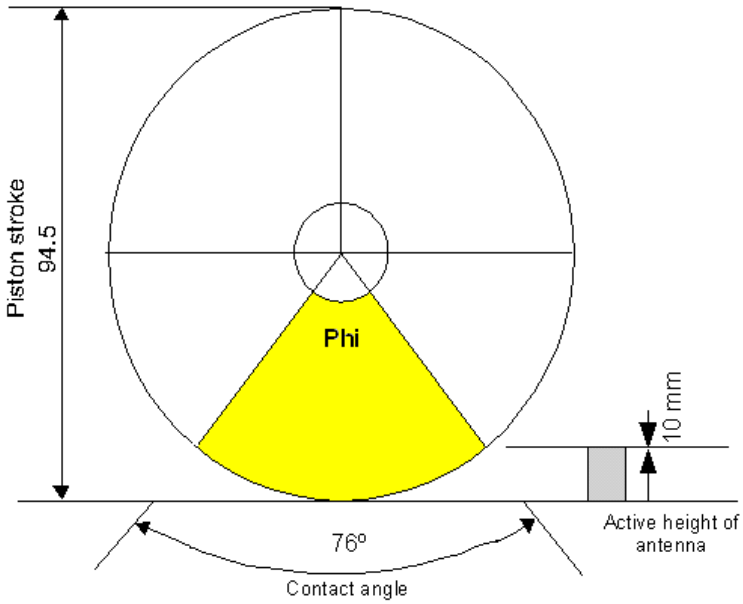

Figure 3.10 Angle of Transmission [104]

Calculating the angle:

$$\text{Phi} = 2 * \arccos\left(\frac{\text{piston stroke} / 2 - \text{active height of antenna}}{\text{Piston stroke} / 2}\right)$$

$$2 * \arccos((94.5 / 2 - 10) / (94.5 / 2))$$

$$= 75.9°$$

Calculating maximum rotational speed:

Minimum contact time	1.5 sec
RPM	60 / 'minimum contact time' * Phi / 360°
	= 60 / 1.5 * Phi / 360°
	= 8472 rpm

Calculating contact time and number of transmissions:

Synchronization time:	0.3 sec

Maximum rotational speed: 5500 rpm

Contact time: 60 / ‘rpm’ * Phi / 360°

= 60 / 5500 * 75.9 / 360°

= 2.3 ms

= minimum 1 transmission time

Two transmissions at: 4860 rpm

.

3.1.5 Temperature Lookup Table procedure

In order to obtain the thermocouple temperatures, the outputs from the evaluation unit must be read and post processing applied in the form of cold junction compensation using the internal temperature of the sensor and the provided lookup tables from www.sensortelemtrie.de (Table 3.1). Output from the evaluation unit is connected to a data acquisition unit and then input to a host PC, where the temperature for each thermocouple is calculated using bespoke client software.

Table 3.1 Lookup table for existing system telemetry signal outputs.

	Values from chart supplied by Manner								
chip mv	428	706	963	1388	1643	1824	1995	2231	2531
Chip temp	20	85	100	125	140	150	160	170	180
t/c temp									
50	149	172	174	165	169	233	317	433	627
100	1011	1034	1036	1029	1030	1093	1180	1294	1485
150	1860	1884	1886	1879	1880	1942	2027	2138	2322
200	2694	2718	2720	2714	2715	2777	2880	2970	3150
250	3537	3580	3561	3557	3557	3619	3692	3805	3987
300	4391	4418	4416	4411	4410	4473	4551	4661	4838
350	5261	5286	5285	5285	5279	5344	5421	5528	5702

The ambient temperature region of interest is 140°C - 180°C and the chip reference voltage must be 7V for the data to be valid. Channel 1 is the chip temperature measured in millivolts, Channel 2 is the 7v reference voltage and Channels 3 to 8 are thermocouple output voltages, measured in millivolts.

The procedure to find the thermocouple temperature is:

a) If channel 2 reference voltage is 7V, then continue reading data.
b) Read channel 1 and locate chip temperature voltage (mV) in the table, where corresponding column gives chip temperature and thus the voltage column to read.
c) Use linear interpolation if chip temperature voltage between two values. In the determined voltage column, find position of thermocouple voltage.
d) The thermocouple temperature is the corresponding index position of the thermocouple voltage index position.

3.2 Piston Instrumentation

The piston and piston structure is described and an explanation is given of a prototype piston development, including dimensional analysis and the machining process, and is followed by an explanation of how components are optimised through the use of finite element analysis and CAD software.

3.2.1 Piston

Increased performance and efficiency, to yield lower fuel consumption, is the source of thermal loading in engine's components. As a result pistons, cylinders, and rings become subject to raised temperatures during engine operation and their integrity is critically

affected and problems to other components and systems may be induced, such as crankshaft and connecting rod assembly, or inefficient lubrication system due to overheated oil.

The piston is the most important component of an internal combustion engine and analysis is performed to provide the necessary information concerning durability and performance efficiency. The two main problems in piston design of a suitable crown are to conduct heat from the combustion chamber to the piston wall and to transfer the thrust of the gas load to the piston bosses and hence to the connecting rod.

Prolonged absorption of excessive heat may cause a permanent molecular change in the piston material, eventually leading to piston failure and volume change of materials have a negative influence on engine performance, reducing power output of the engine.

Piston temperature distribution is the main concern in piston development and it is necessary to prepare pistons for measurements of the temperature difference at various locations.

The piston is a hollow cylinder, closed on the top crown and open at bottom and made from aluminium or iron. It fits closely within the engine cylinder with a small clearance, allowing it to be driven alternatively up and down in the cylinder. The task of the piston is to assist in burning fuel efficiently, transmit power to the crankcase and seal the engine cylinder. The shape of the piston crown increases the gas turbulence and compression ratio inside the cylinder to achieve a better fuel burn. In the engine combustion chamber, when the air-fuel mixture is burned, high pressure acts on the piston head forcing it to move downwards, transferring energy through the connecting rod, resulting in rotational movement of the crankshaft.

The upward movement of the piston results in an increase of pressure and temperature inside the cylinder, with the piston absorbing a high amount of energy in the form of pressure, heat and kinetic energy and therefore it is very important to build a piston to sustain these forms of energy and transfer the energy with minimum losses.

The high and rapid temperature changes inside the combustion chamber cause uneven thermal distribution and therefore uneven expansion of the piston and cylinder. For this reason, piston's rings are in contact with the cylinder wall and used to seal the area between the combustion chamber and the crankcase.

Analysis is performed to create the piston from appropriate material and in the optimum shape. Piston temperature data is measured and used as initial data values for analysis of the temperature distribution for piston design.

Thermocouples are located at positions of high importance (Figure 3.11), which are: top piston land, piston bowl as this creates high turbulent flow in order to assist the combustion process, behind the ring grooves and possibly at the piston skirt as this has the larger contact area with cylinder walls where heat can be transferred to the cooling system.

CAD is extensively used to design, develop and optimize products and components to enable accurate machining and repeatability for the overall process. It has the important benefits of lower product development costs and shortened design cycle, since CAD enables designers to develop virtual designs where flaws can be identified before proceeding to manufacturing process.

3.2.2 Piston Structure

Figure 3.12 shows the structure of a Diesel piston. High gas pressures and inertia forces act on the piston head, the piston pin and the piston grooves. These parts of the piston must be designed to operate under these conditions without failures.

3.2.2.1 Piston Head

An important design measure is the thickness of the piston's head. It is to the piston crown that maximum load is applied and it sustains the maximum pressure and temperature through all stages of the combustion. The demand of higher compression engines has made it necessary to reduce the clearance volume by shaping the piston head for adequate valve clearance when the piston is at TDC and for increased turbulence. The maximum pressure at all the stages must be known in order to calculate the appropriate head thickness of the piston.

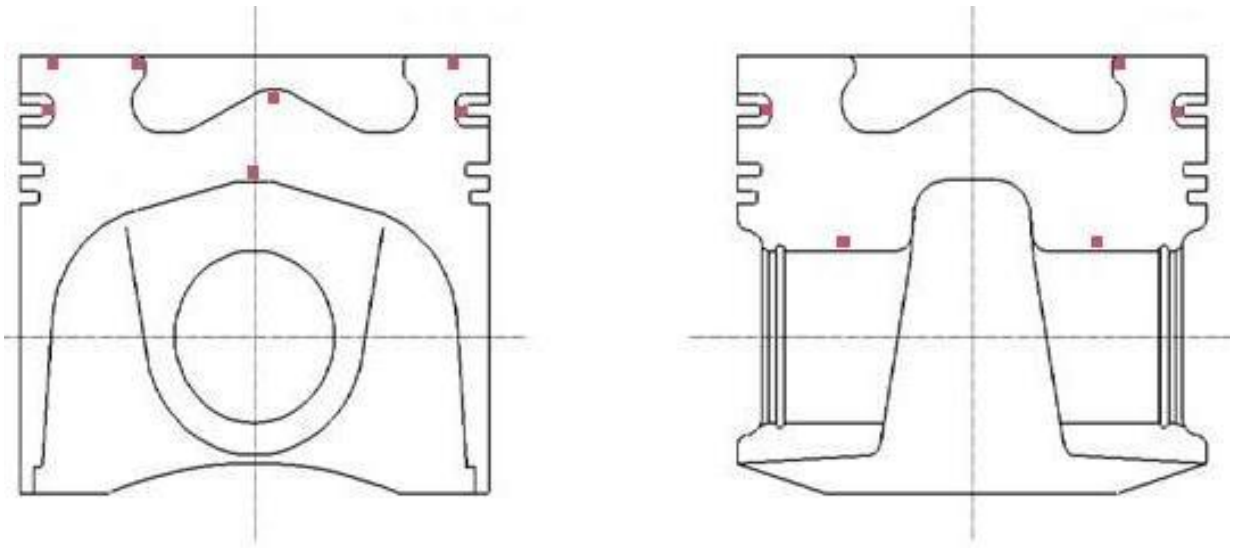

Figure 3.11 Locations of thermocouple tip (red dots) for diesel piston

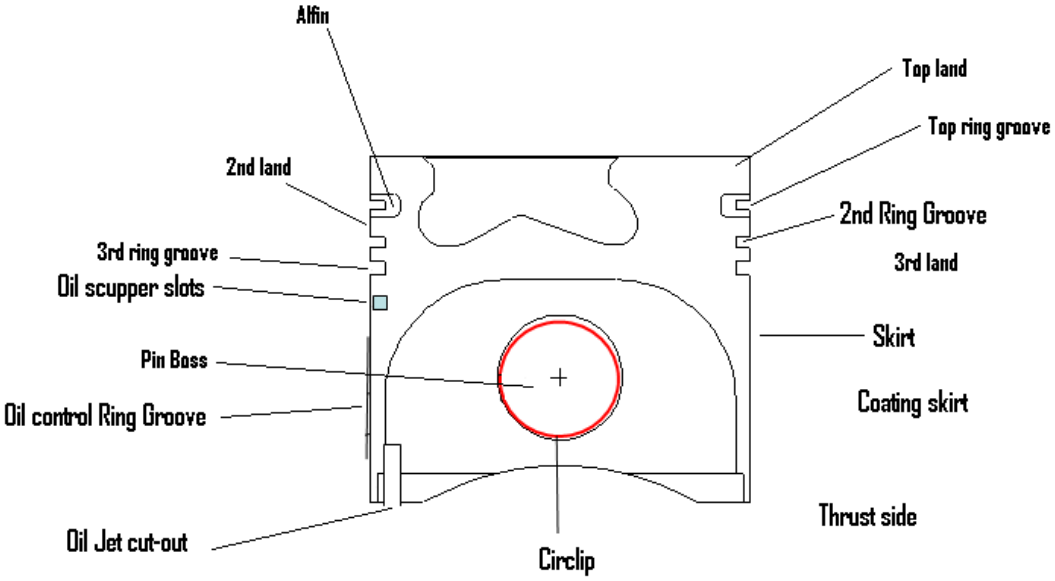

Figure 3.12 Detail of Diesel Piston

Another design aspect is the running temperature of the piston with respect to the piston skirt. If the piston head runs too cool with respect to skirt, thermal efficiency will be reduced due to heat loss through the piston, and the chilling effect of the cold metal on the combustion process will increase the percentage of unburned gasoline escaping in the exhaust gas. If the piston head runs too hot with respect to skirt, surface ignition could result, with related engine roughness and shorter piston life. The piston skirt must run comparatively cool to avoid increased expansion due to the temperature increase.

3.2.2.2 Piston Boss/Pin Boss

The pin boss is responsible for delivering the pressure applied on the piston head to the connecting rod and crankshaft (Figure 3.13). The pin must not cause any deformation at maximum pressure. It is designed to minimum dimensions to reduce weight.

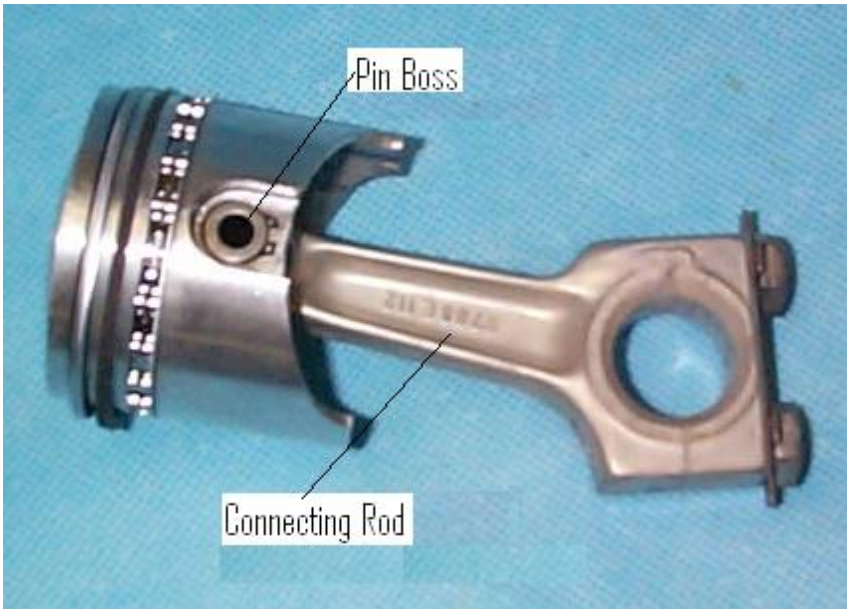

Figure 3.13 Piston, Pin Boss and Connecting Rod.

3.2.2.3 Piston Rings/Groove

The piston rings (Figure 3.14) form a seal between the piston and cylinder wall. Most automotives pistons have 3 piston rings, two for compression sealing and a third for oil sealing.

Compression rings stop gases escaping through to the crankcase, and the oil seal scrapes off excess oil and returning it to the crankcase, leaving only enough oil on the cylinder walls to provide piston and ring lubrication.

3.2.2.4 Cylinder Walls

The cylinder walls are cooled by circulating water in the water jackets, and this cooling effect is carried through the rings by transferring heat from the piston to the cylinder walls.

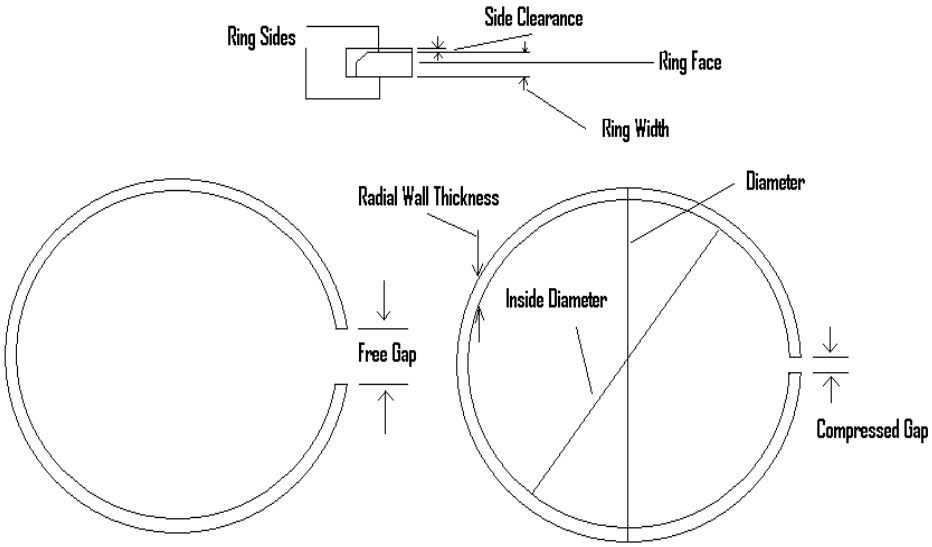

Figure 3.14 Piston Ring Parameters.

3.2.3 Piston Materials

The materials used for piston production is very important in maintaining the engine performance over a long period of time, and the piston operating conditions influence the material used.

One very important factor that has to be considered is the specific weight of the piston. Forces acting on the piston would produce minimum kinetic energy if the piston had relative high specific weight. In order to minimize these inertia forces, and so have better transformation of chemical to kinetic energy, the specific weight of the piston must not exceed specific values. In recent years aluminium is used in piston production, having half specific weight than iron pistons. Aluminium pistons can be either cast or forged and must be heat treated.

The numbers in Figure 3.15 indicate piston temperature values at various points, and Table 3.2 lists approximate temperatures in °C at these points for cast and forged aluminium.

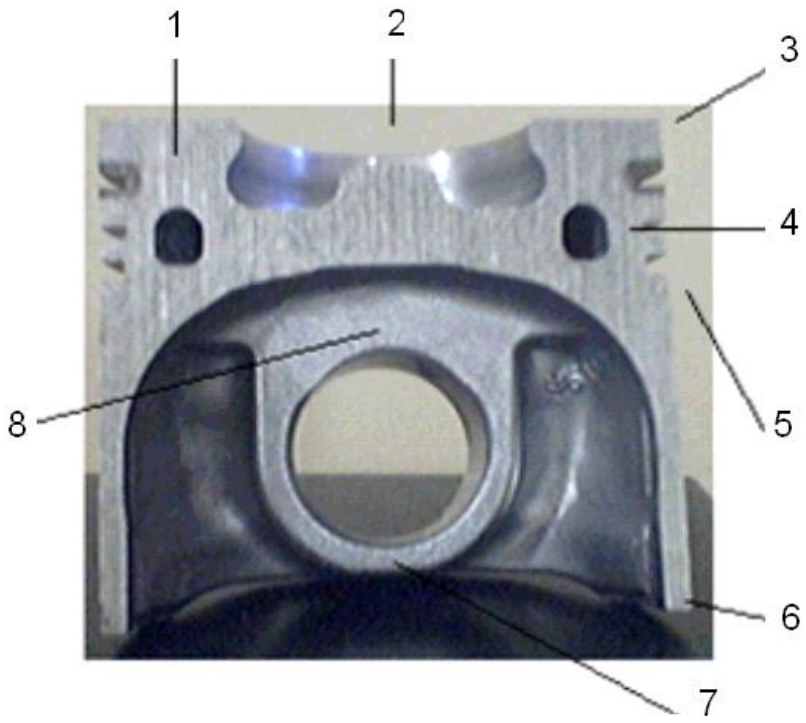

Figure 3.15 Important temperature locations on piston.

Table 3.2 Temperature values at piston locations

Operating Temperature for Aluminium Piston		
	Cast	**Forged**
1	290ºC	230ºC
2	260ºC	220ºC
3	230ºC	210ºC
4	180ºC	150ºC
5	150ºC	120ºC
6	95ºC	90ºC
7	135ºC	150ºC
8	175ºC	190ºC

Another aspect that must be taken into account is the thermal expansion of the piston and cylinder. To ensure the clearance between the alloy piston and cast iron cylinder will remain as small as possible during the entire thermal range of engine operation, the thermal coefficient of expansion of the material properties must be as close as possible. The thermal

coefficient of expansion of the grey cast iron cylinder wall is approx 9 x 10^{-6} m/m x K and for the aluminium piston is 24 x 10^{-6} m/m K. To make the thermal coefficients of expansion as close as possible, iron or silicon inserts, being harder than aluminium, are manufactured into the piston surface.

3.2.4 Dimensional Analysis of the Piston

The dimensions of the piston are of high importance, especially when it has a complex design, such as a diesel engine piston. Therefore the accuracy of the measuring method has to be considered with regards to other factors such as time consumption and complexity of available methods.

The measurement of piston dimensions could be performed using one of four methods: Employing vernier callipers or gauges, use of a photocopier machine or a pc scanner to scan the piston, use of a laser scanner to produce piston drawings and finally the use of a Coordinate Measuring Machine.

Vernier callipers and feeler gauges are limited to basic dimensions of the piston, such as diameter and height and ring gaps width. Other measurement methods are utilised for complex surfaces of the piston. With a piston divided into two halves, cleaned and a matt finish applied to the surfaces to eliminate reflection, it is possible to take an image of the piston section and print onto a piece of paper, or laser scanned onto graph paper. This image then represents the most important information of the piston for drilling the thermocouple holes. The disadvantages of this photocopying are accuracy, orientation, scaling, and measurement of printed images and although scanning had high detail for cylindrical and relief objects, both of these processes can be inefficient and time consuming. A coordinate-measuring machine is a mechanical system that moves a

measuring probe over a surface to determine the coordinate points on a work piece, but even with the finest probes, the complex geometry of the piston bowl could not be represented.

Measuring the external geometry with Vernier callipers is the fastest, simplest and accurate method to create drawings so that drilling is carried out with reference to the external dimensions of the piston.

3.2.5 Prototype Piston Development

To measure the temperature inside the cylinder at the piston's crown surface and at other important areas like the piston ring grooves and pin holes, a number of sensors are used to measure the temperature at these different points. Because of the rapid change of the high temperatures and the uneven distribution of heat, the installation of the sensors become a very important task and requires some modification to the piston in order to install properly and is achieved by drilling a number of holes in the piston where thermocouples will be placed. Figure 3.16 shows the position of the holes at the measurement points and angles from the vertical or horizontal axis in the experiment piston.

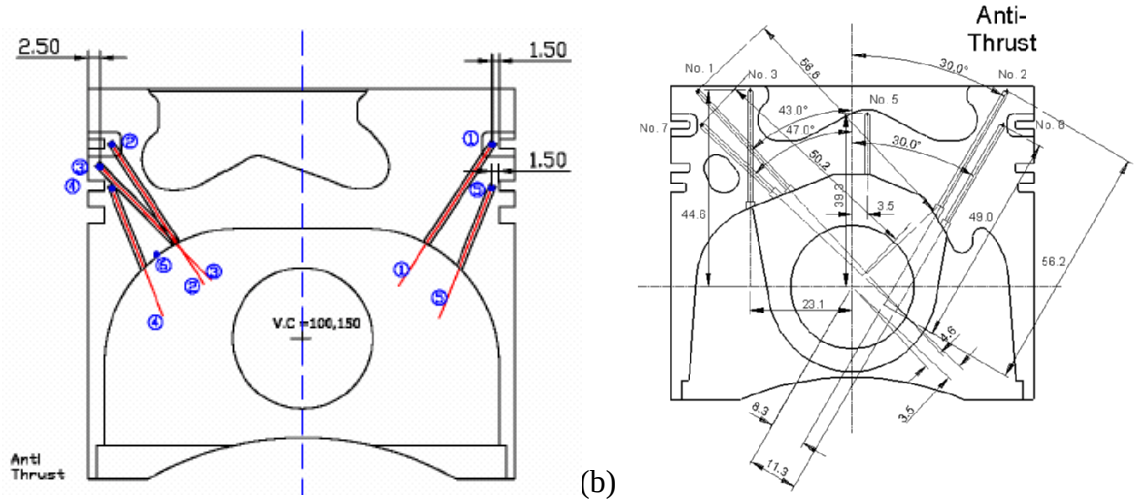

Figure 3.16 Drill locations for thermocouple installation.

To avoid experimental errors on aluminium production pistons, it is practical to design work holding arrangements, drilling processes and CNC code development utilising a prototype ‘dummy’ piston manufactured from inexpensive material with good machining properties. An acrylic piston (Figure 3.17) identical to a 3-D CAD model designed in I-DEAS software was manufactured and optimised CNC code was created for machining on a vertical CNC milling centre. A full size acrylic piston is then manufactured and all the required drilling performed until the complete procedure is correct. When the CNC code is satisfactory, the prototype development piston is drilled and instrumented.

Figure 3.17 Manufacturing the acrylic block.

3.2.6 Machining Process

An adapter was manufactured to hold the piston on a 4-axis CNC machine and dial gauges were used to ensure levelness of the adaptor and to ascertain the alignment and centreline and reference plane of the piston (Figure 3.18).

Figure 3.18 Machining of the Prototype acrylic piston block.

For the selected thermocouple type, the smaller the thermocouple diameter, the less effect it has on the piston integrity, but the more difficult it is to drill the holes. The drill holes of 1.2 mm diameter are 0.2mm greater that the 1 mm diameter of the thermocouple, and drilled to a distance of 0.5 mm from the piston surface or desired sensor location and because of the complex shape of the piston, flat spots are milled on rounded surfaces to aid drilling (Figure 3.19 (a)). A problem encountered was blocking of the drill flute and broken drills, and therefore a new drill was used for each hole. Initially, the process was to drill a hole, then machine a cut away on the piston to determine the accuracy of the drilling, then repeating the process for each hole. It is not an easy task to remove the piston from its fixture when one hole was drilled, cut away the material and then re-align the piston back onto the fixture. As a result, all the holes were drilled in one machining process and then examined for accuracy (Figure 3.19 (b)).

(a)

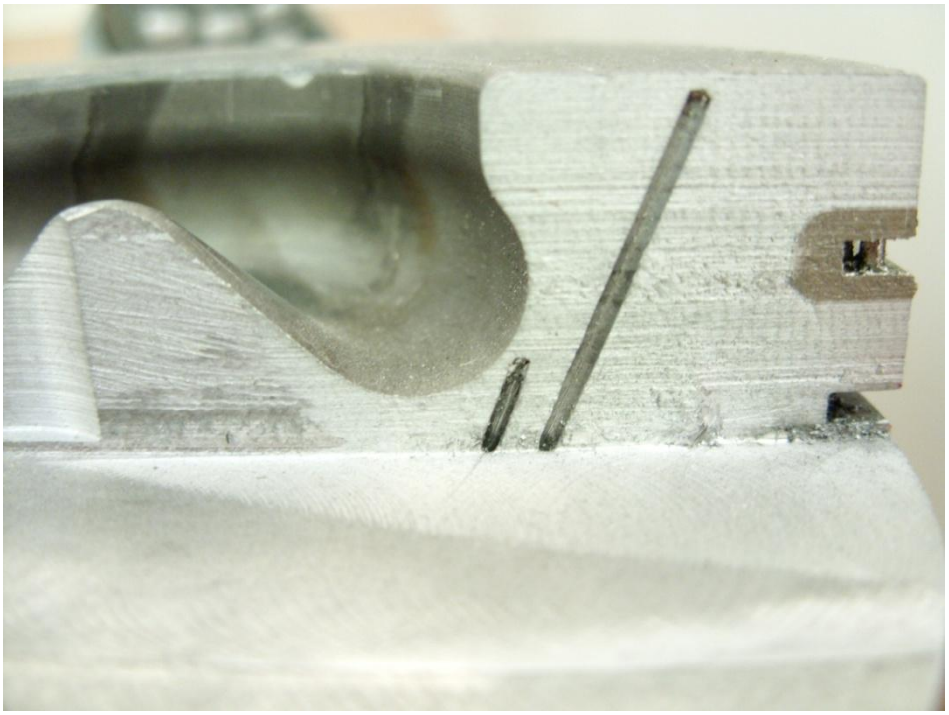

(b)

Figure 3.19 Flat spots at drill positions (a) and cut away of drilled aluminium piston (b)

3.2.7 Finite Element Analysis of Temperature Distribution

In order to analyse a piston, a method is required to calculate the temperature distribution of the piston. This method is known as Finite Element Analysis and is a technique used for analytical solution to any complicated mathematical formulation problem. The main concept is that a structure is divided into a number of elements, called finite elements. These elements are connected to each other with joins called nodes and have boundary conditions imposed. The properties of the elements and nodes describe the structure. Equations for the entire structure are then obtained by combining the equations of each element and node.

3.2.7.1 Important Piston parameters for FEA

To use FEA, and obtain the temperature distribution, it is necessary to know some important values. These are the dimensions (3D structure) of the piston structure, the density, thermal expansion, thermal conductivity and heat transfer coefficient of the piston material. Of the three modes of heat transfer (conduction, radiation and convection), it is convection that expresses the thermal distribution energy exchange on a piston.

As the piston moves inside the cylinder, the temperature of the surrounding fluids causes energy transfer between the piston and surroundings. The piston is influenced mainly by three different heat sources: gases, water and oil (Figure 3.20).

As these three sources influence the temperature and temperature distribution of the piston, then for analysis it is necessary to know the temperature of the surrounding heat source and the heat flow coefficient. The heat transfer coefficient depends on the geometric parameters of the engine and piston speed and the main problem with calculating the heat flow

coefficient is that these coefficients vary from top to bottom and at the sides of the piston, due to the change of gas temperature inside the cylinder. Assumptions are made for gas temperature of 1000 ºC at piston head, water temperature of 85 ºC at piston skirt and oil temperature of 70 ºC at bottom of piston [13].

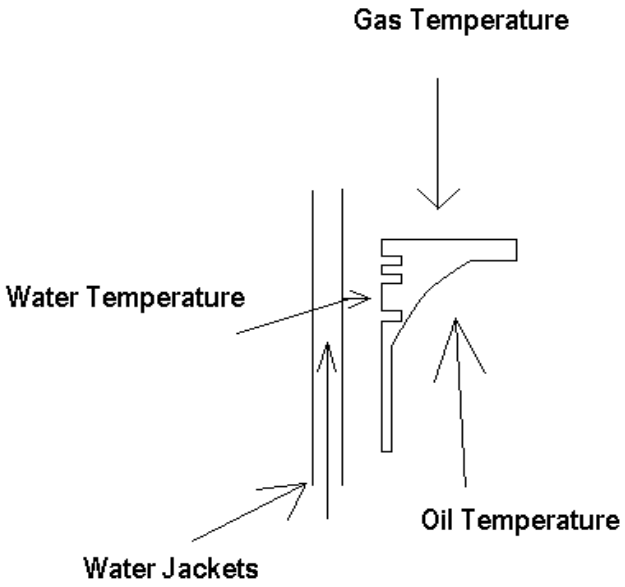

Figure 3.20 Heat transfer to piston

3.2.7.2 FEA Procedure

The steps involved in applying FEA applications are:

- Build the model with all the required dimensions of the piston.
- Mesh the model with a high number of elements for high precision.
- Apply boundary conditions.
- Simulate the model.
- Collect the solved temperature distribution data from the simulation.

3.2.7.2.1 Model the Piston

The structure of the piston is defined as a 3D model. Analysis of models is very computer intensive and complex models take a long time to solve. But if the model is symmetrical, then a smaller section can be solved, thereby reducing computing time (Figure 3.21 (a)).

3.2.7.2.2 Mesh the model

After the piston model is defined, a mesh is applied, comprising of a large number of elements and nodes (Figure 3.21 (b)).

(a) 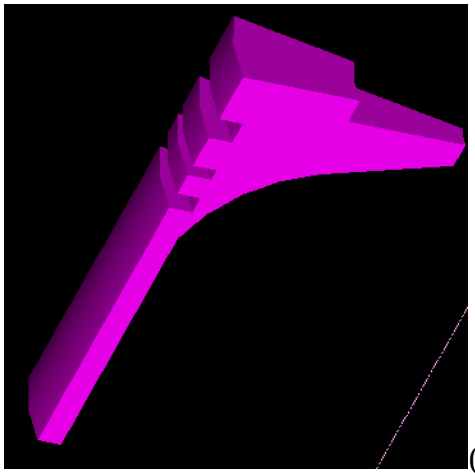 (b) 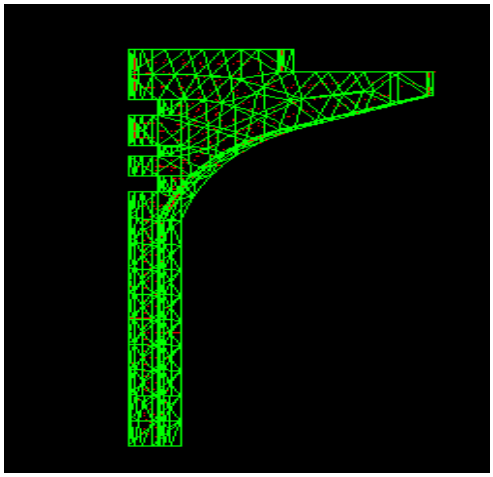

Figure 3.21 A Simple Model of Piston Section (a) and Section Mesh (b) [13].

The size of the elements can be specified by the user which allows for small element size at points of interest and large element size at areas of similar value. The larger the number of nodes, the more time is required for the simulation. After defining the mesh size, boundary conditions - properties externally imposed on the system to be analysed, are defined.

3.2.7.2.3 Simulation of the Model

There are two methods of analysis when using FEA software: theoretical analysis or real analysis. Theoretical analysis uses assumed data values as initial values for the model, whereas real analysis uses real temperature data values as initial values for the model. To be able to do this analysis to a high degree of accuracy it is important to have some points of real temperature measurements that will act as initial points in real time. After applying the necessary boundary conditions to the model, the simulation creates a set of solutions according to the information provided.

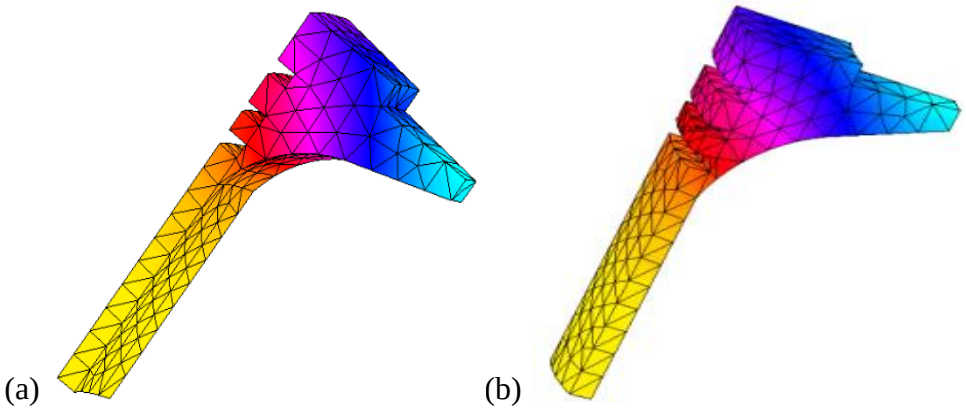

Figure 3.22 Simulation result for cast iron (a) and aluminium (b) piston.

From the analysis (Figure 3.22) it can be seen where the high temperature values are distributed on piston. This type of analysis is used by engineers to determine where alterations are required to optimise the piston shape. By using different material with the same boundary conditions it is possible to rerun the analysis of the temperature distribution on the piston and show the differences that may occur.

By comparing the results from the two analyses that were made it can be seen that the areas of temperature importance are the same. The difference that occur are due to the use of

different materials and the temperature range at those points. In Figure 6.12, the temperature range of a cast iron piston (a) is between 91.7 ºC and 313 ºC and the temperature range of an aluminium piston with some iron inserts (b) is between 84.4 ºC and 275 ºC. There is a difference of 38 ºC at the high temperature points and a difference of 7.2 ºC at low temperature areas.

By applying analysis to a full 3D model of the piston, engineers can view the thermal distribution over the whole piston and thereby predict the temperature distribution of various configurations of piston and design the optimum shape (Figure 3. 23).

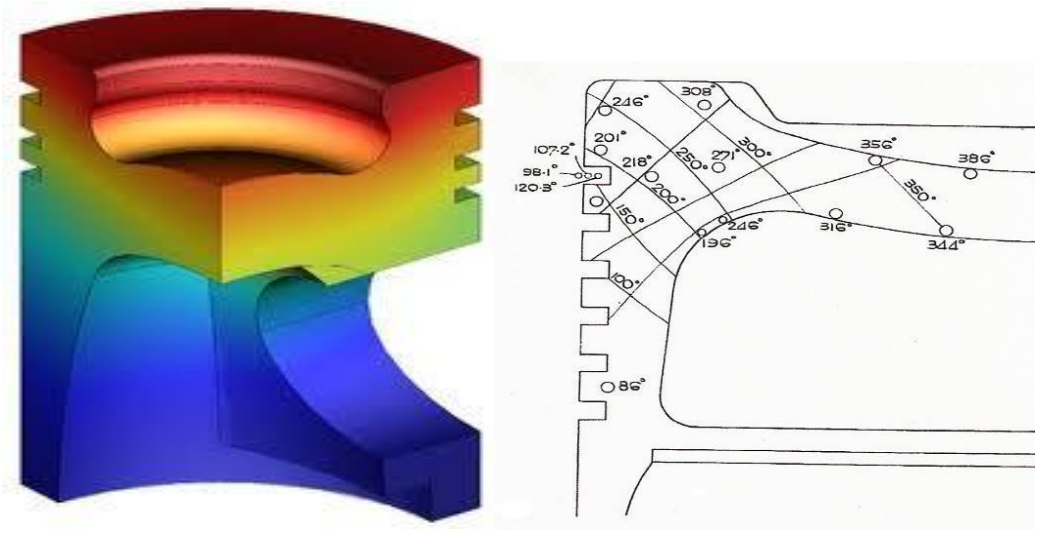

Figure 3.23 Temperature distribution zones on the piston crown.

3.3 Summary

This chapter describes the main issues regarding the existing system that are required to be overcome with the prototype system.

A bespoke sensor includes a 7v signal pin to confirm data validity. Therefore the proposed system must be able to detect a 7v signal, but this is beyond the aim of using low power

and low voltage electronics. An induction stator and rotor require precise alignment and have limited contact time and thus limited transmission time, and the higher the engine speed, the lower the transmission time available to transfer data. A coaxial cable transfers power and data concurrently, but should be separated, therefore this telemetry system needs to be located adjacent to an engine under test. A mains powered evaluation unit has a setup procedure including HF energy regulation that must be within a specific range, otherwise it will be too powerful for the telemetry unit. The acquired signals are subject to multiple stages of signal processing including multiplexing, de-multiplexing to produce 0 -10v data, and cold junction compensation on a host PC. The proposed aim is to substitute the cable with a wireless data link and the mains supply with an independent power supply.

Piston instrumentation explains why temperature thermal distribution is the data to be acquired and the methods developed to produce a piston that can be tested with the proposed wireless telemetry system. The methods are: dimensional analysis to enable modelling of a piston, development of a machining process to position thermocouples and FEA to model a piston and determine the effects of temperature distribution.

4 Proposed System

A new system is proposed that is different from the existing system by employing wireless telemetry transmission on a license free frequency, providing continuous transmission of digital data and eliminating multiple data processing and conversions. Power for the system is from an independent power generator providing power for the full rotation of the piston. Connection to a host is via a USB adapter. Thus is reduced the amount of data processing of the existing system and the elimination of cabling and induction coil issues.

Bluetooth wireless technology can be employed as a serial cable replacement technology to simplify connection to other devices and to eliminate the electrical interference. The Bluetooth stack is a set of protocols, profiles and services required to establish a connection to another device and with lower power requirements reduce the size of the proposed power generator and thus lower costs. It has robust digital data transfer and uses standard protocols to maintain links and data transfer.

Thermocouples are the most widely used temperature sensor and their use simplifies signal processing required for voltage conversion. Characteristics of the thermocouple are provision of a low voltage output that corresponds to temperature, but the non linear output voltage requires conversion by either look up tables or polynomial equations.

4.1 Bluetooth transmission

The Bluetooth stack implements the Bluetooth protocol and has two functions: control of the Bluetooth device and communication with other Bluetooth devices [105]. The Bluetooth device attempts to establish a connection with other devices within the transmission range. If successful, information is exchanged on functionality (services), behaviour (profiles), the communication protocol and any security required for data transfer. For successful data transmission, the Bluetooth radio adheres to the specified standards and is optimized for physical size and power by design of the antenna and employment of a transmission technique that reduces or eliminates interference from other devices. A Bluetooth module requires a constant power source because loss of power or moving out of range closes a connection. Power-up or re-entering within range requires a new discovery and connection procedure, which takes seconds to accomplish due to the Bluetooth connection protocol. A device may be put into sleep mode but still requires a valid connection for the time a wake message is sent. Power consumption is minimised if a device is entered into sleep, but will consume maximum power when in active mode and transmitting data.

4.1.1 Bluetooth Stack

A stack is a layered set of functional units implementing a protocol. Each layer has clearly defined duties and responsibilities, and clearly defined interfaces to adjacent layers in the protocol stack [106].

Because the Bluetooth radio is part of a mobile device, a Bluetooth device must be able to dynamically locate other devices within its transmission area and to determine which services are available [107]. In the discovery process, the Bluetooth device finds the other

devices in the area. In the service discovery process, the Bluetooth device determines which services the other devices have running on them.

The discovery process is known as an inquiry. When a device issues an inquiry, other devices respond with their Bluetooth address, a 6 byte ID assigned by manufacturer, and a class device record, which describes the type of device and gives a general indication as to services available.

A Bluetooth device may be discovered by one of four methods:

(1) Inquiry. A Bluetooth device transmits inquiry messages to find other devices within range of its radio. Devices scanning for inquiries reply with the information needed to make a connection [106].
(2) Cache. Devices found by previous inquiry. [107].
(3) Pre-known. A register of pre-known devices with which the device can connect to immediately without having to issue an inquiry message [107].
(4) Trusted. A device which is paired with another device and is explicitly marked as trusted in a security database [106].

4.1.1.1 Service discovery

Services are tasks the Bluetooth device can perform. The Bluetooth Special Interest Group [108] describe standard services such as: LAN access services, File Transfer services, Printing services, custom services, etc, which are identified by Bluetooth Assigned Numbers.

4.1.1.2 Protocols

A communication protocol is a set of rules for how devices should behave towards one another when communicating. It is essential that devices follow the same protocol [106].

Specific protocols are defined depending on the task to be performed such as: data transfer, audio transmission, or internet data transfer. New protocols may be defined by building on top of existing protocols. Apart from data encapsulation and audio / video transfer, there are three major protocols used by Bluetooth, implementing the three most common methods of data transfer [107]:

- Logical Link Control and Adaptation protocol (L2CAP) packet transfer
- RFCOMM data streaming
- Object Exchange (OBEX) object exchange

L2CAP exchanges data packets between the protocol upper layers and the Bluetooth radio. RFCOMM provides serial port emulation services that use the serial interface. OBEX transfers data objects between devices. OBEX is built on RFCOMM but is not specific to Bluetooth (Figure 4.1). It can be implemented on any transport method such as IrDA, TCP/IP, etc.

4.1.1.3 Profiles

A profile is a set of rules for how a device uses the Bluetooth stack [106]. It describes how applications are to use the Bluetooth stack and defines standard ways of using selected protocols and protocol features [107]. Every profile depends on the Generic Access Profile which defines the generic procedures related to establishing connections between two devices. There are three transport profiles: Serial Port Profile (SPP), Service Discovery

Application Profile (SDAP), and the Generic Object Exchange Profile (GOEP), which are designed to be building blocks, with higher level application profiles being dependant on the functionality of lower level transport profiles [107].

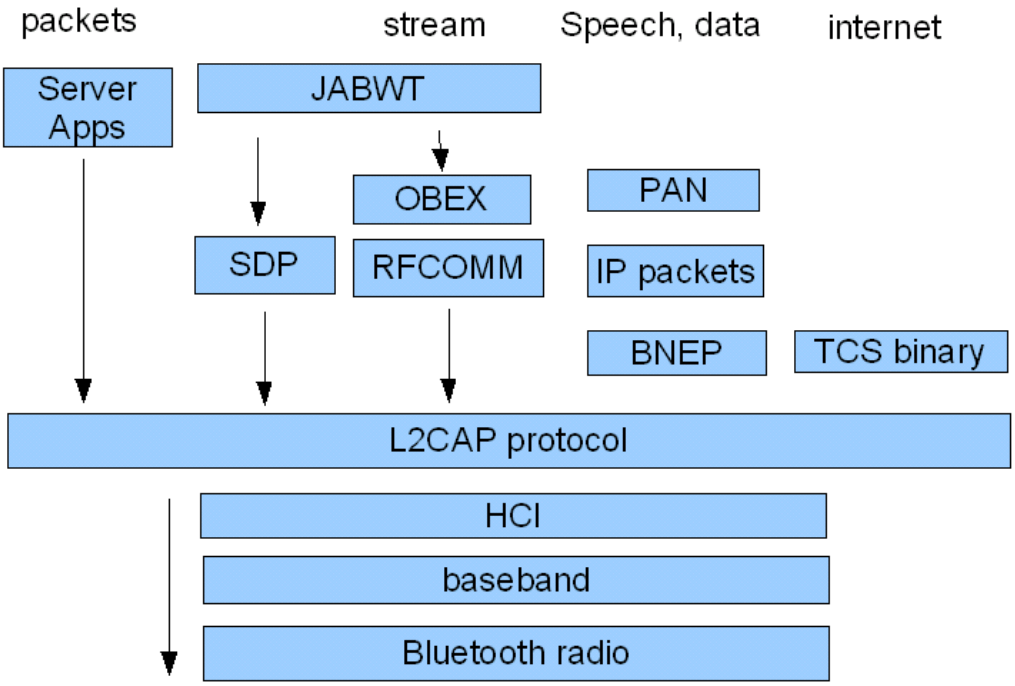

Figure 4.1 Bluetooth Stack and Java API [107].

4.1.1.4 Security

Security can be applied at four levels, but is not obligatory.

(1) Pairing. Where each device has a common code or Personal Identification Number (PIN) [105].

(2) Authentication. Two Bluetooth devices verify that they both have the same secret key [106].

(3) Authorisation. A device is given permission to access a particular service [106].

(4) Encryption. Data is encrypted using encryption keys [105].

4.1.1.5 Connection

A Bluetooth device may connect to another device using various topologies, described in Table 4.1.

Table 4.1 Bluetooth Connection Topologies

Connection	
Client / Server	A Bluetooth client requests services or data from a server, and the server provides services or data to a client. A Bluetooth device can be either a client or server or both, depending on the other devices it is connected to.
Master / Slave	A Bluetooth device can explicitly be a master to any other connected devices, or designated as master at connection time. A Bluetooth device can be a master to one device and also a slave to another device at the same time on different simultaneous connections
Peer to Peer	A peer to peer connection occurs when two devices make a connection without connecting through an intermediary device.
Piconet	If a device is behaving as a master, then up to six slaves can be connected to it. This group of up to seven devices is called a piconet.
Scatternet	If a device is a master to other slaves, forming a piconet, but is itself a slave to another master device, then two or more piconets can be combined to form a scatternet.

4.1.1.6 Software

The Bluetooth SIG [108] defines the Bluetooth specification and Bluetooth Assigned Numbers define the services available on a Bluetooth device. The Bluetooth specification defines over-the-air behaviour for ensuring compatibility of Bluetooth devices from different vendors, it does not standardise a software API (Application Programming Interface) for use by Bluetooth applications.

The Bluetooth stack can be written in any development language, either a native language such as C, C++, assembler, etc, or Java. A Bluetooth stack written in a native language is not required to have a standard interface, it only needs to implement the Bluetooth specification. A Bluetooth stack written in Java does have a standard interface called the Java API for Bluetooth Wireless Technology (JABWT).

4.1.2 Device Development

A Bluetooth device consists of three elements, a Bluetooth radio that transmits data between two or more Bluetooth devices, the Bluetooth stack which is either a hardware, firmware, or software implementation that enables the device to behave as a Bluetooth device, pass data to the radio and communicates with other Bluetooth devices, and thirdly, a software API to communicate between the end user application and the Bluetooth stack.

4.1.2.1 Radio

A Bluetooth radio consists of five aspects, antenna, transmission, power, frequency range, and data transfer rate.

4.1.2.2 Antenna

There are three types of antenna used in Bluetooth devices (Figure 4.2), dipole (a), integrated (b) and ceramic (c), and are described in Table 4.2 [109].

Figure 4.2 Three main Bluetooth antenna types [109].

Table 4.2 Bluetooth Antenna types

Antenna Type	Description
Dipole	A dipole antenna consisting of an electrically conducting wire or rod one half the maximum desired wavelength and connected via a balun to a coaxial cable.
Integrated (Printed) dipole	Integrated dipoles are embedded internal antennas printed on the PCB.
Ceramic	Ceramic antennas are small-form and high-performance with dimensions as small as 6 x 1.5 x 0.6 mm

4.1.2.3 FHSS (frequency-hopping spread spectrum) Transmission

Every transmitting system has a characteristic signature, including signal frequency and signal bandwidth, when modulated with the signal waveform. Signals are mostly represented in the time domain, but can also be represented in the frequency domain.

A spectrum is the frequency domain representation of the signal. A spread spectrum system is one in which a signal is transmitted over a frequency band much wider than the minimum bandwidth required for the signal and the single frequency is deliberately spread over a wide band of frequencies.

There are two spread spectrum technologies: Direct Sequence Spread Spectrum (DSSS) and Frequency Hopping Spread Spectrum (FHSS).

DSSS takes the data signal at the sending station and combines it with a higher data rate bit sequence and divides the data according to a spreading ratio.

Bluetooth employs FHSS, a transmission technology where the data signal "hops" in a pseudo random sequence over a wide band of frequencies determined by the master Bluetooth device. This technique reduces interference because a signal from one band will

only affect the spread spectrum signal from another device if both are transmitting at the same frequency at the same time and with the introduction of adaptive frequency hopping into the Bluetooth system, the performance can be greatly improved by eliminating channels with known interference. The transmission frequencies are determined by a spreading, or hopping, code and the receiver must be set to the same hopping code [110].

Current regulations require 75 or more frequencies per transmission channel with a maximum dwell time (time spent at a particular frequency during any single hop) of 400 ms, giving a maximum time for the hopping sequence of 30 seconds, but Bluetooth devices default to a fast hopping frequency of 1600 hops per second, over 79 channels, with a 1 MHz spacing and switching time of 625 μs [110].

4.1.2.4 Power Ratings

Bluetooth devices are designed to be low power devices, using from 10 mW to 100 mW. The actual power consumption is defined by a class type (Table 4.3) [105], which also defines the devices operating distance. Bluetooth v2.0 uses half the power of v1.0.

Table 4.3 Bluetooth V1.0 class power ratings

Power Classes	Power	Distance
Class 1	100 mW	100 m
Class 2	2.5 mW	20 m
Class 3	1 mW	10 m

4.1.2.5 Frequencies

Bluetooth is one of a number of devices that use the Industrial Scientific Medical (ISM) radio frequency range of 2.4 GHz. The actual frequency range is 2.4 GHz – 2.483 GHz,

giving a spectrum spread of 85.3 MHz. Table 4.4 lists the devices that use the 2.4 GHz frequency band [107].

Table 4.4 Devices that use the 2.4 GHz frequency band

Devices that transmit over the 2.4 GHz frequency band	
Devices	**IEEE Standard**
Bluetooth	802.15.1
ZigBee	802.15.4
Wireless LAN	802.11b, 802.11g
Cordless phones	

4.1.2.6 Data transfer rate

Table 4.5 compares the data transfer rates of devices that use the 2.4 GHz frequency range. Although Bluetooth 2.0 has an increased data rate over v1.0, it is still slower than wireless LAN. ZigBee is a low data rate, low power device and is not designed for fast wireless data transmission.

Table 4.5 2.4 GHz device data transfer rates

Device	IEEE standard	Transfer rate
Bluetooth v1.0	802.15.1	700 Kbits
Bluetooth v2.0	802.15.1	3 Mbits
ZigBee	802.15.4	250 Kbits
Wireless LAN	802.11b	11 Mbits
Wireless LAN	802.11g	54 Mbits
Wireless LAN	802.11n	150 Mbits

4.1.3 Data Transmission

The Bluetooth transmission channel is sub-divided into time slots using time division duplexing (TDD). The master device transmits on even numbered time slots and slave devices transmit on odd-numbered slots immediately after receiving a packet from the

master device (Figure 4.3). The time slot length is a function of the frequency hop rate resulting in a nominal length of 625 μs for a hopping frequency of 1600. Data is transmitted between the master and slaves in packets that are contained within the time slots [87, 111]. A device may use one, three, or five consecutive time slots for a single packet as coordinated by the master. If a packet is greater than one time slot, then frequency hopping is skipped during packet transmission [112].

Figure 4.4 shows the size of the Bluetooth data packets and the proportion of the payload [113]. As can be seen, the access code and header are constant size, as is a guard band to eliminate interference with the next packet, therefore, the more time slots used for transmission, the larger the payload can be.

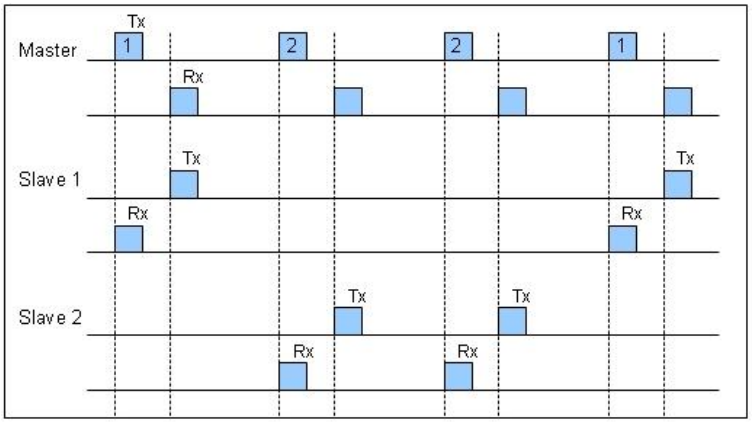

Figure 4.3 Master / Slave Transmit and Receive Timings [112].

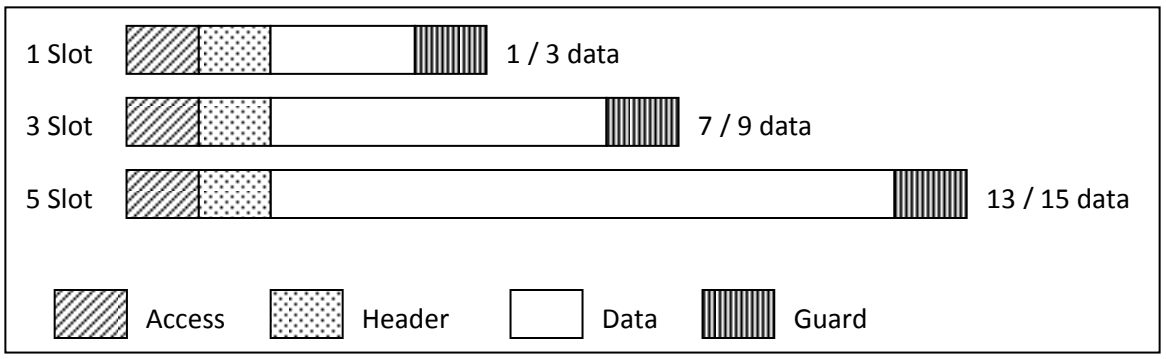

Figure 4.4 Payload in Bluetooth Packets [113].

4.1.3.1 Digital Frequency Modulation

The Bluetooth core specification was initially designed to operate with a peak data rate of 1 Mb/s using frequency shift keying (FSK) techniques. With the introduction of the Enhanced Data Rate (EDR), support for 2 Mb/s and 3 Mb/s peak data rates using phase shift keying (PSK) techniques is incorporated [114].

The payload contains the user data that is modulated onto the RF carrier using one of several different modulation schemes such as GFSK as specified in Bluetooth v1.0 and v1.2, and π/4-DQPSK or 8DPSK modulation schemes for the v2.0+ EDR specification [111].

4.2 Transducer installation

A transducer detects a physical phenomenon and converts one type of energy to another, and for temperature measurements a thermocouple is used to acquire data. The heated metals in a thermocouple are subject to the Seebeck effect, which affects the output voltage. Thermocouples are calibrated to 0°C and a method called cold junction compensation, using polynomials or lookup tables, is applied to obtain the correct temperature.

4.2.1 Seebeck Effect

In 1821, Thomas Johann Seebeck discovered that a heated metal bar would create a voltage across the length of the bar (Figure 4.5a). This voltage is known as the Seebeck voltage, and it differs for various metals or metal alloys. If two wires of the same material with the same temperature differential are measured, then the wires will have the same voltage across them and there would be no voltage difference (0V) between the open ends of the

wires at T_a. If different metals are used for each wire, however, a voltage difference is created between the wires at T_a that is proportional to the temperature difference between them (Figure 4.5b) [115].

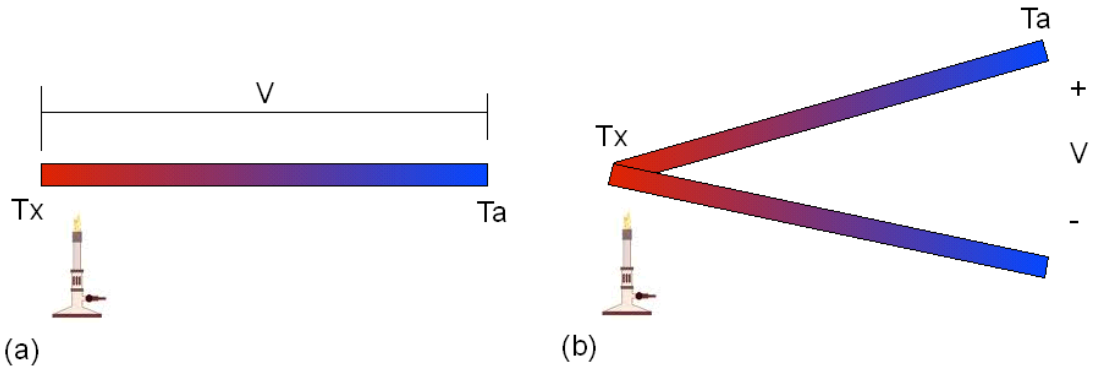

Figure 4.5 Seebeck Voltage (a) Creation. (b) Proportional to temperature [115].

4.2.1.1 Thermocouple

The thermocouple is the most popular transducer for measuring temperature. It is very rugged and inexpensive and can operate over a wide temperature range. However, it has some unique signal conditioning requirements. It is made by connecting together two wires made of different materials. By choosing materials that have different Seebeck voltages, a measureable voltage V_{AB} will be created that depends on the temperature difference between T_X and a reference, T_{REF} (Figure 4.6) [115].

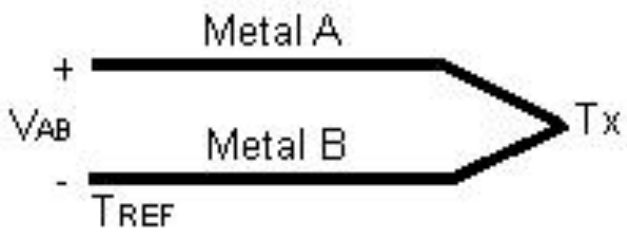

Figure 4.6 Voltage Measured at Thermocouple Leads.

At T_{REF} the Seebeck voltage varies with temperature. For small changes in temperature, the voltage is approximately linear:

$$\Delta V = S\Delta T \qquad (4.1)$$

where:

ΔV is the change in voltage.

S is the Seebeck coefficient.

ΔT is the change in temperature.

The Seebeck coefficient (S), in µV per °C, also varies with changes in temperature, causing the output voltages of thermocouples to be nonlinear over their operating ranges, i.e. the voltage is nonlinear with respect to temperature. The Seebeck coefficient of the thermocouple can vary by a factor of three or more over the operating temperature range of the thermocouple. A type K thermocouple has a Seebeck coefficient of 39.48 µV/°C at 0°C [116].

4.2.1.2 Cold junction

The output of the thermocouple is relative, not absolute. If the probe and measurement circuit ends have the same temperature, the measured voltage will be zero. If the probe end is hotter, a positive voltage will be measured. If it is colder, a negative voltage will be measured.

In order to determine the actual temperature at the probe end, the temperature at the circuit end also needs to be known. Historically, this was accomplished by keeping the temperature at the circuit end at 0°C. Consequently, the connection between the thermocouple and the measuring circuit (reference junction (Figure 4.7)) came to be known

as the 'cold junction'. The process of using the reference junction temperature to calculate the actual temperature is referred to as Cold Junction Compensation [117].

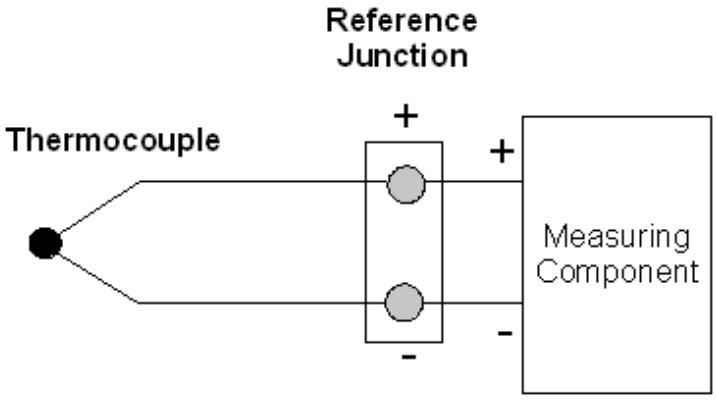

Figure 4.7 Thermocouple Connected to a Measuring Component.

4.2.1.3 Isothermal block

The physical connection point where the thermocouple wires meet the copper circuit wires must be the same temperature, i.e. isothermal, and for this reason, both thermocouple and measuring circuit are connected to an isothermal block that contains a reference junction temperature sensing device (Figure 4.8) to directly measure the actual temperature of the cold junction [117].

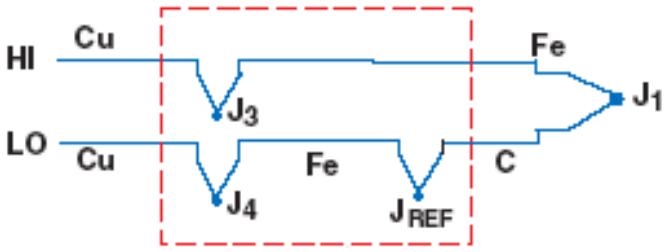

Figure 4.8 Connection at the isothermal block [109].

If the thermocouples leads are not located close together and at the same temperature, then there will be an error [115]. A difference in temperature between leads and reference point will directly affect the accuracy of the temperature measurement.

4.2.2 Calculating Cold Junction Compensation

There are two general approaches to cold-junction compensation – hardware and software compensation.

Hardware cold-junction compensation uses a special circuit that applies a variable voltage to cancel the cold-junction voltage, but each thermocouple type must have its own compensation circuit that works at all ambient temperatures, and can be expensive [118].

Software cold-junction compensation requires only knowledge of the ambient temperature. If a sensor is used to directly measure the ambient temperature at the cold junction, then software can compute the appropriate compensation [118].

4.2.3 Cold Junction Compensation

Cold junction compensation temperature reference tables were created using the ice bath method by the National Institute of Standards and Technology (NIST) for the different thermocouple types [119]. Table 3.1 shows a list of common thermocouple types together with their temperature range in °C, their output voltage range in mV and their Seebeck coefficient [77]. The temperature references are available in two forms; either in polynomial equations or as look-up tables for the conversion values.

For type K thermocouples, NIST used the following equations to determine the voltage output for a given temperature. Coefficients, a_0 , a_1 , a_2 , and c_i , of reference equations give

the thermoelectric voltage, E, as a function of temperature, t , for the indicated temperature ranges.

The equation below 0 °C is of the form:

$$E = \sum_{i=0}^{n} c_i (t)^i \qquad (4.2)$$

The equation above 0 °C is of the form:

$$E = \sum_{i=0}^{n} c_i (t)^i + a_0 \, e^{a_1 (t - a_2)^2} \qquad (4.3)$$

where :

e is the natural logarithm constant

E is in mV

t is in °C.

Table 4.6 Thermocouple Voltage Output (mV).

TC type	Conductor		Temperature Range	Voltage Range (mV)	Seebeck Coefficient (µV/°C)
	Positive	**Negative**			
E	Chromel	Constantan	-270° to 1000°	-9.835 to 76.358	58.70 at 0°C
J	Iron	Constantan	-210° to 1200°	-8.096 to 69.536	50.37 at 0°C
K	Chromel	Alumel	-270° to 1372°	-6.548 to 54.874	39.48 at 0°C
T	Copper	Constantan	-270° to 400°	-6.258 to 20.869	38.74 at 0°C
S	Platinum-10% Rhodium	Platinum	-50° to 1768°	-0.236 to 18.698	10.19 at 600°C
R	Platinum-13% Rhodium	Platinum	-50° to 1768°	-0.226 to 21.108	11.35 at 600°C

The equations are used to produce the polynomial coefficients for popular thermocouple types. For k type thermocouples there are NIST polynomial coefficients [120] and look-up tables for the 0 - 300°C temperature range [121].

4.2.4 Thermocouple temperature curve using polynomials

The thermocouple voltage-versus temperature curve can be approximated using polynomials in the following form:

$$T = c_0 + c_1 v + c_2 v^2 + ... + c_n v^n \qquad (4.4)$$

Where:

T is the temperature in degrees Celsius

c_0 through c_n are coefficients for the specific thermocouple type.

v is the thermocouple voltage in volts

As can be seen from Table 4.7, type K thermocouples are defined to 10^{th} order polynomial [115]. As the order increases, the accuracy of the polynomial improves, but the polynomial fit rapidly degrades outside the temperature range and should not be extrapolated outside the limits of the selected type. A representative number is n = 9 for ± 1°C accuracy [122].

If the slope of the Seebeck coefficient curve is plotted against temperature, it can be seen that the thermocouple is a non-linear device. Output voltages for the more common thermocouples are plotted as a function of temperature in Figure 4.9. A horizontal line would indicate a constant coefficient, i.e. a linear device. It can be seen that the slope of the type K thermocouple approaches an approximate constant over a temperature range from 100°C to 1000°C and could be used as such for non critical applications.

Table 4.7 Polynomial orders for types k thermocouples.

Thermocouple Type	Temperature Range for Polynomials (°C)	Polynomial Order
K	-270 - 0 0 - 1370	10^{th} 9^{th}, + $ae^{b(t-c)\wedge 2}$

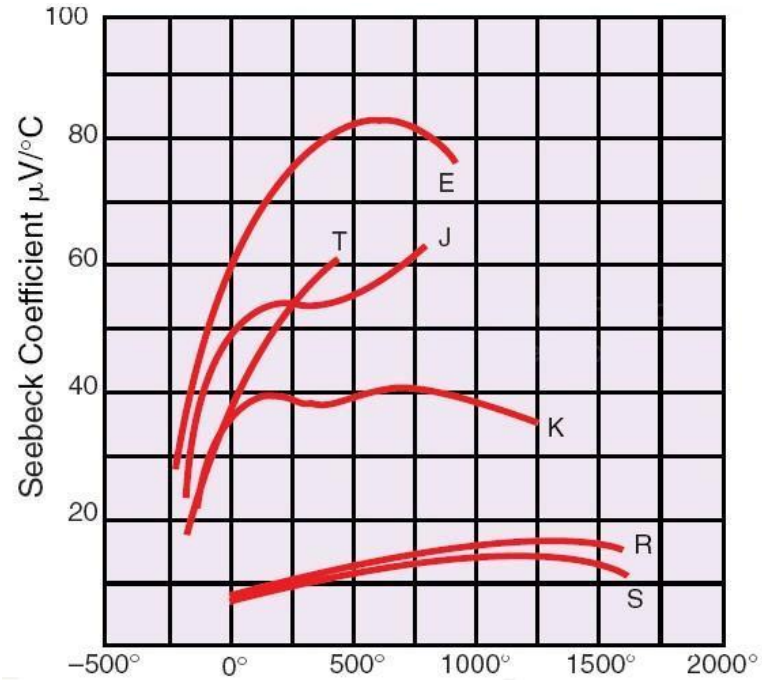

Figure 4.9 SEEBECK coefficient Vs temperature [122].

4.2.5 Simplifying Temperature Measurement

The calculation of high-order polynomials is a time consuming task for a computer but time can be saved by using a lower order polynomial for a smaller temperature range [115]. There are ways to simplify the computations without a significant loss of precision. For small changes in temperature, a linear approximation provides a good correlation between voltage and temperature. For wider temperature ranges, an alternative method is to divide the entire range into several smaller ranges, and use a different linear approximation for

each of the sub-ranges. Figure 4.10 shows a characteristic thermocouple curve divided into eight sectors, with each sector approximated by a third order polynomial ($Ta = bx + cx^2 + dx^3$) [122], assuming the thermocouple voltage can be measured accurately and easily with a sensitive measuring system.

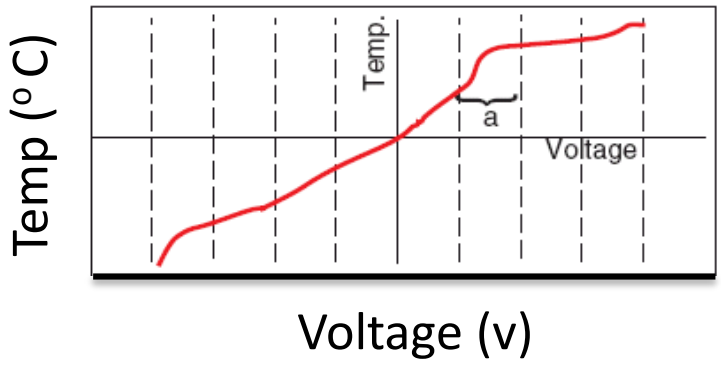

Figure 4.10 Characteristic Curve Divided into Sectors [122].

4.2.5.1 Gain / Amplification

It is necessary to ensure that the low-level signals of the transducer match the full scale input voltage of the measuring device as close as possible by selecting a gain factor that amplifies the signals to match the full scale voltage rating. Also, ADC resolution should not be over-specified. A 12-bit ADC has an accuracy of 0.024% while that of a 16-bit ADC is 0.0015%, which is excessive for a transducer with ±1% accuracy [123].

4.3 Summary

Bluetooth wireless technology is a serial cable replacement technology. It has a simple connection procedure, eliminates interference with other devices and has a variable data transmission rate.

The Bluetooth stack is a set of protocols, profiles and services required to establish a connection to another device. Although the software is complex, it presents a simple setup procedure to the user. By employing adaptive frequency hopping, channels that are detected to contain interference are removed from the hopping sequence. Bluetooth master and slave devices communicate on alternate clock cycles. Data is transferred between master and slave in packets, whose size may be extended to transfer larger packets of data.

The advantages of Bluetooth for proposed system are: lower power requirements reduce the size of the proposed power generator and thus lower costs, the use of a ceramic antenna enables placing the system in a smaller space and the engine will not have to be modified to accommodate a dipole antenna, using peer to peer connection eliminates requirement for the search procedure to detect other devices, use of packet transfer for a robust digital data transfer, use of standard protocols to maintain links and data transfer and employing the Microsoft Bluetooth stack to reduce development time and costs compared to development of a bespoke stack or purchasing a proprietary stack.

Thermistors and other sensors require specific signal processing to be performed on the host too enable conversion to temperature. The use of thermocouples simplifies signal processing to voltage conversion.

Thermocouples are the most widely used temperature sensor and perceived wisdom is that unless a different type is specifically required for an application, then to use a k type, which also adequately covers the temperature range to acquire.

Characteristics of the thermocouple are provision of a low voltage output that corresponds to and is proportional to temperature, but the output voltage is non linear and requires conversion by either look up tables or polynomial equations. The characteristics of the

Seebeck effect require that the probe end and the voltage sensing end are apart as much as possible. The closer the probe end and sensing end, the smaller the temperature gradient will exist between them, and thus the less accurate the measurement will be.

When a temperature reading is acquired, a method of temperature conversion is required, calculation by polynomial equations, lookup tables & interpolation, bespoke software functions or a sensor incorporating signal processing. With the use of a thermocouple amplifier, the non linearity of the Seebeck effect is overcome by cold junction compensation being performed on the sensor, and the higher the resolution of the reading, the more accurate the temperature reading.

5 Power Generator

This chapter explains magnetism as current and e.m.f through a coil and graphically representing magnetisation and de-magnetisation of a magnetic force with a hysteresis curve. Types of magnets and magnet properties are described. Power generation construction, theory of a generator, rectification, filtering, regulation, and design of a simple generator are examined.

5.1 Magnetism

When a conductor carries a current, a magnetic field is produced around that conductor in the form of concentric fields along the whole length of the conductor (Figure 5.1). The direction of the field depends on the direction of the current.

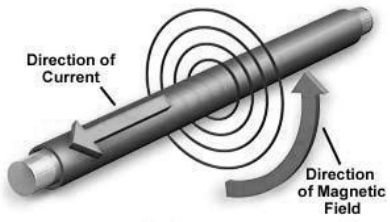

Figure 5.1 Direction of Force Through a Conductor [124].

If two current-carrying conductors placed side by side, a force, measured in Newtons, will exist between them due to magnetic flux. The direction of this force will depend on the direction of the current flow. If current flow is in the same direction, then there is more flux between the conductors and they will be forced apart. If current is in the opposite direction then flux between the conductors tends to cancel out, leaving more flux on the outside of the conductors, thus forcing them together.

If a current-carrying conductor is placed at right angles to a magnetic field, a force will be exerted on the conductor. If the process is reversed and a conductor moves through a magnetic field, cutting across the flux, then a current would flow in the conductor, and if a current flows then an electromotive force (e.m.f.) must be producing it. This e.m.f. is called an induced e.m.f., whose direction is the same as that of the current flow [125].

When a magnet is moved towards and inside a coil of wire, or a coil towards a magnet, a current is induced inside the wire. It does not matter which is moving, so long as one is moving in relation to the other. The same effect occurs in a stationary wire in a changing magnetic field. A stationary wire in an unchanging magnetic field will not have a current induced. A wire which is unconnected at both ends will have a difference in voltage between the ends (induced voltage), but current can only flow when the wire is part of a complete circuit [126].

The size of the induced current can be made larger either by using a stronger magnet, moving the magnet at a faster speed, or using more turns of wire on the coil. The direction of the current can be reversed by moving the magnet in the opposite direction or by reversing the magnet face from north to south [8].

5.1.1 Magnetisation

All ferromagnetic materials have atomic magnetic moments that are aligned within regions called domains. In the absence of a magnet field the direction of each domain is randomly oriented. During magnetization of the material, domain magnetisation is in the direction of the applied field and they will rotate to be aligned parallel to the applied field (figure 5.2).

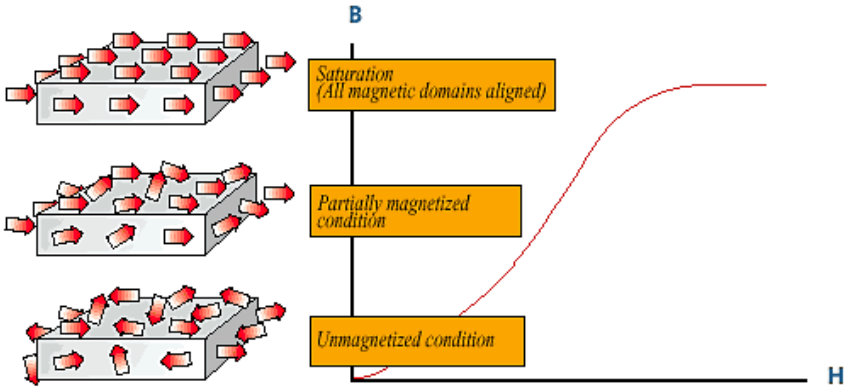

Figure 5.2 Field Alignment Towards Saturation [127].

5.1.2 The B-H Curve Hysteresis Loop

The hysteresis loop or B-H curve, is a graphical representation of the relationship between an applied magnetic field and the resulting induced magnetisation within a magnet material and describes the cycle of a magnet brought to saturation, de-magnetised, saturated in the opposite direction, and then de-magnetised again under the influence of an external magnetic field (Figure 5.3). The three most important characteristics of the curve are the points at which the B and H axes intersect and the point at which the product of B and H are at a maximum.

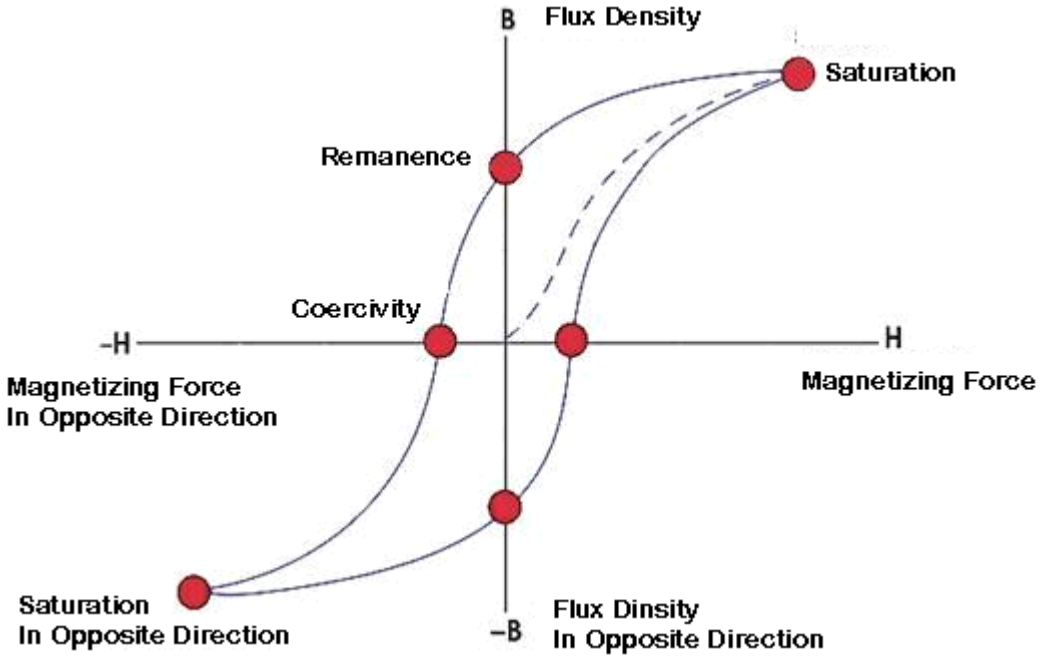

Figure 5.3 B-H curve or Hysteresis Loop [128].

Saturation is the maximum energy product, the point at which the product of B and H are maximum ($BH_{max)}$.

During magnetisation, an increasing magnetic field (H) is applied to the material until a saturation point is reached. When this applied field is removed, the permanent magnet material does not return to zero flux density, but follows the path of the hysteresis loop, retaining some of its magnetism (Remanence or B_r). Coercivity is the point at which the magnet becomes de-magnetised under the influence of an additionally applied magnetic field. BH_{max} is the maximum energy density of the magnetic field in the air gap. The higher this BH product, the smaller the volume of the magnet needs to be.

5.1.3 Orientation of Flux

Some applications require magnets oriented in a particular direction with a high degree of accuracy. If the required direction does not coincide with a geometrical plane of the magnet

of anisotropic materials, then special measurement, testing, cutting and machining is undertaken. Isotropic materials may be magnetised in any direction (Figure 5.4) [127].

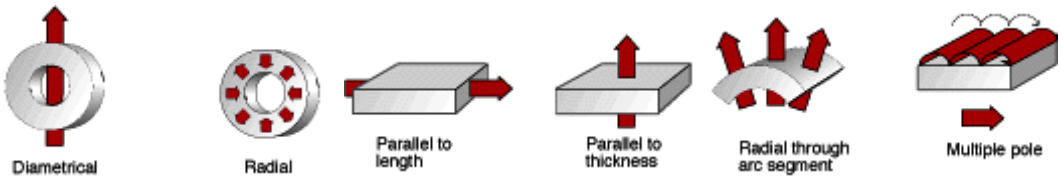

Figure 5.4 Field Orientation For Magnet Types [127].

For the proposed power generator, magnets orientated along the central axis, axial flux, are used. With the magnet placed facing the planar coil, the magnetic flux cuts the coil at 90°, inducing a voltage and current. If the magnetic flux cuts the coil at less than 90°, then less voltage is induced.

5.2 Modern Magnet Materials

There are four general classes of modern commercial magnets, based on material composition (Table 5.1). Each class has a number of grades that have their own magnetic properties [126].

Table 5.1 Classes of modern commercial magnets.

Types of modern commercial magnets	
Neodymium Iron Boron	NdFeB
Samarium Cobalt	Smco
Ceramic	Ferrite
Alnico	AI-Ni-Co

Neodymium magnets are extremely strong for their small size, metallic in appearance and found in simple shapes such as rings, blocks and discs and are used in servo motors and DC motors. Samarium Cobolt (SmCo) is an alternative to Neodymium magnets, has a more

stable output over a much wider temperature range and can be used in critical applications such as aerospace and military applications. But it is a brittle material and could shatter if mishandled and care should be taken when assembling with the SmCo magnets.

Alnico is made from a powdered mixture of ingredients that are pressed into a die under pressure or cast to a variety of shapes and sizes, but does not lend itself to conventional machining because it is hard and brittle. Ceramic magnets have a lower flux density compared to other magnets and is limited to simple shapes because tooling is expensive and finishing requires precision grinding.

Neodymium magnets are selected because it has the highest flux density, because of the handling issues of SmCo and Alnico magnets (brittleness) and working temperatures are not in the range where SmCo magnets would have a flux density advantage.

5.2.1 Super Neodymium Magnets

Neodymium magnets (Nd-Fe-B) are composed of neodymium, iron, boron and a few transition metals. These magnets are extremely strong for their small size, metallic in appearance and manufactured in simple shapes such as rings, blocks and discs (Figure 5.5). The Attributes of Neodymium magnets are: A very high resistance to de-magnetisation; High energy for given size; Low working temperatures, but good in ambient temperature; Requires coating as the material is corrosive [72]. Data sheets state that samarium cobalt magnets start to outperform neodymium magnets at temperatures above +150°C, the rotor is located at a position where the temperature is lower than this value. The magnet shape selected for the power generator is the disc magnet, as, by drilling only a hole, it is the simplest shape with which to construct the rotor.

Figure 5.5 Neodymium magnet shapes: Blocks, Discs and Rings [129].

5.3 Prototype Power Generator Design

The prototype generator design is an axial flux, permanent magnet, single phase, single stator, single rotor, power generator, with stator coils connected in series.

There are constraints on the size and diameter of the rotor and stator due to space limitations of the engine cylinder dimensions. A 2 ltr Ford Puma engine allows a diameter of 100 mm for the stator and rotor. The connection rod big end crankshaft bore is 60 mm, which therefore, allows a 20 mm diameter for magnets or coils. The magnets are magnetized axially with the north pole on one face and the south pole on the opposite face (Figure 5.6)

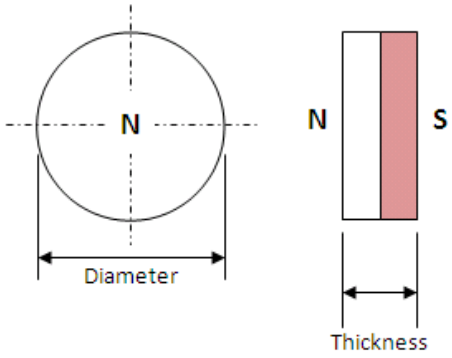

Figure 5.6 Disc Magnet Axial Flux Magnetic Poles.

The magnets are arranged circumferentially around the rotor with alternating north and south poles, which increases the flux transition rate. Simulation by Finite Element Analysis shows that axial flux density is formed as sinusoidal peaks around the axial center of the

magnet. The simulation plot (Figure 5.7) shows the flux density distribution of alternating north and south flux density peaks corresponding to alternating north south arrangement of the magnets.

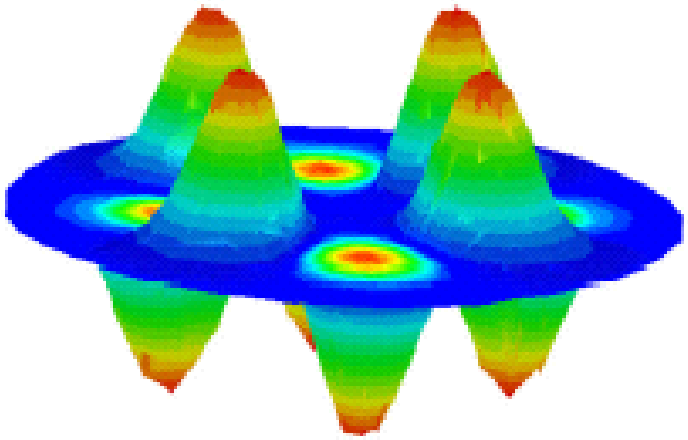

Figure 5.7 Disc Magnet Axial Flux Density Simulation [73].

5.3.1 Flux density (β) at a distance from magnet

A rod magnet is defined as having a length greater than diameter, and therefore, a disc magnet has a diameter greater than length. In the following formula both types are used interchangeably.

To estimate the flux density β on the central axis at a distance x from the magnet, the following formula can be used [130]:

$$\beta = \frac{B_r}{2} \cdot \left[\frac{(X+T)}{[R^2 + (X+T)^2]^{1/2}} - \frac{X}{[R^2 + X^2]^{1/2}} \right] \quad (5.1)$$

Where:

= Remanence of the magnet

R = Radius

T = Thickness

X = Distance from magnet

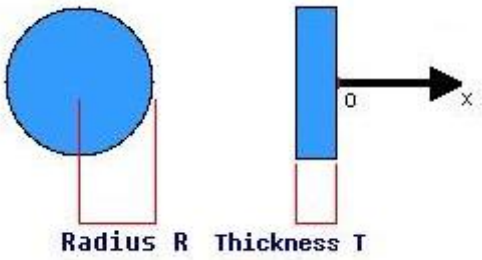

Figure 5.8 Magnet Parameters.

Figure 5.8 shows the required parameters for the formula and is applied to 10mm x 5mm disc magnets, where a Br of 1.3 Tesla is obtained from NdFeB data sheets, R = 5 mm, T = 5 mm and X is a variable value corresponding to distance from the magnet.

Equation 5.1 is the formula for calculating the flux density at the magnet face, or at a specified air gap from the magnet face. Flux density calculators that use the equation are available online for different types and shapes of magnet. The online calculator was used for various sizes of grade 42 NdFeB disc magnets at various air gaps.

Table 5.2 shows the flux density, in Tesla, at various distances from the magnet face, for selected magnet sizes. For a proposed air gap of 0.5 mm in the generator, it can be seen that 6 mm diameter by 4 mm thick magnet has the highest flux density at this air gap.

Should the air gap increase, then the flux density of the 6 mm x 4 mm magnet decreases rapidly, and it is the 10 mm x 5 mm magnet that has the highest flux density between an air

gap of 0.5 mm and 2 mm (Figure 5.9). If a stator coil is utilized with multiple layers, as opposed to a single layer planar coil, then the air gap between each coil layer is increased and the 10 mm by 5 mm magnet would produce the highest flux density value.

Table 5.2 Flux Density at various air gaps for specified magnets

Flux Density (Tesla)						
Air Gap (mm)	**Magnet Dimensions** (mm) Diameter x Thickness					
	20 x 3	**15 x 1**	**15 x 4**	**10 x 4**	**10 x 5**	**6 x 4**
0.1	0.19	0.09	0.31	0.41	0.46	0.51
0.3	0.19	0.09	0.30	0.39	0.44	0.48
0.5	0.19	0.09	0.30	0.38	0.42	0.44
0.9	0.18	0.08	0.28	0.35	0.39	0.37
1.3	0.18	0.08	0.27	0.31	0.35	0.31
1.7	0.17	0.08	0.25	0.28	0.32	0.26
2.1	0.16	0.07	0.24	0.25	0.28	0.21
2.5	0.16	0.07	0.22	0.23	0.25	0.18
2.9	0.15	0.07	0.21	0.20	0.23	0.15
3.3	0.15	0.06	0.19	0.18	0.20	0.12
3.7	0.14	0.06	0.18	0.16	0.18	0.10
4.1	0.13	0.05	0.17	0.14	0.16	0.09
4.5	0.13	0.05	0.15	0.13	0.14	0.07

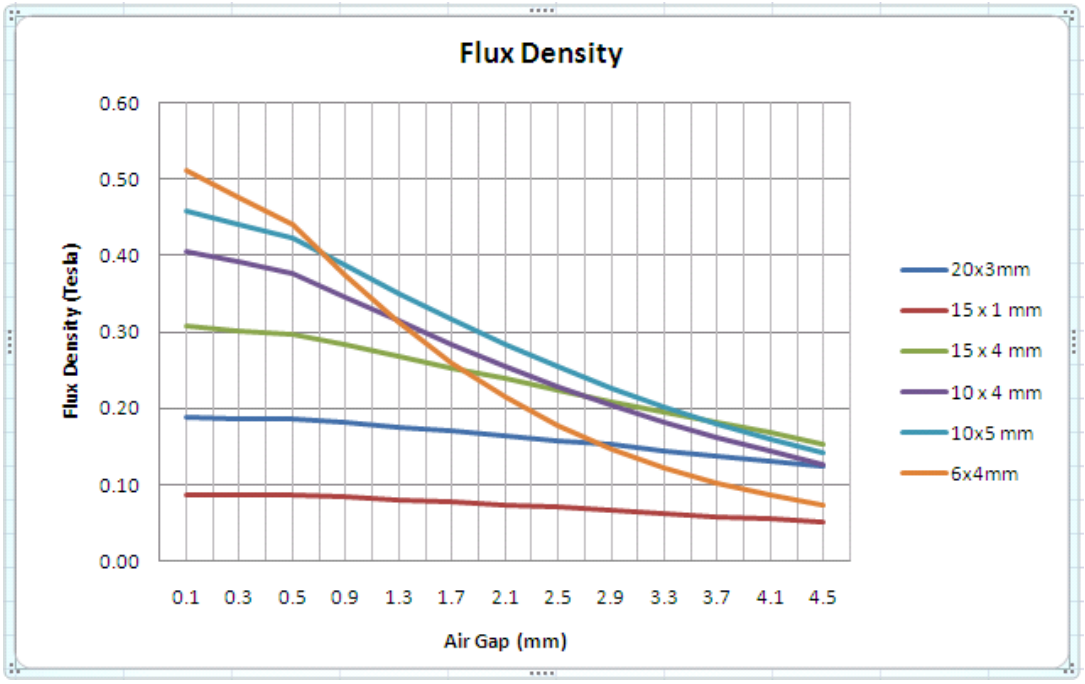

Figure 5.9 Flux Density of Various NdFeB Magnets.

The coils are arranged in a slotless, air core, concentrated, single phase configuration. Being slotless eliminates cogging, the air core reduces iron losses and eddy current losses and the single phase allows a magnet to coil ratio of 1:1.

The coils are arranged circumferentially around the stator in series form, with adjacent coils being wound in the opposite direction, corresponding to the alternating poles of the magnets and thereby adding the induced voltages at each transition.

The stator diameter of 100 mm permits 12 coils of 20 mm diameter, but for ease of winding, coils with outer diameter of 16mm and inner coil diameter of 5 mm are wound (Figure 5.10(a), with Figure 5.10(b)) showing the rotor dimensions using 10 mm diameter magnets. When magnet selection has been made, induced voltage to into the coil can be calculated based on flux density of the magnet.

For 0.4 mm wire (gauge 26), the induced voltage can be calculated by

$$V = A \times M \times N \qquad (5.2)$$

Where

V	=	induced voltage	
A	=	cross sectional area of the wire (m^2)	$0.7845 \times d^2$
M	=	rate of change of flux (T/sec)	revs / sec x number of magnets
N	=	number of turns	

There is a voltage constraint from the generator of 5V due to maximum input voltage of the electronic components and DAQ system. A disadvantage of a single phase stator system is lack of voltage control and therefore the magnets and coils must be calculated to not exceed an induced voltage of 5V at the desired maximum rpm.

Table 5.3, 10 mm x 4 mm magnets, and Table 5.4, 10 mm x 5 mm magnets, show the parameters for a generator consisting of 12 magnets and 12 coils and the voltages induced into one coil and 12 coils at selected rpm. For each size of magnet, the number of turns (N) parameter is chosen so that it produces 5v or less at the maximum speed of the test rig.

Table 5.3 Parameters and induced voltage for a 10mm x 4mm magnet

				rpm	Voltage
M	0.38	Tesla		1000	0.847
A	0.000013	m^2		2000	1.693
N	70			3000	2.490
				4000	3.336
				5000	4.183
				6000	4.980

Table 5.4 Parameters and induced voltage for a 10mm x 5mm magnet

				rpm	Voltage
M	0.42	Tesla		1000	0.842
A	0.000013	m^2		2000	1.684
N	63			3000	2.477
				4000	3.319
				5000	4.161
				6000	4.953

These values are an example of the trade off that has to be made in that if space constraints dictate less thickness of the magnet, then this will require more turns on the stator coil for the same voltage output.

5.3.2 Power Generator Design For Pistons

Taking into account various ideas from research and applying ideas from wind generator technology, the power generator is designed using a disc rotor containing NdFeB

permanent magnets so that induction occurs for the whole of the piston cycle. The rotor is permanently connected to the crankshaft so that it rotates as the piston reciprocates. The stator is connected to the piston connection rod in a manner so as to stay static, compared to the rotor, as the piston reciprocates (Figure 5.11a), in this way, as the piston reciprocates, the magnets rotate past the stator coils and induce a voltage.

The telemetry electronics are connected as a system and attached to the piston big end (Figure 5.11b). The stator output is passed to the full wave rectifier and step up converter, and from there to the Bluetooth DAQ module and sensor. The cabling from the thermocouples is taken down the side of the connection rod to the thermocouple amplifier sensor.

A rectifier circuit converts AC to DC by means of either semiconductor diodes or an IC rectifier [8]. The effect of rectification is that the DC output contains a ripple component that is minimised or eliminated using a filter capacitor. Voltage regulators limit the output of the power supply, but require a minimum operating input voltage which is higher than the regulated output.

Permanent magnets induce a current and voltage into the coil. A DB101G119 1A [131] full-wave IC bridge rectifier rectifies the AC output from the coil to DC and a 100 nf electrolytic capacitor filters the DC ripple. A MAX756 [132] 5v step-up converter provides a constant 5v supply to the Bluetooth module and sensor devices (Figure 5.12 a & b).

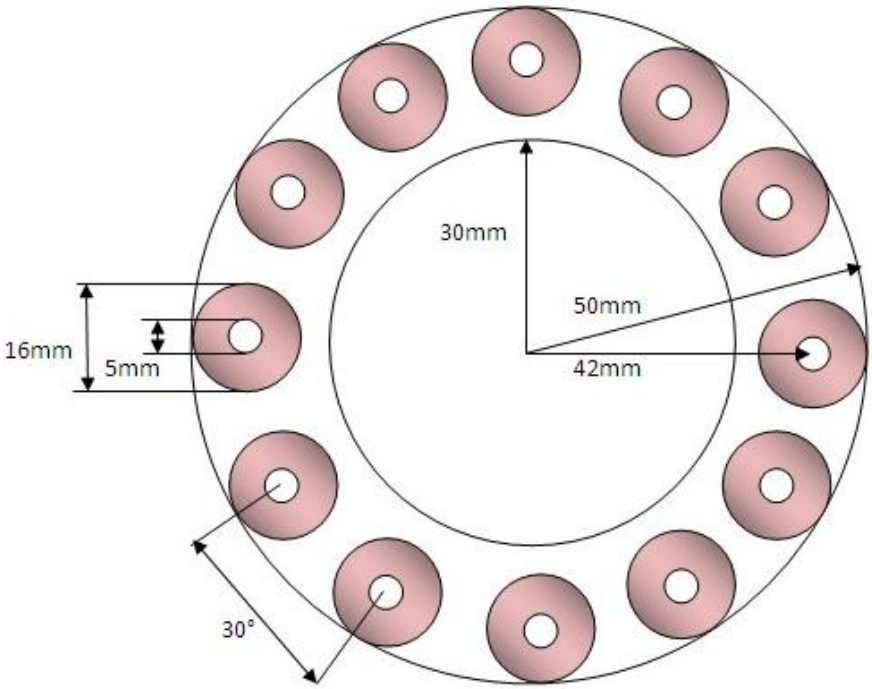

(a)

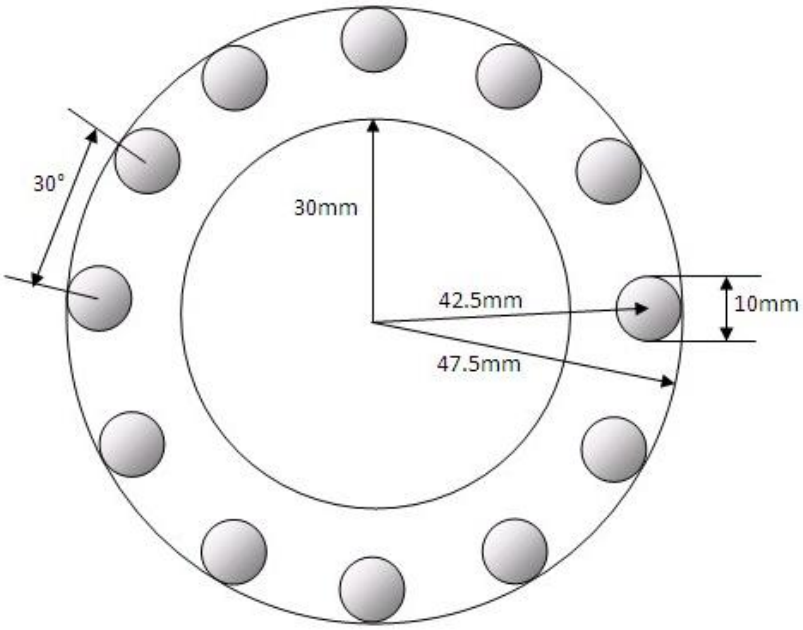

(b)

Figure 5.10 Dimension of stator (a) and rotor (b).

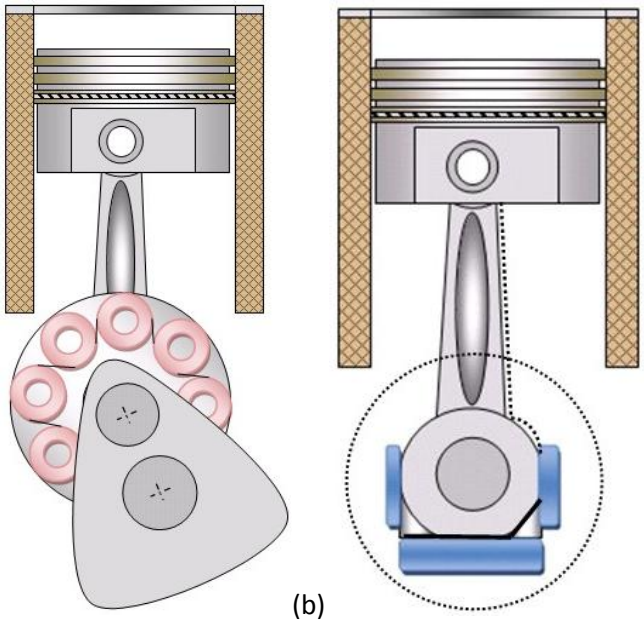

(a) (b)

Figure 5.11 Diagram of stator (a) and telemetry electronics (b) attached to piston.

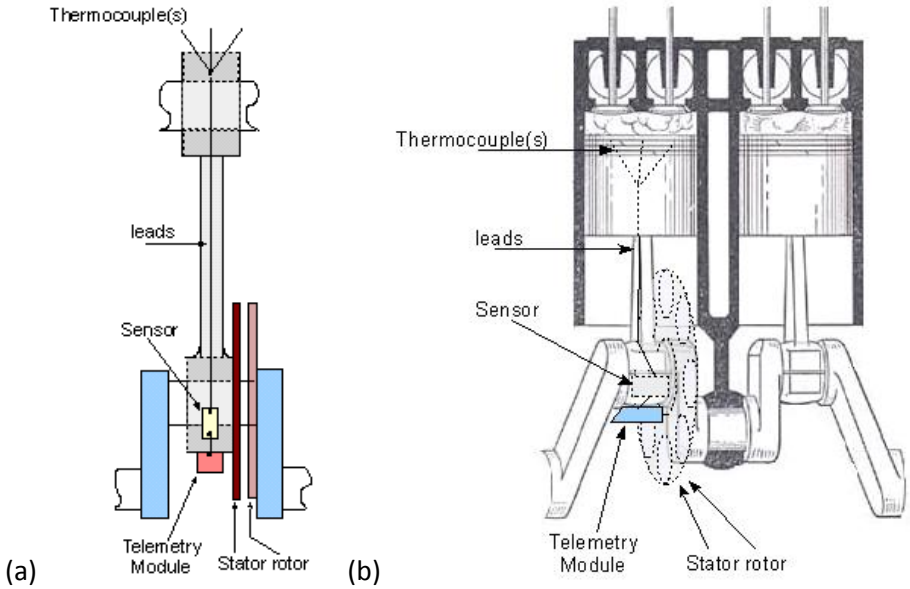

(a) (b)

Figure 5.12 Schematic (a) and 3D (b) representation of power generator and piston.

5.4 Summary

A BH curve shows the residual magnetism remaining in a magnet material, how the orientation of flux can be applied to modern magnetic materials in standard or customised directions, and by analysis of magnet characteristics, the selection of Neodymium magnets is made for the power generator because of highest flux density for a selected size and the handling and manufacturing issues of SmCo and Alnico magnets (brittleness).

The generator design incorporates the selection of axial flux magnets, and through flux density simulation, the shape of the axial flux density map for a circumferential arrangement of magnets shows how the axial flux of the magnet will be at 90° to the coil, and therefore induce optimum voltage. The axial orientation of flux allows both rotor and stator to be constructed as flat discs in a very compact design.

Flux density value calculations are required because it is the interrelationship of flux density, magnet size, coil size, and velocity of flux transition that determines the induced voltage into the stator coil. The air gap between magnet and coil is a very important parameter as flux density decreases with distance from the magnet. Calculated flux density values are tabulated to compare different size magnets at various air gaps, to determine the optimum size magnet for the size constraints of the stator and rotor.

The prototype system is designed for a piston, showing the dimensions of the stator and rotor, and the location of electronic components on the connection rod and crank shaft without any machining of engine parts. Components are located on the connection rod big end to be at the lowest temperature location of the engine, giving a wider temperature gradient between sensor and thermocouples and therefore making temperature readings more accurate.

6 Prototype Telemetry System

The prototype short distance system comprises of hardware and software. The complete system comprises of sensors, a power supply, a data acquisition system and a telemetry system. The hardware is in the form of thermocouples, thermocouple amplifiers, a Bluetooth data acquisition module and a USB Bluetooth adapter that acts as a host receiver. By utilising low power, commercial off the shelf (COTS) components to create a low component count modular mechatronic data acquisition system that has flexibility in the choice of sensor connection, The system reads low power thermocouple temperature data, performs signal processing and transmits the data values to a host via wireless telemetry.

The software is the Bluetooth stack, an aggregation of software development modules and the resultant firmware is loaded onto the DAQ module microprocessor which is configured to read either analogue or Serial Peripheral Interface (SPI) digital input data, but is in digital form for Bluetooth transmission. Figure 6.1 shows a prototype digital Bluetooth telemetry system.

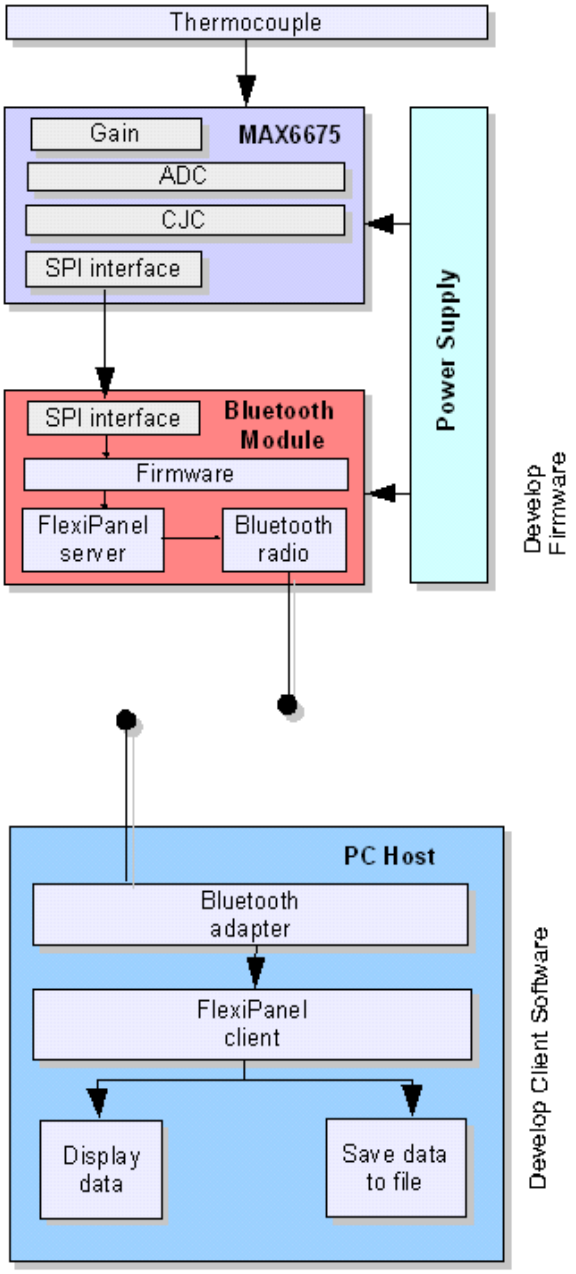

Figure 6.1 Example Bluetooth telemetry system.

6.1 Hardware

The system hardware consists of a thermocouple, thermocouple amplifiers, an embedded Bluetooth adapter for the transmitter and a USB Bluetooth adapter for the receiver on a PC host.

6.1.1 Thermocouple

If cold junction compensation is not integrated in the thermocouple amplifier, then a separate temperature sensor is also required and connected as close as possible to the thermocouple connection (isothermal block). These two thermocouple and temperature sensor readings must then be digitised and cold junction compensation methods employed to obtain the correct temperature of the thermocouple.

By using a dedicated thermocouple amplifier that includes gain and cold junction compensation, the analogue output can be converted to a digital value by the microcontroller, or a digital output read directly by the microcontroller digital interface (SPI). The SPI device has a 12 bit resolution for data compared to the microcontroller ADC resolution of only 10 bits. If a thermocouple amplifier is not used, then the corresponding analogue circuit is more complex and has a higher component count.

6.1.2 Analog Devices AD595C Thermocouple Amplifier

The AD595C [133] is an instrumentation amplifier and thermocouple cold junction compensator with a pre-calibrated amplifier producing a 10 mV/°C output directly from a type K thermocouple signal input. The C class amplifier has an accuracy ±3°C and is designed to be used from 0°C to +50°C ambient temperature. The minimum error at is calibrated +25°C. When powered from a single ended +5 V supply with a supply current of 160 µA, the AD595 provides a measuring range from 0°C to +300°C.

6.1.2.1 AD595 Packaging

The AD595C is packaged as a 14 pin, ceramic, hermetically sealed, Dual In Line IC, as shown in Figure 6.2. As can be seen from the pin layout, the thermocouple wire inputs connect to pins 1 and 14 either directly from the measuring point or via thermocouple extension wire type.

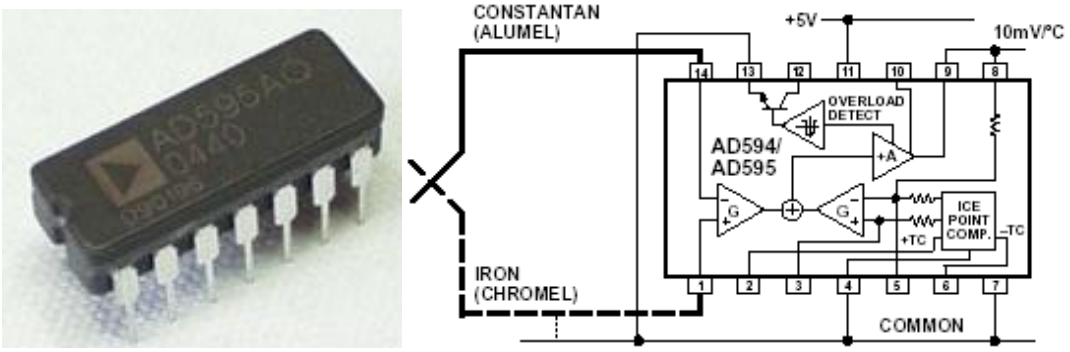

Figure 6.2 AD595 Thermocouple amplifier and internal functionality [133].

6.1.2.2 AD595 Output Voltages

To achieve a temperature output of 10 mV/°C and accurately compensate for the reference junction, the AD595 gain is trimmed to match the transfer characteristic of K type thermocouples of 40.44 µV/°C at 25°C, resulting in a gain of 247.3. The absolute accuracy trim induces an input offset to the output amplifier characteristic of 11 µV, because the AD595 is trimmed for a 250 mV output for a 25°C thermocouple input.

Because a thermocouple output voltage is nonlinear with respect to temperature, and the AD595 linearly amplifies the compensated signal, the following transfer function (equation 6.1) is used to determine the actual output voltage:

$$AD595\ output = (Type\ K\ Voltage + 11\ \mu V) \times 247.3 \qquad (6.1)$$

Since a type K thermocouple deviates from straight line approximation, the AD595 reads 2.7 mV at 0°C.

Table 6.1 Sensor Voltage Ouputs.

Thermocouple Temperature (°C)	Type K voltage (mV)	AD595 output (mV)
0	0	2.7
10	0.397	101
20	0.798	200
25	1.000	250
30	1.203	300
40	1.611	401
50	2.0.22	503
60	2.436	605
80	3.266	810
100	4.095	1015
120	4.919	1219
140	5.733	1420
160	6.539	1620
180	7.338	1817
200	8.137	2015
220	8.938	2213
240	9.745	2413
260	10.560	2614
280	11.381	2817
300	12.207	3022

Table 6.1 lists the ideal AD595 output voltages for a reference junction at 25°C. The output values for intermediate temperatures can be interpolated, or calculated using the output equations and ANSI thermocouple voltage tables.

6.1.3 MAXIM DALLAS MAX6675 Thermocouple Amplifier

The MAX6675 [134] thermocouple amplifier is a thermocouple-to-digital converter with a built-in 12-bit analog-to-digital converter and contains cold-junction compensation sensing and correction, a digital controller and a SPI interface. It is designed to work in conjunction with an external microcontroller or other intelligent monitoring applications. It produces a

12 bit digital output directly from type K thermocouple signal inputs, and is powered from a +5 V supply to provide a measuring range from 0°C to +1023.75 °C. The output range is 0.25 °C per bit.

6.1.3.1 MAX6675 Packaging

The MAX6675 is packaged in an 8 pin SOIC (Small Order Integrated Circuit). It can be soldered directly to a circuit board (Figure 6.3(a)), or connected to a circuit board via a SOIC to DIL adapter (Figure 6.3(b)). Figure 8.4 shows the thermocouple connection to the device and a mains ripple by-pass capacitor.

Figure 6.3 MAX 6675 SOIC package (a), SOIC to DIL converter (b) [134].

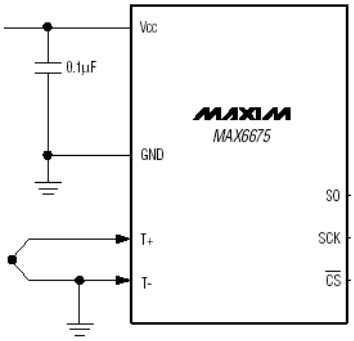

Figure 6.4 MAX6675 Thermocouple Connection [134].

6.1.3.2 MAX6675 Temperature Conversion

The signal-conditioning hardware reduces the introduction of noise errors from the T+ and T- thermocouple wires and converts the thermocouple's signal into a voltage. For type-K thermocouples, the MAX6675 transfer characteristic is 41µV/°C, approximating the thermocouple characteristic with the following linear equation:

$$V_{OUT} = (41\mu V / °C) . (T_R - T_{AMB}) \qquad (6.3)$$

Where:

V_{OUT} is the thermocouple output voltage (µV).

T_R is the temperature of the remote thermocouple junction (°C).

T_{AMB} is the ambient temperature (°C).

The MAX6675 reads the thermocouple hot end in the range from 0°C to +1023.75°C. The isothermal block (cold end) is in the range from -20°C to +85°C.

The ADC adds the cold-junction measurement with the amplified thermocouple voltage and outputs the 12-bit result onto the SO (Serial Out) pin. A sequence of all zeros is a reading of 0°C and a sequence of all ones is +1023.75°C.

The data reading from the thermocouple is processed and transmitted through a serial interface. Forcing pin CS (Chip Select) high initiates a new data conversion. Forcing CS pin low immediately stops any conversion process and applies a clock signal on pin SCK (Serial Clock) to read the results at pin SO. A complete data read requires 16 clock cycles.

BIT	DUMMY SIGN BIT	12-BIT TEMPERATURE READING												THERMOCOUPLE INPUT	DEVICE ID	STATE
Bit	15	14	13	12	11	10	9	8	7	6	5	4	3	2	1	0
	0	MSB											LSB		0	Three-state

Figure 6.5 12 bit ADC Resolution within 16 bit Digital out SPI frame [134].

The first bit, D15, is a dummy sign bit and is always zero. Bits D14–D3 contains the converted temperature in the order from the most significant bit (bit 14) to the least

significant bit (bit 3). Bit D2 is normally low and goes high when the thermocouple input is open. D1 is low to provide a device ID for the MAX6675 and bit D0 is three-state (Figure 6.5). The accuracy of the MAX6675 is susceptible to power supply coupled noise, which is minimized by placing a 0.1µF ceramic bypass capacitor close to the supply pin of the device (Figure 6.4).

6.1.4 Toothpick 2.1

Toothpick 2.1 [102] is an embedded Bluetooth module that integrates a low power Microchip PIC18LF6722 microcontroller [135] and a LinkMatik Bluetooth radio, preloaded with Toothpick Services firmware including FlexiPanel user interface server, Wireless Field Programming and Toothpick Slave host-controlled operation.

6.1.4.1 Toothpick 2.1 Packaging

The Toothpick 2.1 Bluetooth adapter is packaged on a 28 pin, 0.7”, DIL printed circuit board as shown in Figure 6.6(b) and Figure 6.6(a) shows the pin layout. Table 6.6 summarises the Toothpick electrical characteristics.

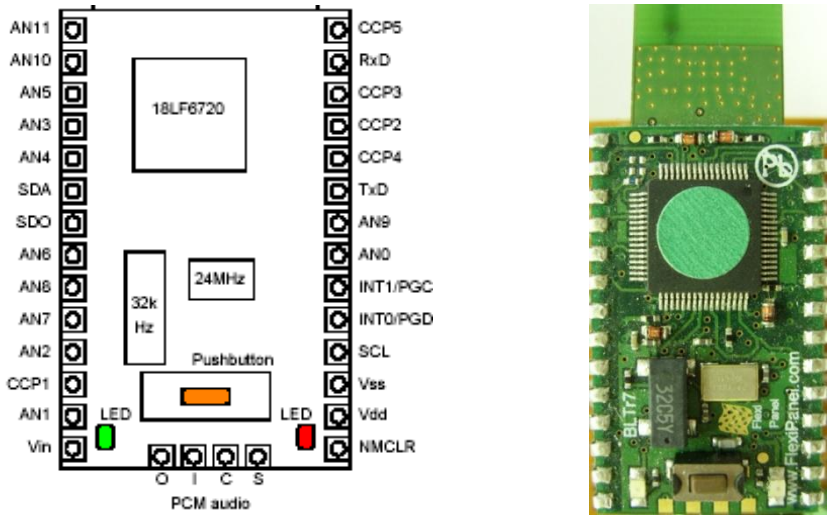

Figure 6.6 Pin Layout Toothpick 2.1. (a) schematic. (b) photograph [102].

6.1.4.2 Power Regulation

Toothpick power consumption is dominated by the LinkMatik radio, whose current consumption is 55mA during connection and device discovery. The Toothpick may be powered with a 3.2V – 5.5V regulated input to the Vdd pin. Alternatively, an unregulated input between 3.2V and 10V may be applied to the Vin pin where it will be regulated by a 400mA regulator. In this case, the Vdd pin functions as a 5V regulated power source for external circuitry. The total current draw in all I/O pins including Vdd must not exceed 200mA. The power regulator is a low-dropout type and will operate as an unregulated power source below 5V.

LinkMatik is separately regulated to operate at 3.2V – 5.0V, but requires 5V in transmit and receive modes. A 1µF tantalum capacitor is provided between Vin and Vss and a 100nF tantalum capacitor is provided between Vdd and Vss. When the Toothpick module is turned off, the 18LF6722 typically draws 10mA (plus I/O pin current drain) when clocked with the 20MHz oscillator and 50µA with the 32kHz oscillator.

6.1.4.3 Linkmatik 2.0 Bluetooth Radio Transceiver

LinkMatik 2.0 [136] is a serial to Bluetooth data link and can be interfaced to many standard Bluetooth devices, *e.g.* Laptop computers, PDA's, Mobile phones *etc*. The radio is a 2.4GHz Class I Bluetooth device with an integral antenna. The PIC microcontroller communicates with the Linkmatik radio via a UART serial port, with a wide range of baud rates up to 230 Kbaud over the serial port or 50 – 90 Kbaud over-the-air. Table 6.2 summarises the Bluetooth radio characteristics on the Linkmatik 2.0 radio.

Table 6.2 Bluetooth radio characteristics on the Linkmatik 2.0.

Characteristic	Value
Class	1
Maximum RF power output	100 mW / +20dBm
RF frequency range	2.402 GHz to 2.480 GHz
RF channels	79
Frequency hopping	1600 Hz
Range	100m
Data Rate	230 Kbaud
Maximum data rate over the air	50 – 90 Kbaud
Communication latency µP to µP	8 ms to 15 ms

6.1.4.4 USB Bluetooth Adapter

The USB adapter that receives the transmissions from the LinkMatik Bluetooth radio is a low power Ezurio 2.0+ EDR (Enhanced Data Rate, up to 3Mbps) Bluetooth adapter [137], incorporating Adaptive Frequency hopping to cope with interference from other wireless products and providing open field connectivity in excess of 300 metres (Figure 6.7). The USB adapter contains a fully compliant Bluetooth HCI interface enabling it to run with any approved Bluetooth protocol stack including Microsoft Windows XP SP2 and Windows CE.

Figure 6.7 Ezurio USB Bluetooth adapter [137].

6.1.5 Power Requirements

All the components for the telemetry system, either analogue or digital, have specific power requirements. Voltage input to the whole system is 5V because the AD595 is a 5V device and the Bluetooth radio drops out under 4.5V. Table 6.3 shows the power characteristics for

the AD595 and Table 6.4 for the MAX6675. Table 6.5 shows the power requirements for the Linkmatik Bluetooth radio and Table 6.6 for the Toothpick module.

Table 6.3 AD595 Power Characteristics.

	Voltage	**Current**	**Power**
AD595C	5V	160 □A	0.8 mW
MAX6675 idle	5V	1.5 mA	7.5 mW
MAX6675 Serial Out	5V	50 mA	250 mW
Toothpick module + Bluetooth	5V	60 mA	300 mW

Table 6.4 MAX6675 Power Characteristics.

	Voltage	Current	Power
MAX6675 idle	3.0V	1.5 mA	4.5 mW
MAX6675 Serial Out	3.0V	50 mA	150 mW
PICμC + signal input	3.0V	25 mA	75 mW
Toothpick module + Bluetooth	3.0V	60 mA	180 mW

Table 6.5 Electrical characteristics for the Linkmatik 2.0 Radio.

Characteristic	Function	Value
Supply Voltage	Regulated	3.2V – 5.1V
Average Current	Idle	3 mA
	Connection & Discovery	55 mA
	Connected & Tx	22 mA
	Connected & Rx	33 mA
	Sleep mode	370μA – 1.5mA
Maximum Voltage	Any IO pin	-0.4V – Vdd + 0.1V

Table 6.6 Electrical characteristics for the Toothpick 2.1

Characteristic	Function	Value
Supply Voltage	Regulated	3.2V – 5.5V
	Unregulated	3.2V – 10V
Average Current	Idle	10 mA
	Connection & Discovery	60 mA
	Connected & Tx	30 mA
	Connected & Rx	40 mA
	Lowest sleep mode	370µA
Maximum Voltage	Any IO pin	-0.5V – Vdd + 0.1V
Maximum Current	Any IO pin	25 mA
	Total on all pins	200 mA

6.1.6 Sampling Rates

The PIC18LF6722 has selectable clock frequencies and minimum and maximum data acquisition times, described in the PIC18LF6722 data sheet [135]. Taking the maximum clock period and maximum acquisition time gives a theoretical sampling frequency of 3306 Hz. Using the minimum clock periods and minimum acquisition times, gives a maximum sampling frequency of 54945 Hz. SPI slave device interfaces output data at frequencies determined by the master device. The MAX6675 can output data at up to 4 MHz, or any frequency below this. As stated previously, the Bluetooth radio transmits over-the-air at between 50 to 90 Kbaud. As one byte requires 10 bits to transmit, and therefore two bytes require 20 bits to transmit, then 50 Kbaud can transmit upto 2500 samples/sec and 90 Kbaud can transmit upto 4500 samples/sec for 16 bit integer values. The PIC is hardware sampling, whereas firmware is software sampling. The exact sampling rate is undetermined at this juncture because software sampling involves the overhead of function calls and instruction set execution times, which add to the time taken to call the sampling function.

6.1.7 Bluetooth Module Firmware

The PIC18LF6722 microcontroller controls the connected amplifiers through firmware uploaded into controller memory. The simplest method to create the firmware is to employ an Integrated Development Environment (IDE) suite for writing source code and converting to Hex files (firmware). The embedded firmware requires Hex files for uploading to the microcontroller. Any software development language may be used to create the source code for the Hex file, but most common is C or assembler. A method for uploading the firmware to the microcontroller is also required. This may be via hardware (cable) upload or via a wireless link.

6.2 Software

The system software components include a Bluetooth stack for communication between two or more Bluetooth devices, a software development suite and IDE to create the firmware that is uploaded to the microcontroller, and a user interface design program.

6.2.1 Bluetooth

The Bluetooth stack used by The Toothpick Bluetooth DAQ module is the Microsoft Bluetooth stack Windows XP SP2 implementation. The Bluetooth adapter on the host PC must also use this implementation.

6.2.2 Application Development

There are four methods in which to develop an application for the Toothpick: (1) Develop applications in C using MPLAB C18 from Microchip. This allows the developer to take advantage of the FlexiPanel Toothpick Services; (2) Develop applications using any other suitable microcontroller development system, although the Toothpick Services will no

longer be available with this method; (3) Use a pre-compiled FlexiPanel standalone firmware solution such as Data Acquisition and Remote Control; (4) Use the Toothpick Slave Firmware Solution to allow Toothpick to be controlled by a host processor.

6.2.2.1 User Interface Development

Applications that use the FlexiPanel User Interface Server use the FlexiPanel Designer to create user interfaces. User interfaces for firmware solutions are programmed into Toothpick directly using the Bluetooth link. User interfaces developed for applications using C18 are encoded as files to be included in a MPLAB development project [102].

6.2.2.2 Development Using MPLAB C18

Applications developed using MPLAB C18 can take advantage of the pre-loaded Toothpick Services and can be programmed either conventionally using In Circuit Programming or using the wireless field programmer [102]. Wireless Field Programming reduces costs as upgrades can be distributed electronically using a TEAclipper programming clip [138].

6.2.2.3 Alternative Development Systems

Toothpick applications can be developed using PIC development environments other than MPLAB, although complete erasure of the pre-loaded Toothpick Services will be necessary, making them unavailable to the application [102].

6.2.2.4 Standalone Firmware Solutions

Standalone Firmware Solutions are compiled using MPLAB C18 and the available source code allows developers to use them as starting points for custom applications. Precompiled,

or user developed standalone firmware solutions are converted to ‘Service Packs’ and loaded via Wireless Field Programming [102].

6.2.2.5 Development Using Toothpick Slave

Toothpick can be connected as a slave, in which case it would be controlled by an external microcontroller via a serial interface.

6.2.3 MPLAB

The Microchip MPLAB Integrated Development Environment (IDE) [139] is an editor, project manager and design desktop for application development using Microchip PIC microcontrollers and dsPIC DSCs. Application code is created that is executable by a target PIC microcontroller. The source code files are then built into executable code using language tools (assemblers, compilers, linkers, etc.).

6.2.4 C18

MPLAB C18 [140] is a cross-compiler that runs on a PC and converts standard ANSI C code into machine code to build the .hex file that can be programmed into a Microchip PIC18xxxx device. Blocks of program source code (.C files and .H files), library files, and data are “linked” by the compiler and placed into the various memory regions of the PIC18LF6722 microcontroller. The MPLAB graphical user interface serves as a single environment to write, compile and debug code for embedded applications. Flexipanel firmware code can be developed with MPLAB to retain the Toothpick services within the application.

6.2.5 MPLAB SIM Testing Code with the Simulator

A debug tool is a hardware or software tool that is used to inspect code as it executes a program or selected PIC microcontroller instructions. Hardware tools execute instruction code in real devices although they typically cannot monitor all registers and all memory in real time. A Simulator is a software program that runs on a PC to simulate the execution of the instructions for the selected PIC microcontroller. MPLAB SIM [139] simulator integrates with MPLAB to test the developed PIC source code. It does not run in "real time," since the simulator program is dependent upon the speed of the PC, the complexity of the code, overhead from the operating system and how many other tasks are running. However, the simulator accurately measures the time it would take to execute the code if it were operating in real time in an application.

MPLAB SIM execute instructions, communicates with peripherals through function registers, allows viewing of register and variable values and the stimulus generator can simulate real world input and send signals to pins or registers in the simulator. Activity of the simulator can be sent to a Log file for later analysis. Figure 6.8 shows The MPLAB SIM interface displaying the project folder, the source code pane, the watch window, allowing variable values to be monitored, and the output window.

6.2.6 Flexipanel

Flexipanel is a design environment for the Toothpick 2.1 module to create the firmware, including servers or client interfaces and incorporates the proprietary Flexipanel services.

6.2.6.1 Flexipanel Designer

When FlexiPanel Clients connect to FlexiPanel Servers, the server tells the client to display the desired user interface (Figure 6.9). The server may modify the contents and appearance of the controls at any time [141]. FlexiPanel Clients provide all the requested controls on the user interface, but interface appearance may vary on different devices.

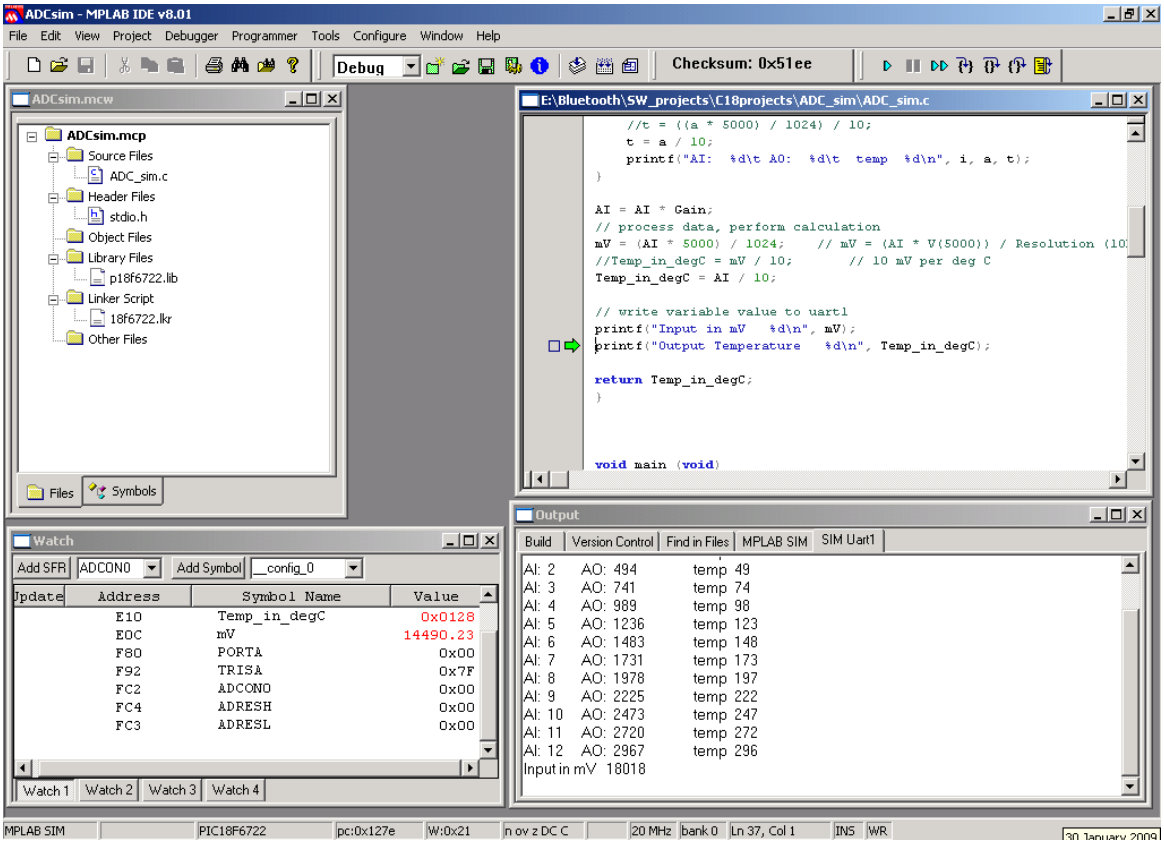

Figure 6.8 MPLAB SIM interface [139].

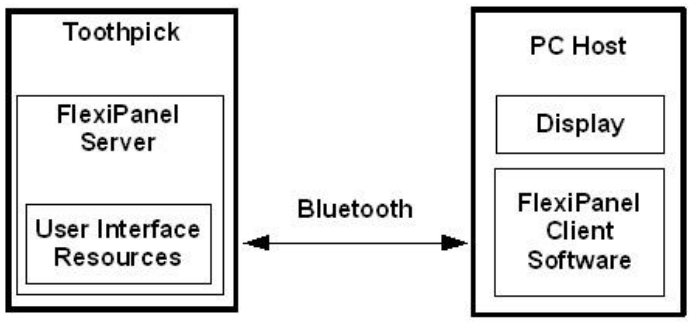

Figure 6.9 Transmission between Toothpick and PC host [141].

FlexiPanel Designer manages the different aspects of the user interface controls, such as how they appear on specific client software, etc (Figure 6.10) and then programmed into a specific target such as a FlexiPanel DARC (Data Acquisition Remote Control) module [142]. The communication standard used by FlexiPanel Designer 3.0 to communicate with clients is FlexiPanel Protocol 3.0.

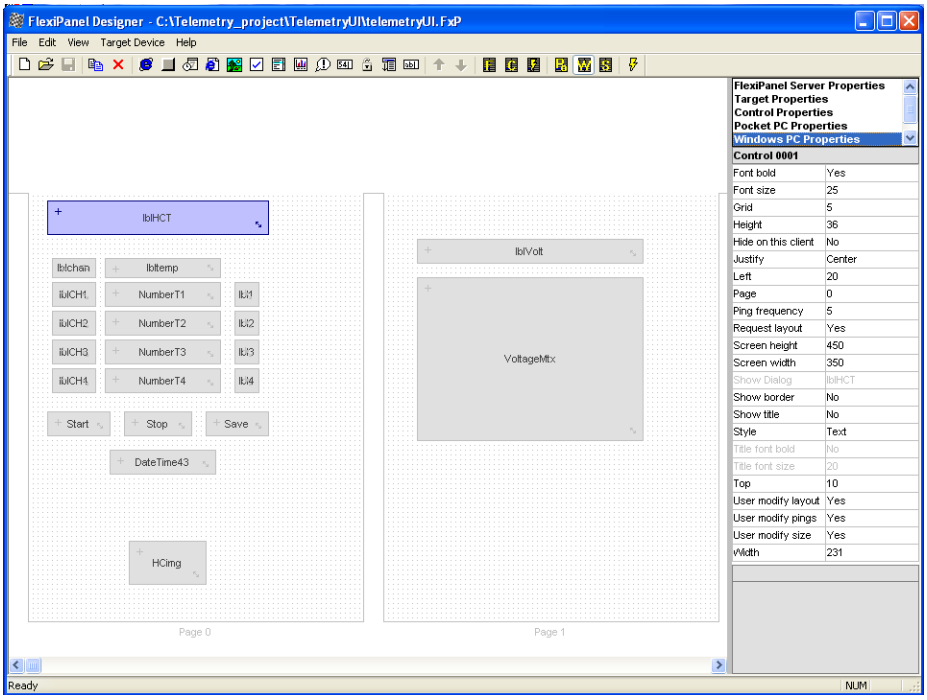

Figure 6.10 FlexiPanel designer control layout [141].

6.2.6.2 Flexipanel Server

The FlexiPanel server allows remote devices such as Windows PCs, handheld devices and cell phones to display user interfaces on its behalf using FlexiPanel client software. The interface specifications are stored on the server and transmitted to the client using the FlexiPanel Bluetooth Protocol. The user interface specification is created using FlexiPanel Designer software. Server and client communicate by passing messages. The server

transmits processed data to clients by transmitting information about the 'logical' user interface. Messages begin with a 20 byte header detailing the message content, followed by the actual data content. Error correction is assumed to be managed by the Bluetooth protocol.

6.2.6.3 Flexipanel firmware

Firmware can be created by one of three methods: Firmware developed with Flexipanel designer; saving hex files as a service pack; or using a pre-compiled service pack. Hex files can be created by using the MPLAB environment to develop and compile code to obtain the resultant hex file. A Service pack can be created by executing the toothpickWFP.exe utility and saving the hex file as a service pack. The designer firmware or service pack can then be uploaded to the microcontroller via the Bluetooth link.

6.2.6.4 Wireless Field Programming

Toothpick's wireless field programmer allows both developer and Toothpick Services firmware to be uploaded using a Bluetooth-equipped PC, and firmware can be upgraded at a later date as required. FlexiPanel proprietary services implement the Bluetooth stack on the Toothpick device and the PC host, via a USB adapter, and manage the data transfer between the PIC microcontroller and LinkMatik Bluetooth radio.

6.2.6.5 HexWax

HexWax Explorer [143] is a firmware management utility for charging TEAclipper programming clips with firmware via a USB adapter (Figure 6.11). Firmware can be the hex file created by MPLAB and charged to the TEAclipper instead of creating a service pack with FlexiPanel.

Figure 6.11 TeaClipper programmer and USB adapter [143].

6.2.7 Proteus PCB design

Proteus PCB design [144] is an integrated suite of tools for professional PCB Design. Proteus 7.2 can also simulate ARM and Microchip PIC controllers and peripherals.

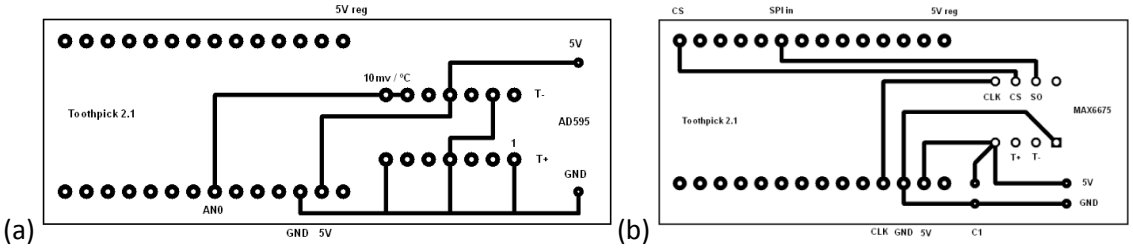

Figure 6.12 PCB Pin layout for AD595 (a) and MAX6675 (b).

Figure 6.12 shows The PCB layout for the Toothpick 2.1 embedded Bluetooth module and the AD595 thermocouple amplifier (a) and MAX6675 thermocouple amplifier (b).

6.3 Summary

A description is given of the hardware components used in the prototype telemetry system and the software used to develop the data acquisition firmware. The hardware consists of thermocouples and thermocouple amplifiers, a Bluetooth data acquisition module incorporating a Bluetooth radio and microprocessor to which firmware is uploaded. Power requirements for the system are indicated and how various characteristics of the hardware influence the sampling rates of the system. For the software utilised, a description of how the Bluetooth stack is incorporated into the data acquisition module is given, then, by using

MPLAB develop suite, how firmware is written in C and tested before uploading to the microprocessor, and using Flexipanel Designer to develop the user interface. PCB CAD design software is employed to design the printed circuit boards for the system components.

7 Test and Results

A test rig is employed to test the power generator and electronics to confirm that it can produce the required output. The velocity of the rotor is calculated for various test speeds and voltage readings taken for various test speeds and air gaps between rotor and stator. A piston and connection rod are instrumented with the power generator and electronic circuits and output data is displayed on a client interface on a host PC. The power generator output is determined for the magnet type, velocity of the magnet passing the coil and the number of turns of the coil. Empirical voltage measurements of the generator output were taken to confirm the calculated output.

7.1 Test Rig

The test rig comprises of a Griffn & George AC motor 9 with a speed range of 2000 rpm to 6500 rpm, as measured with a digital tachometer, an acrylic disc incorporating twelve 10mm x 5mm permanent NdFeB magnets [72], an acrylic disc supporting twelve stator coils (Figure 7.2(b)), an AD595 analogue thermocouple amplifier [133], a MAX6675 digital thermocouple amplifier [134], a MAX756 DC-DC step-up converter [132], a DB101G full-wave bridge rectifier [131]. The induction coil is 0.4mm enamelled copper wire.

7.1.1 Thermocouple Simulation

A resistor potential divider board simulates thermocouple analogue voltages input to four AI channels on the Toothpick DAQ module which performs analogue to digital conversion. The AD595 has a temperature range of 0 to 300°C and outputs 10mV / °C, therefore the output voltage range of the potential dividers are set between 10mV for 1°C and 3V for 300°C.

7.1.2 Induction Power Generator

The induction generator comprises the motor, a 10 cm diameter rotor disc of twelve permanent magnets, and a 10 cm diameter stator disc, with various windings. The windings are twelve 2mm thick coils of 35 turns each, twelve planar coils of 20 turns and twelve planar coils of 15 turns. The stator coils are formed with 0.4mm enamelled copper wire.

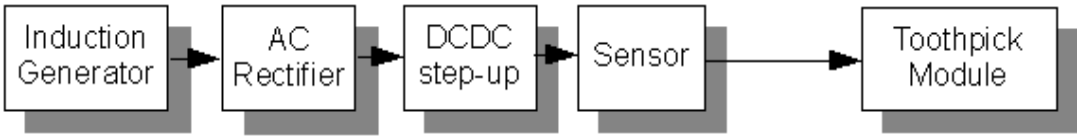

Figure 7.1 Block Diagram of Power Generation.

Figure 7.1 shows a block diagram of the power generator, transducer and DAQ module and Figure 7.2 shows the rotor (a) and power generator (b). The AC motor turned the magnet disc, inducing an AC current in the coil. The AC current is rectified by a DB101G full-wave rectifier to produce a DC voltage output. A capacitor filters (smoothes) the rectified output to reduce the ripple that is present on all rectifier circuits. The smoothing capacitor is an electrolytic type. Values of 47µF and 470µF were used.

[a] 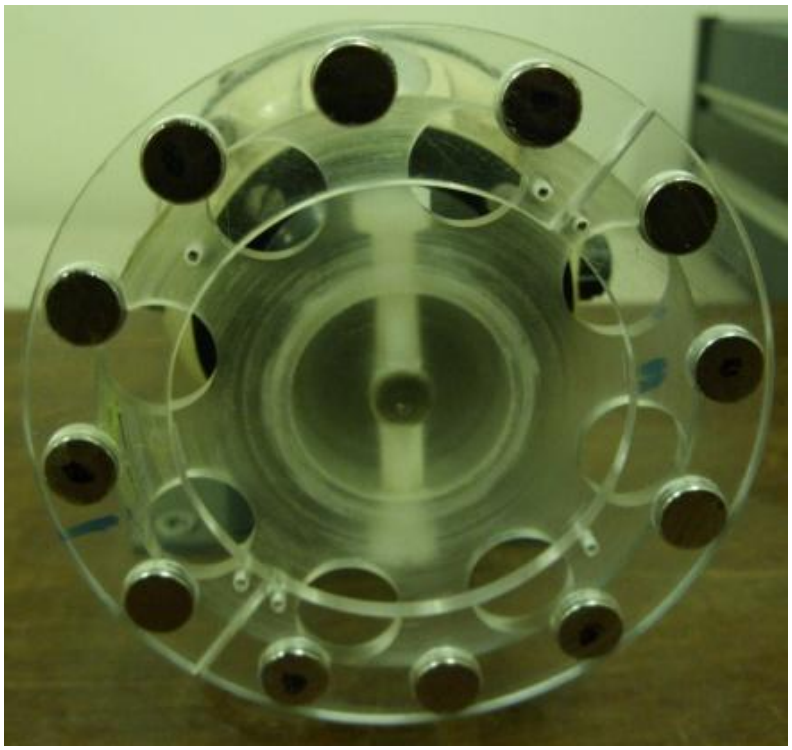

[b] 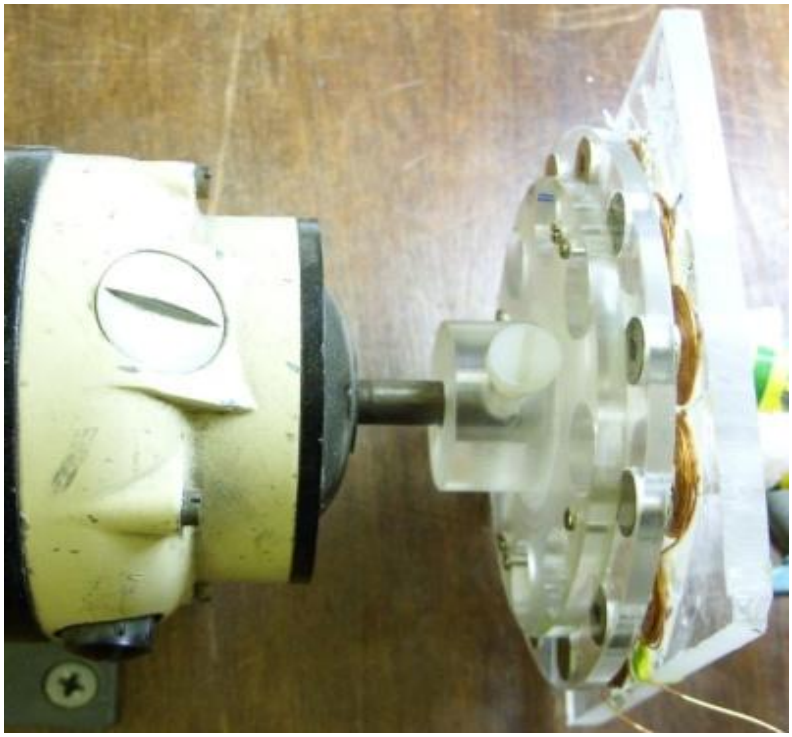

Figure 7.2 Rotor (a) and motor test rig (b).

The output from the capacitor is then fed to the input of the MAX756 step-up converter, where the input voltage is converted to 5V output. The output of the step-up converter drives the thermocouple amplifier which is connected to the ‘cold end’ of a type K thermocouple (Figure 7.3). The output from an analogue thermocouple amplifier is taken to an analogue IO pin on the Toothpick Bluetooth module DAQ device, whereas a digital thermocouple amplifier output is connected to the SPI interface of the Toothpick Bluetooth module DAQ device.

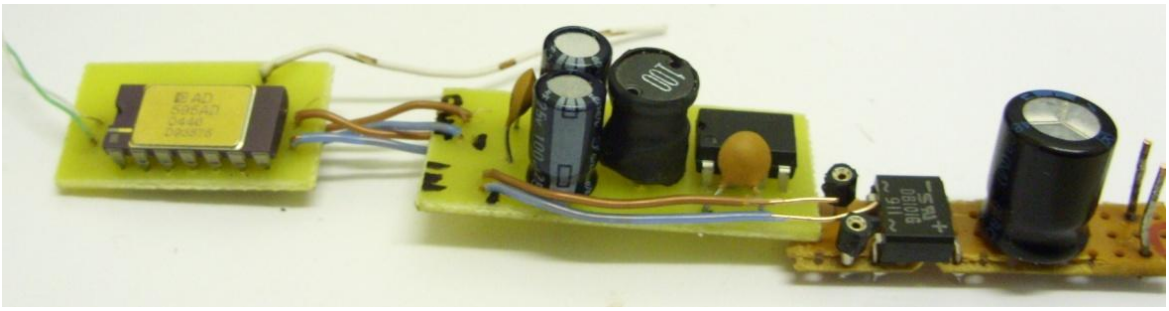

Figure 7.3 Analogue sensor, step-up converter and rectifier.

The MAX756 datasheet states that a voltage as low as 0.7V can be input to the device in order to produce the 3V or 5V output. Initially, approximately 2.0V is required to start the MAX756 device, and then may be reduced to 0.7V to continue operation.

The expected signals are an AC induced voltage at the power generator, DC voltage after the rectifier and 5V from the step up converter. The thermocouple voltage is 0 – 12mV (0 - 300°C) and is converted by the thermocouple amplifier to 0 – 3V output (0 - 300°C). The electronic devices require up to 5V supply and the step up converter requires a voltage in the range of 0.7V – 5V.

7.2 Voltage Produced by Inductor

When magnets pass a coil, they instigating a north-south transition of magnetic polarity through to the coil. It is this north-south transition that induces a current, and therefore a voltage, in the coil. The flux density value is calculated for the dimensions of the magnet and the magnetic remanence value is obtained from the magnet data sheet. The motor speeds were selected with a manual selector, from minimum position of 2000 rpm, ¼ position of 3125 rpm, ½ position of 4250 rpm, ¾ position of 5375 rpm and maximum position of 6500 rpm. Table 7.1 shows the velocity of a single magnet and therefore the velocity of north-south transitions. Equation 7.1 states the equation to calculate the voltage induced in a coil of a given dimension.

Table 7.1 Magnet Velocity at Selected Motor Speeds

Magnet Velocity at Selected Motor Speeds					
Disc Diameter (cm)	10	Circumference (cm)			31.4
Magnets	12				
Motor Speed (rpm)	2000	3000	4000	5000	6500
Magnet Velocity (m/s)	126	188	251	314	408

Voltage produced by inductor [145]:

$$\varepsilon = \beta.l.v \quad \text{volts} \qquad (7.1)$$

Where:

β = flux density Tesla

l = length of coil metres

v = velocity m/s

$$l = 2\pi \times R_{avg} \times N \qquad (7.2)$$

Where:

R_{avg} = average radius of spiral coil mm

N = number of turns

$$R_{avg} = (Di + N(W+S)) / 2 \qquad (7.3)$$

Where:

Di = inner diameter of spiral coil mm

N = number of turns

W = wire diameter mm

S = spacing between wire mm

$$v = (\pi D) / 100) \times (rpm / 60) \qquad (7.4)$$

Where:

D = diameter of rotor cm

The voltage readings are taken to determine the rotor speed at which 5V is output in order to drive the electronics, and the speed at which the step up converter activates (approx. 1.4V) and minimum activation speed (0.7v).

The test rig was run at the selected speeds, with the stator coils at three different air gaps from the rotor of 1mm, 3mm and 5mm. Charts of the induced voltages for the 15 turn

planar coil (Figure 7.4), 20 turn planar coil (Figure 7.5) and 35 turn multi layer (2 mm deep) coil (Figure 7.6) are shown for comparison of how coils influence induced voltage.

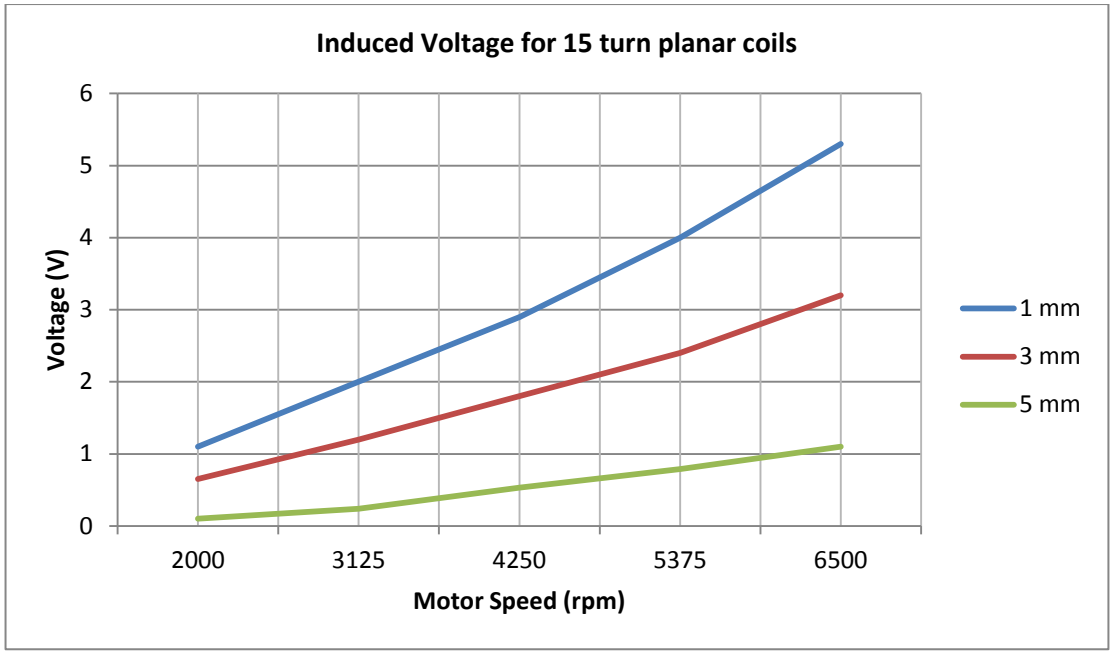

Figure 7.4 Induced Stator Voltage for 15 turn Planar Coils.

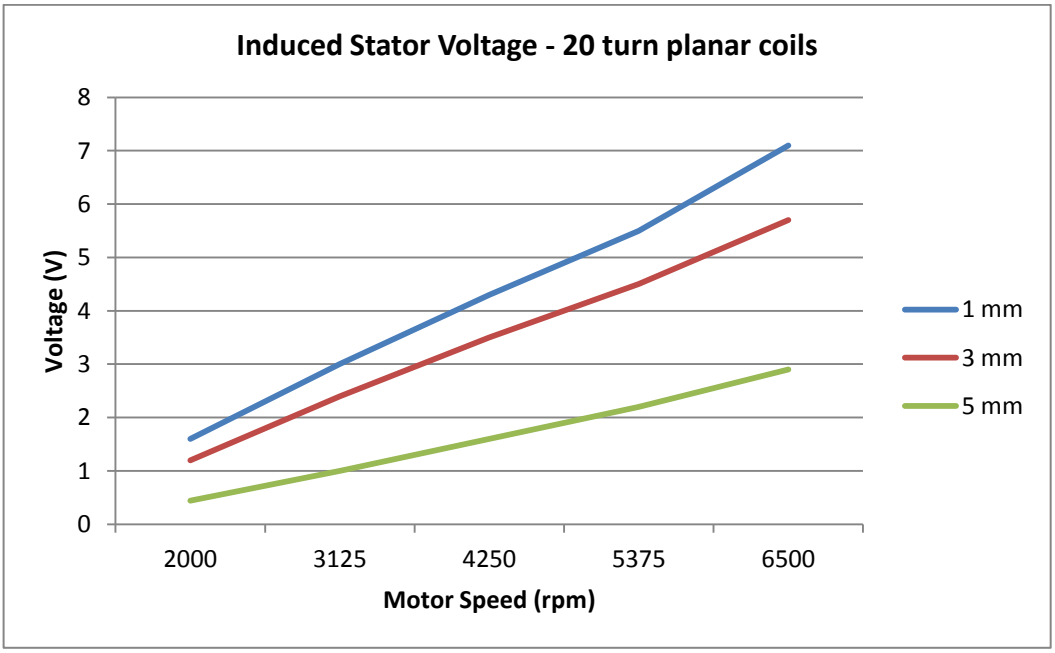

Figure 7.5 Induced Stator Voltage for 20 turn Planar Coils.

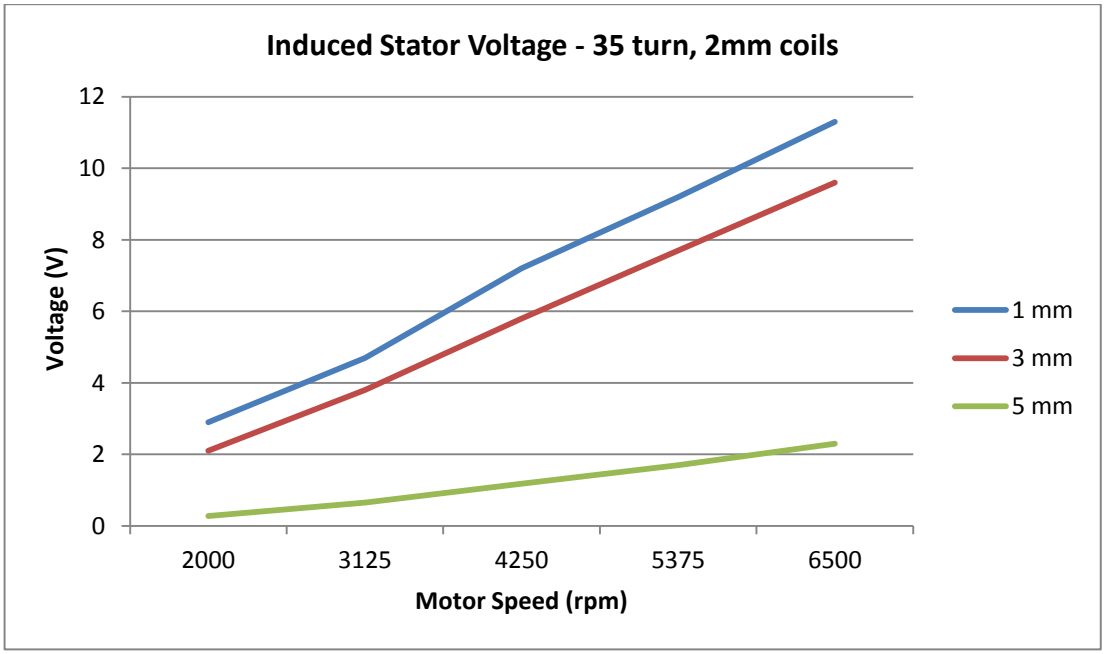

Figure 7.6 Induced Stator Voltage for 2 mm deep Coils.

Four parameters affect the induced voltage, the size of magnets, the size of coil (diameter and number of turns), speed of the rotor (north-south transition frequency) and the air gap between magnet and coil. Increasing any of the first three parameters will increase the induced voltage. Increasing the forth, air gap, will reduce the induced voltage. The figures (7.4, 7.5 and 7.6) show that for a constant magnet size and constant coil size, it is the rotor speed that increases the induced voltage. The figures also show that if the air gap is increased, then not only is the amount of induced voltage lower, but the rate of increase is also diminished.

If the air gap is increased, the flux density value decreases and thus the induced voltage is lower. As the air gap increases, the flux density does not decrease linearly but is a curvilinear plot (Figure 7.7). Inversely therefore, as the air gap decreases, the rate at which voltage is induced increases.

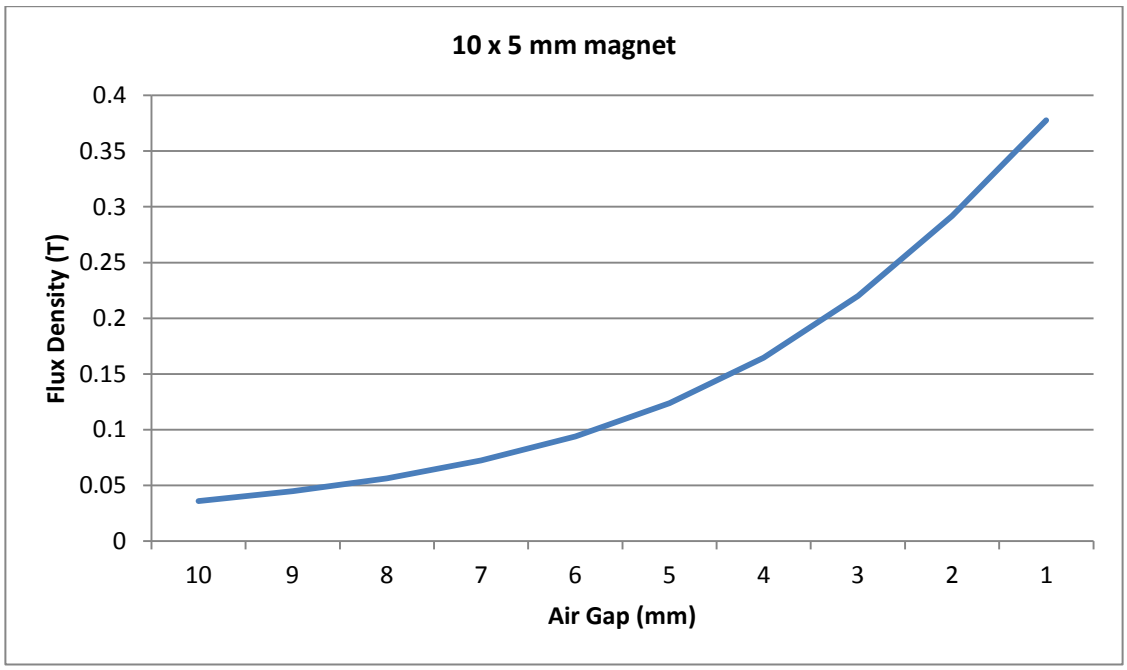

Figure 7.7 Plot of flux density as air gap decreases

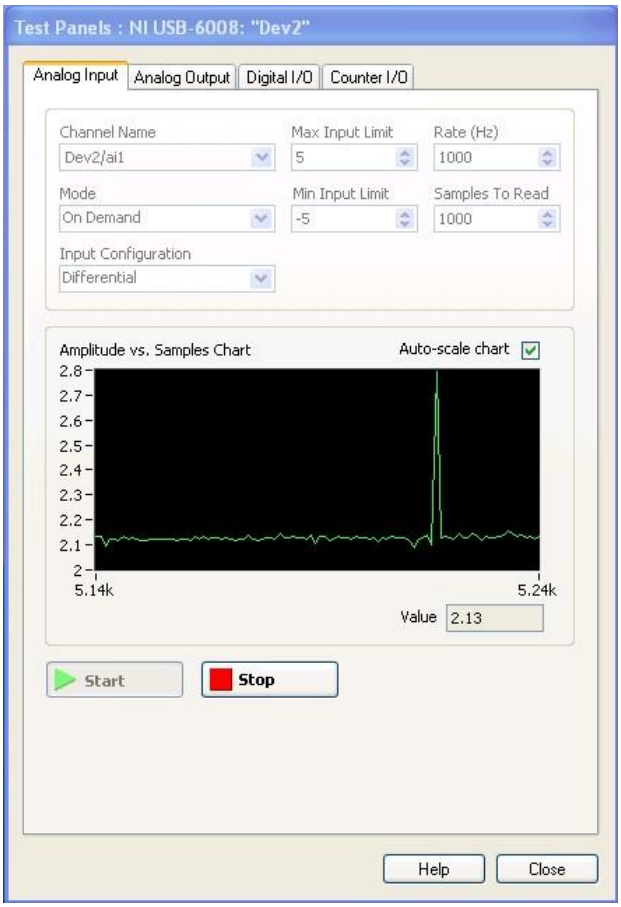

Figure 7.8 NI USB 6008 test panel

Figure 7.8 shows the NI USB 6008 DAQ device test panel displaying the acquired analogue signal from the AD595 amplifier when connected to a type K thermocouple, whose probe end is applied to a heat source. The DAQ device reads an average of 2.13V which, at 10mV / °C, equates to 213°C temperature.

7.2.1 Location of components on piston

The stator coils are wound onto a split acrylic stator ring formed to shape of piston con rod big end (Figure 7.9). The ring also includes formers that are the diameter of the inner coil (5 mm) and height of the multi layer winding (2 mm). Figure 7.10 shows the stator positioned on piston big end (a) and on a crankshaft (b).

Figure 7.11 shows an AD595 thermocouple amplifier positioned on con rod big end with the thermocouple leads taken to the piston. It is positioned at the big end for two reasons, one, to place it at a lower temperature than inside the piston, and two, to have a wider temperature difference between the sensor isothermal block and the thermocouple hot end, for a more accurate reading. Figure 7.12 shows the sensor, power generator electronics and Bluetooth DAQ device positioned on the piston big end.

Figure 7.9 Stator Ring.

(a)  (b) 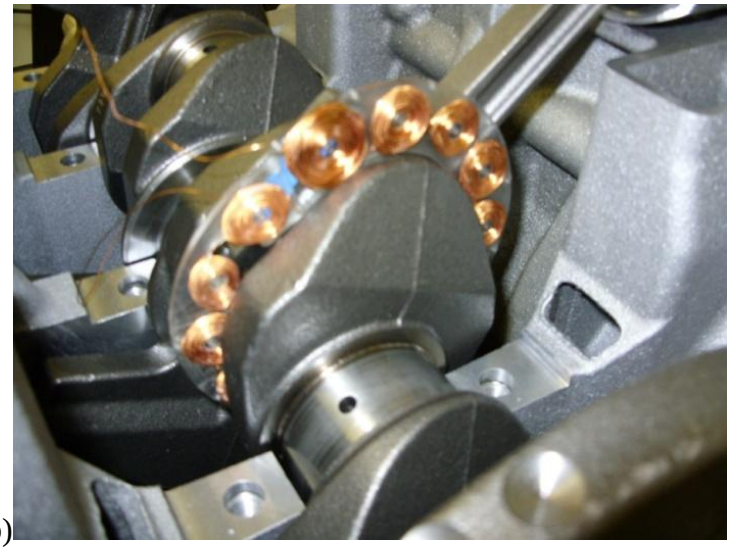

Figure 7.10 Stator on Piston (a) and Crankshaft (b)

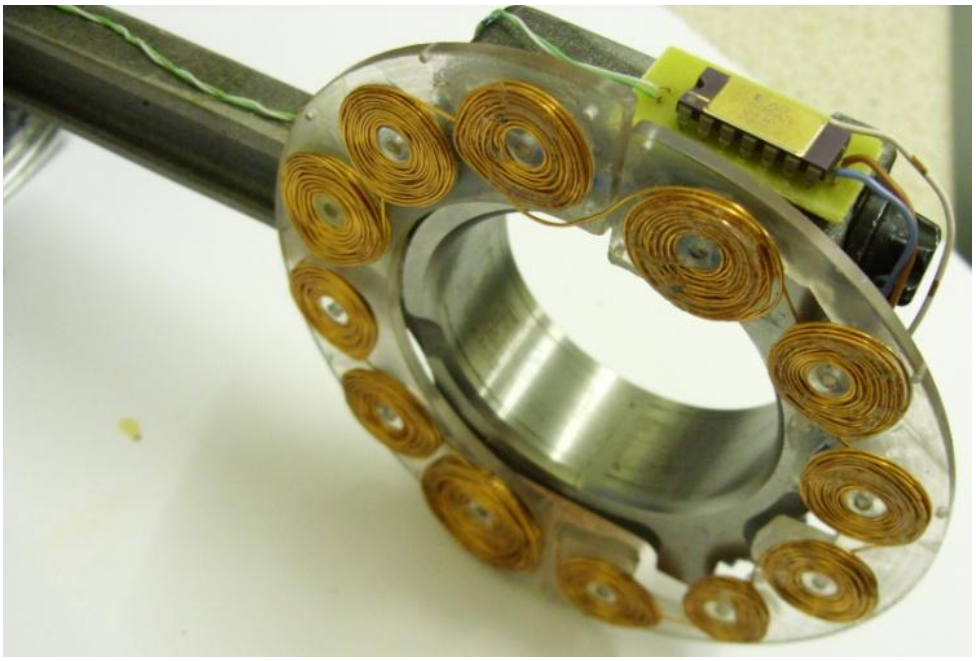

Figure 7.11 Sensor positioned on big end

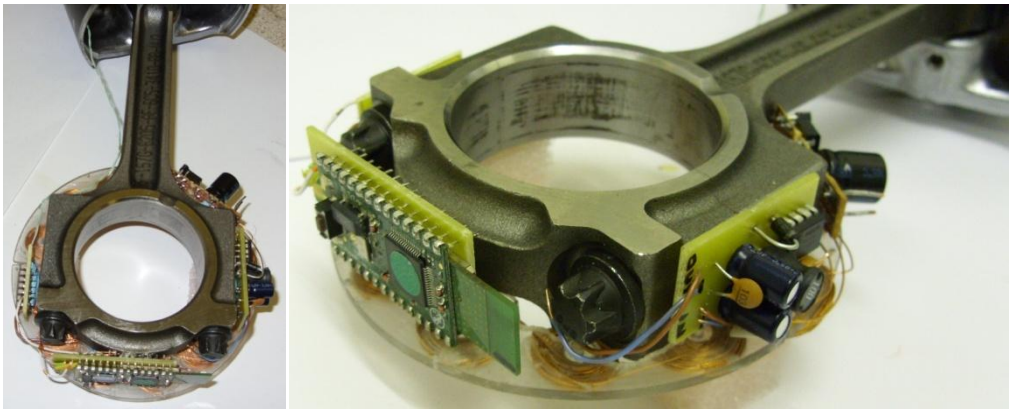

Figure 7.12 Telemetry electronics positioned on big end

7.2.2 Host Client Interface

The electric motor turns the rotor so that the power generator delivers a voltage to the data acquisition system and telemetry system to show they are working. The input to the Toothpick Bluetooth module DAQ device is processed by the embedded firmware and converted to the appropriate temperature value. These temperature values are then displayed on the client interface of the host PC. The values can be displayed as numerical values on the user designed interface, as a graphical plot, or as a list of values that can then be saved to an Excel file in CSV format. If the data is to be saved, then the amount of data that can be saved is dependant on the available free memory, which is dependant on the size of the firmware code that is uploaded to the embedded device. Extra memory (up to 1Mb) can be connected to the PIC microcontroller, but as the PIC is integrated into the Bluetooth module, any external memory must be connected externally to the Toothpick device itself.

Figure 7.13 shows the client interface when connected to an analogue thermocouple amplifier (a) and a digital thermocouple amplifier (b). The analogue amplifier interface (a)

is designed with two pages (dialogues), and the second page displays the analogue voltage input as a graph (Figure 7.14 (a)). Selecting the hash button (#) from the plot window displays the analogue voltage as a list of values with associated timestamp (Figure 7.14 (b)). Selecting a save button saves the data to an Excel file in either CSV format (,) or CSV format (;).

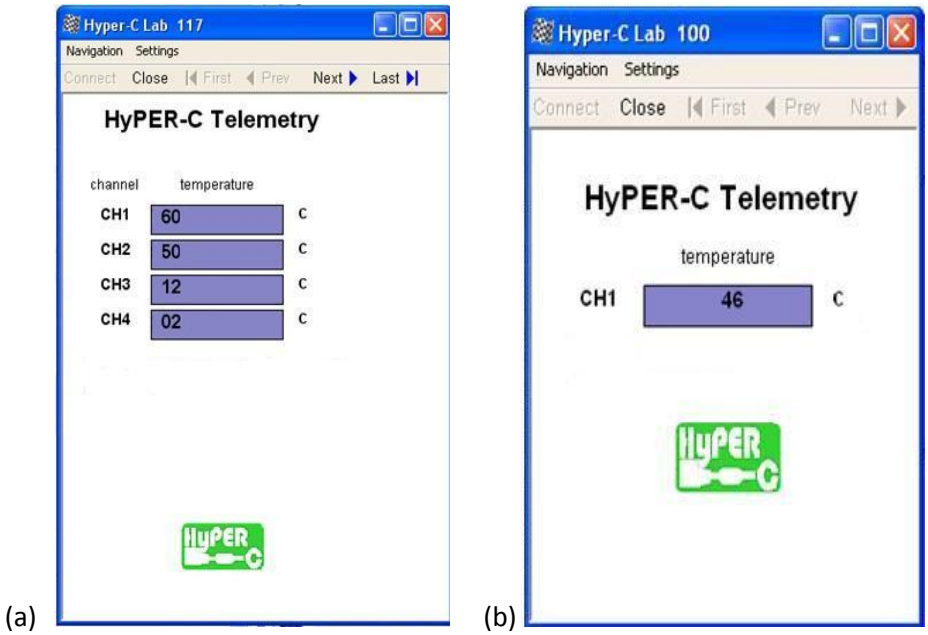

Figure 7.13 Client Interface (a) analogue DAQ (b) digital DAQ.

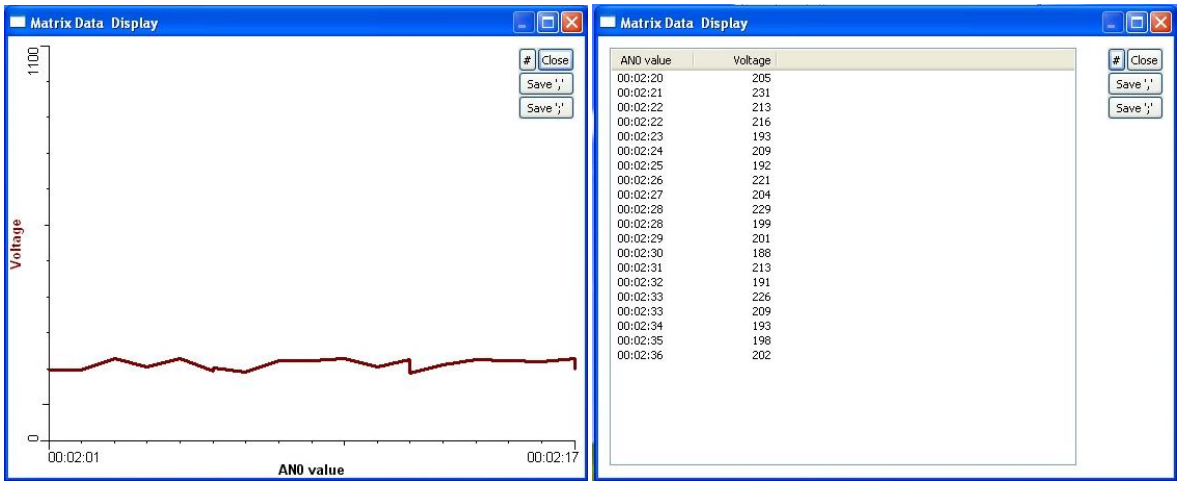

Figure 7.14 Analogue channel voltage: (a) plot (b) by value.

The C code firmware listings for analogue input and SPI interface for digital input are in the appendix.

7.3 Summary

A test rig is constructed to implement a test procedure to confirm that the power generator generates a voltage and current by rotating the rotor adjacent to the stator.

Calculations are shown to indicate the theoretical induced voltages of the power generator for the stated magnet size and coil size and empirically measured voltages output from the power generator after rectification to DC are shown as a table and as plots to confirm the expected voltage output. The electronics for the telemetry system, to be supplied by the power generator, are located on the piston connection rod big end and photographs show the components can be adequately located at this position without the necessity for connection rod modification. User interfaces show analogue and digital input, and signals displayed as a plot or as a value table that could be saved to a spreadsheet.

8 Conclusions and Future Work

8.1 Conclusion

In this work the telemetry system described is a prototype, whose scope excludes harsh environments, and is developed to take measurements of voltages that represent temperature. In order to reduce emissions and fuel consumption as regulations become stricter, there is a requirement for a more precise control of the engine and temperature measurements. Piston telemetry can help achieve this and is extensively used in research and development to acquire the temperature data used to design more efficient engines and pistons. The prototype system is robust, reliable and a more cost effective method than existing systems or techniques available at the moment, such as Manner Sensortelemetrie, one of the best available systems.

It is a wireless telemetry system that has been selected for development with low power requirements provided by an independent power generator, integrated signal processing and the high integrity of digital data transmission.

The mechatronic design of the prototype, incorporating an independent low voltage power generator, provides a complete wireless telemetry system, without the requirement for slip rings, power cables or transmission cables.

The prototype telemetry system is a compromise between components, functionality and software development. Ease of firmware development in the C language with a public domain IDE and over the air (wireless) firmware uploading contributes to the flexibility and modularity of the system.

The power generator is designed to be compact and to be easily attached to a piston connection rod, thereby eliminating the need to machine any engine components for fitting purposes. The physical size of the generator can be adapted to meet application requirements by selecting parameters for magnet size, diameter of wire, number of turns in the coil and rotational speed of the generator to produce the desired output voltage. In other induction systems a mains power supply is required to transfer power to and data from a telemetry unit, necessitating that data acquisition is always performed in the vicinity of the engine.

The prototype generator comprises of a single stator disc and single rotor disc. The axial flux magnet/coil configuration results in a compact design producing power for the whole rotational cycle of the piston. The simple configuration of concentrated single phase planar coils is without the cogging, core losses and eddy current loss complexities of a 3 phase induction machine.

The operating speed of the power generator is not a trivial choice to make and consideration of the rpm range of the engine is required. With a high number of coil turns, a large induced voltage could destroy the electronic components, so therefore a linear regulator is required at high rpm, but at low rpm, insufficient voltage is produced to drive the regulator. With a low number of coil turns, at low rpm sufficient voltage is produced to drive a step-up converter, but at high rpm may produce a large voltage to destroy

components. If temperature data is acquired at high rpm, then reducing the size of coil and / or the number of turns to provide a low voltage to drive a step-up converter, keeps the size of the generator compact.

When employing RF methods, the temperature data is modulated onto a carrier signal for telemetry transmission. The raise in temperature in the engine will cause the carrier frequency of the telemetry signal to drift and a compensating electronic circuit must be created to calibrate the carrier signal so that it can be demodulated by the receiver. Bluetooth receiver design includes processing of the carrier frequency to eliminate drift.

The present system has limitations of space constraints when applied to small engines, but can be easily developed for large pistons that have the capacity to accommodate the DAQ telemetry system internally.

This system reduces the amount of signal post processing required. Signal processing is transferred from software processing on a PC to electronic hardware processing on the sensors. The results are then transmitted to a host and displayed via a generic interface available on a number of devices instead of a bespoke interface on a single device.

Bluetooth is well known technology and is able to connect to many types of devices including a PC or smart phone, transmitting digital data, not voltage level values as in the Manner system.

The Manner telemetry system requires a significant amount of signal processing and post processing. Precise alignment of induction coils is required and transmission is available for only 76° of the rotational cycle. The employment of a mains power supply and voltage signals in the 0 – 10V range exceed the voltage requirements of modern electronics.

Bespoke software development is then required to develop a user interface and perform signal post processing by using lookup tables for temperature values.

8.2 Recommendations for Further Work

To place the telemetry system within a harsh environment and to investigate thermal adhesives and thermal insulation materials to encapsulate the components and thus lower the environmental ambient temperature.

To reduce the power requirements by investigating the feasibility of a printed circuit board stator in order to reduce the thickness of the generator. As MEMS devices evolve to produce higher power, investigate an array of accelerometers or thermal scavengers that may be employed to drive thermocouple amplifiers. Develop a dual current induction power generator with high current generation for the toothpick module and low current for the low power electronics. Investigate Ultra Low Power Bluetooth (WiBree) integrated with a low power microcontroller to establish feasibility of a low power Bluetooth DAQ system.

Develop WEB connectivity. The Toothpick DAQ module allows files to be sent to the client. The primary use is to pass HTML files, so a web browser on the client could display the files. As the files are stored on Toothpick module, an internet connection is not required to transmit the files to the client. The acquired temperature data could be passed to a web service that transfers the data as an XML file to an Adobe flex application in a remote web browser, displaying the data in any desired format, e.g. as a plot graph.

Reference

1. Bellis, M. *Telemetry*. http://inventors.about.com/library/inventors/bltelemetry.htm. Sep 2007

2. *NI Webcast: Wireless Technologies for Data Acquisition*. www.ni.com. Mar 2009

3. *Telemetry Systems Overview*. http://www.l-3com.com/tw/tutorial/telemetry_system_overview.html. Sep 2007

4. *Federal Mogal*. www.federalmogal.com. Nov 2010

5. Haycock, R.F., *Automotive Lubricants Reference Book*. 2 nd ed. 2004: SAE International.

6. Horler, G. *Market Forecast: Automotive Digital Wireless Telemetry*. http://www.frost.com. Dec 2007

7. Chapman, S.J., *Electric Machinery Fundamentals*. 4th ed. 2005: McGraw-Hill.

8. Floyd, T.L., *Electronics Fundamentals, Circuits, Devices, and Applications*. 6th ed. 2004: Pearson, Prentice-Hall.

9. *How to Specify a Slip Ring*. http://www.moog.com/products/slip-rings/how-to-specify-a-slip-ring/. Oct 2007

10. Torregrosa, A., P. Olemeda and B Degraeuwe, *A concise wall temperature model for DI Diesel engines.* Journal of Applied Thermal Engineering, 2006. **26**(11 - 12): p. 1320 - 1327.

11. Mohammadia, A., M. Yaghoubi, and M. Rashidia, *Analysis of local convective heat transfer in a spark ignition engine*. International Communications in Heat and Mass Transfer, 2008. **35**(2): p. 215 - 224.

12. Esfahanian, V., A. Javaheria, and M. Ghaffarpour, *Thermal analysis of an SI engine piston using different combustion boundary condition treatments* Applied Thermal Engineering, 2006. **26**(2-3): p. 277 - 287.

13. Chatzakis, M., *Piston Instrumentation For Temperature Telemetry In Internal Combustion Engines, School of Engineering, Design and Technology*, 2007, University of Bradford.

14. Vignesh, C., C Jebaraj and S Manivasagam, *Prediction of Heat Flow and Temperature for Pistons With Improved Cooling Methods*, in *ASME Internal Combustion Engine Division Fall Technical Conference*. 2005: Canada. p. pp. 497-503.

15. Karamangil, M.I., O. Kaynakli, and A. Surmen, *Parametric investigation of cylinder and jacket side convective heat transfer coefficients of gasoline engines.* Energy Conversion and Management, 2006. **47**(6): p. 800-816.

16. *Racing Secrets*. www.racingsecrets.com. Nov 2010

17. *Piston surface plot of the temperature distribution.* http://www.comsol.com/showroom/gallery/205/. Dec 2010

18. Kajiwara, H. and Y Fujioka, *An analytical approach for prediction of piston temperature distribution in diesel engines,* JSAE Review, 2002. **23**(4): p. 429-434.

19. Yamada, Y., M Emi, H Ishii and Y Suzuki, *Heat loss to the combustion chamber wall with deposit in D.I. diesel engine: variation of instantaneous heat flux on piston surface with deposit,* JSAE Review, 2002. **23**(4): p. 415-421.

20. Takamatsu, H. and T. Kanazawa, *Piston temperature measurement method for high-speed gasoline engines.* JSAE, 1999. **20**(2): p. 259-261(3).

21. Burrahm, R.W., K Davis and W D Perry, *Development of a Piston Temperature telemetry System.* SAE International, 1992(920232).

22. Wiczynski, P.D. and R.G Varo, *New Piston Telemetry Applied to Spherical Joint Piston Development.* SAE International, 1996(900056).

23. Silva, F.S., *Fatigue on engine pistons – A compendium of case studies* Engineering Failure Analysis, 2006. **13**(3): p. 480-492.

24. Uchimi, T., K Taya and Y Hagihara, *Heat loss to combustion chamber wall in a D.I. diesel engine — First report: Tendency of heat loss to piston surface,* JSAE Review, 2000. **21**(1): p. 133-135.

25. Furuhama, S. and Y. Enomoto, *Piston temperature of Automobile Gasoline Engine in Driving on the Road.* JSME, 1973. **16**(99).

26. Wu, H. and C. Chiu, *A Study of temperature Distribution in a Diesel Piston – Comparison of Analytical and experimental Results.* SAE International, 1986(861278).

27. Barna, G.L., D.B. Brumm, and C.L. Anderson, *An Infrared Telemetry technique for making Piston Temperature measurements.* SAE International, 1991(910051).

28. Varo, R.G. and S.A. Archuleta, *Piston-mounted power generator, especially for telemetry systems* 1995, Cummins Engine Company, Inc. : United States.

29. Horler, G.D. and D.J. Picken, *A Digital Electronic Solution to Piston telemetry.* SAE International, 2000(2000-01-2032).

30. Horler, G.D., *Wireless remote control system for engine piston*. 2004, INSTR LTD, United States.

31. Kato, N. and M Moritsugu, *Piston temperature Measuring Technology Using Electromagnetic Induction.* SAE International, 2000. **16**: p. 325-330.

32. Suster, M., W.H. Ko, and D.J. Young, *An Optically Powered Wireless Telemetry Module for High-Temperature MEMS Sensing and Communication.* Journal of Microelectromechanical Systems, 2004. **13**(3): p. 536-541.

33. Lee, H.-W., C-H Oh, S K Kauh and K-P Ha, *Development of a multipiston temperature telemetry system using Bluetooth networks, IMechE 2006 Part D*. 2006: Professional Engineering Publishing.

34. Vandevoorde, G. and R. Puers, *Wireless energy transfer for stand-alone systems: a comparison between low and high power applicability.* Sensors and Actuators 2001. **A 92**: p. 305-311.

35. Wang, N., N. Zhang, and M. Wang, *Wireless sensors in agriculture and food industry—Recent development and future perspective.* Computers and Electronics in Agriculture 2006. **50**: p. 1–14.

36. *Telemetry*. http://en.wikipedia.org/wiki/Telemetry. Sep 2007

37. Puers, R., and M Catrysse, *A telemetry system for the detection of hip prosthesis loosening by vibration analysis.* Sensors and Actuators 2000. **85**: p. 42–47.

38. Van Ham, J. and R. Puers, *A power and data front-end IC for biomedical monitoring systems.* Sensors and Actuators 2008. **A 147** p. 641–648.

39. Catrysse, M., B. Hermans and R. Puers, *An inductive power system with integrated bi-directional data-transmission.* Sensors and Actuators 2004. **A 115**: p. 221–229.

40. Chi, B., J Yao, S Han and X Xie, *Low power high data rate wireless endoscopy transceiver*. Microelectronics Journal 2007. **38**: p. 1070–1081.

41. Lenaerts, B. and R. Puers, *An inductive power link for a wireless endoscope.* Biosensors and Bioelectronics 2007. **22**: p. 1390–1395.

42. Lenaerts, B. and R. Puers, *Inductive powering of a freely moving system.* Sensors and Actuators 2005. **A 123–124** p. 522–530.

43. Coosemans, J., B. Hermans, and R. Puers, *Integrating wireless ECG monitoring in textiles.* Sensors and Actuators 2006. **A 130–131**: p. 48–53.

44. Lichtenbelt, W.D.V.M. and H A M Daanen, *Evaluation of wireless determination of skin temperature using iButtons.* Physiology & Behavior 2006. **88**: p. 489–497.

45. Milenković, A., C. Otto and E. Jovanov, *Wireless sensor networks for personal health monitoring: Issues and an implementation.* Computer Communications, 2006. **29**(13 - 14): p. 2521-2533.

46. Shin, D.I., K H Shin and I K Kim, *Low-power hybrid wireless network for monitoring infant incubators.* Medical Engineering & Physics, 2005. **27**(8): p. 713-716.

47. Shin, D.I., S J Huh and T S Lee, *Web-based remote monitoring of infant incubators in the ICU.* International Journal of Medical Informatics 2003. **71**: p. 151—156.

48. Neihart, N.M. and R.R. Harrison, *Micropower Circuits for Bidirectional Wireless Telemetry in Neural Recording Applications.* IEEE Transactions On Biomedical Engineering, 2005. **52**(11).

49. Serra, P.A., G Rocchitta, G Bazzu and A Manca, *Design and construction of a low-cost single supply embedded telemetry system for amperometric biosensor.* Sensors and Actuators, 2007. **B**(122): p. 118-126.

50. Rocchitta, G., R Migheli and S Dedola, *Development of a distributed, fully automated, bidirectional telemetry system for amperometric microsensor and biosensor applications.* Sensors and Actuators 2007. **B 126**: p. 700–709.

51. Chen, Y., H-C Chiu, M-D Tsai and H Chang, *Development of a personal digital assistant-based wireless application in clinical practice.* Computer Methods And Programs In Biomedicine 2007. **85**: p. 181–184.

52. Kagohashi, M., T Nakazato and K Yoshimi, *Wireless voltammetry recording in unanesthetised behaving rats.* Neuroscience Research 2008. **60**: p. 120–127.

53. Crowley, K., J Frisby and S Murphy, *Web-based real-time temperature monitoring of shellfish catches using a wireless sensor network.* Sensors and Actuators 2005. **A 122**: p. 222–230.

54. Lapray, D., J Bergeler and E Dupont, *A novel miniature telemetric system for recording EEG activity in freely moving rats.* Journal of Neuroscience Methods 2008. **168**: p. 119–126.

55. Ativanichayaphong, T., *A combined wireless neural stimulating and recording system for study of pain processing.* Journal of Neuroscience Methods 2008(170): p. 25–34.

56. Valdastri, P., S Rossi and A Menciassi, *An implantable ZigBee ready telemetric platform for in vivo monitoring of physiological parameters.* Sensors and Actuators A: Physical, 2008. **142**(1): p. 369-378.

57. Yea, X., P Wang, J Liua and S Zhang, *A portable telemetry system for brain stimulation and neuronal activity recording in freely behaving small animals.* Journal of Neuroscience Methods 2008. **174**: p. 186–193.

58. Chestek, C.A. and P Samsukha, *Microcontroller-Based Wireless Recording Unit for Neurodynamic Studies in Saltwater.* IEEE Sensors Journal, 2006. **6**(5): p. 1105-1114.

59. Chien, C.N. and F.-S. Jaw, *Miniature telemetry system for the recording of action and field potentials.* Journal of Neuroscience Methods, 2005. **147**: p. 68–73.

60. Harpster, T., B. Stark, and K. Najafi, *A passive wireless integrated humidity sensor.* Sensors and actuators 2002. **A 95**: p. 100-107.

61. Atta, R.M.H., *Multi-layer double coil micro-fabricated transformer.* Sensors and Actuators 2004. **A 112**: p. 61–65.

62. Wise, K.D., *Integrated sensors, MEMS, and microsystems: Reflections on a fantastic voyage.* Sensors and Actuators 2007. **A 136**: p. 39–50.

63. Holladay, J. and E O Jones, *Microfuel processor for use in a miniature power supply.* Journal of Power Sources, 2002. **108**: p. 21–27.

64. Peirs, J., D. Reynaerts, and F. Verplaetsen, *A microturbine for electric power generation.* Sensors and Actuators 2004(A 113): p. 86–93.

65. Harb, J .N., R M LaFollette, and R H Selfridge, *Microbatteries for self-sustained hybrid micropwer supplies.* Journal of Power Sources 2002(104): p. 46-52.

66. Yamazaki, Y., *Application of MEMS technology to micro fuel cells.* Electromechanical Actuators 2004. **50**: p. 663–666.

67. Kuehne, I., D Marinkovic, and G Eckstein, *A new approach for MEMS power generation based on a piezoelectric diaphragm.* Sensors and Actuators A: Physical, 2008. **142**(1): p. 292-297.

68. Raisigel, H., O. Cugat, and J. Delamare, *Permanent magnet planar micro-generators.* Sensors and Actuators A: Physical, 2006. **130-131**: p. 438–444.

69. Kim, S., et al., *Low frequency properties of micro power generator using a gold electroplated coil and magnet.* Current Applied Physics 2008. **8**: p. 138-141.

70. Lee, K., J Yi, and B Kim, *Micro-energy storage system using permanent magnet and high-temperature superconductor.* Sensors and Actuators A, 2008. **143**: p. 106-112.

71. Cavagnino, A., M Lazzari, and F Profumo, *A Comparison Between the Axial Flux and the Radial Flux Structures for PM Synchronous Motors.* IEEE Transactions On Industry Applications, 2002. **38**(6): p. 1517 - 1524.

72. Javadi, S. and M. Mirsalim, *A Coreless Axial-Flux Permanent-Magnet Generator for Automotive Applications.* IEEE Transactions On Magnetics, 2008. **44**(12): p. 4591 - 4598.

73. Fei, W. and P.C.K. Luk, *Design and Performance Analysis of a High-Speed Air-Cored Axial-Flux Permanent-Magnet Generator with Circular Magnets and Coils*, *IEEE International Electric Machines and Drives Conference*. 2009: IEEE.

74. Moury, S. and M.T. Iqbal. *A Permanent Magnet Generator with PCB Stator for Low Speed Marine Current Applications*. in *1st International Conference on the Developments, Renewable Energy Technology* 2009.

75. Bumby, J.R. and R. Martin. *Axial-flux permanent-magnet air-cored generator for small-scale wind turbines*, *IEE Proceedings Electric Power Applications*. 2005.

76. Javadi, S. and M. Mirsalim, *Design and Analysis of 42-V Coreless Axial-Flux Permanent-Magnet Generators for Automotive Applications.* IEEE Transactions On Magnetics, 2010. **46**(4): p. 1015 - 1023.

77. Ferreira, A.P., A.M. Silva, and A.F. Costa, *Prototype of an axial flux permanent magnet generator for wind energy systems applications, European Conference on Power Electronics and Applications*. 2007. p. 1 - 9.

78. Hosseini, S.M., M. Agha-Mirsalim, and M. Mirzaei, *Design, Prototyping, and Analysis of a Low Cost Axial-Flux Coreless Permanent-Magnet Generator.* IEEE Transactions On Magnetics, 2008. **44**(1): p. 75 - 80.

79. Profumo, F., A Tenconi and M Cerchio, *Axial Flux Plastic Multi-Disc Brushless PM Motors: Performance Assessment, Nineteenth Annual IEEE Applied Power Electronics Conference and Exposition*. 2004: IEEE.

80. Luand, L. and C. J.C., *Reduced size microstrip patch antenna for Bluetooth applications*, in *Electronics Letters*. 2005.

81. Vermeeren, G., H Rogier and D De Zutter, *Simple low-cost planar antenna for indoor communication under the Bluetooth protocol*, in *Electronics Letters*. 2001. p. 1153-1154.

82. Dou, W. and M.Y.W. Chia. *Single-layer miniature broadband microstrip antenna using wire bonding technique*. in *IEE Proceedings Microwave Antennas Propagation*. 2001.

83. Jan, J.Y. and T.-M. Kuo, *CPW-fed wide band planar monopole antenna for operations in DCS, PCS, 3G, and Bluetooth bands*, in *Electronics Letters*. 2005.

84. Tibenderana and Weiss, *Efficient and Robust Detection of GFSK Signals under Dispersive Channel, Modulation Index, and Carrier Frequency Offset Conditions.* EURASIP Journal on Applied Signal Processing, 2005. **16**: p. 2719–2729.

85. Seshadri, R.I. and V. M.C. *A Capacity-Based Approach for Designing Bit-Interleaved Coded GFSK with Non coherent Detection*. in *Proceedings International Symposium Information Theory* 2006. Seattle.

86. Feng, W., A. Nallanathan, and H.K. Garg, *Impact of interference on performance of Bluetooth Piconet in 2.4GHz ISM band*, in *Electronics Letters*. 2002. p. 1725.

87. Lindholm, T., *Setting up a Bluetooth Packet Transport Link*. 2000: Department of Computer Science, Helsinki University of Technology.

88. Golmie, N., N. Chevrollier, and E. Bakkouri, *Interference Aware Bluetooth Packet Scheduling*, in *Global Telecommunications Conference*. 2001, IEEE: San Antonio, TX , USA. p. 2857-2863.

89. Shih, C.H., K. Wang, and H.-C. Shih, *An adaptive Bluetooth packet selection and scheduling scheme in interference environments.* Computer Communications, 2006. **29**: p. 2084–2095.

90. Nagl, L., et al. *Wearable Sensor System for Wireless State-of-Health Determination in Cattle*. in *Engineering in Medicine and Biology Society, 2003. Proceedings of the 25th Annual International Conference of the IEEE*. 2003.

91. Warren, S., et al. A Distributed Infrastructure for Veterinary Telemedicine. in *Medicine and Biology Society, proceedings of the 25th Annual International Conference of the IEEE* 2003.

92. *Bluetooth low energy technology*. http://www.bluetooth.com/English/Products/Pages/low_energy.aspx. Dec 2009

93. *ZigBee SoCs provide cost-effective solutions IEEE 802.15.4 and ZigBee basics*. http://www.zigbee.org/LearnMore/WhitePapers.aspx. Aug 2009

94. Alves, M. and E. Tovar, *Real-time communications over wired/wireless PROFIBUS networks supporting inter-cell mobility* Computer Networks, 2007. **51**(11): p. 2994-3012.

95. Golmie, N. and I. Matta, *Applications and services in wireless networks.* Computer Communications, 2005. **28**(14): p. 1603-1604.

96. Hsu, C., W-Y Liao, C-H Luo, and T-C Chou, *The 2.4 GHz biotelemetry chip for healthcare monitoring system.* Sensors and Actuators A: Physical, 2007. **139**(1 - 2): p. 245-251

97. Helleputte, N.V., J.M. Tomasik and W Galjan, *A flexible system-on-chip (SoC) for biomedical signal acquisition and processing.* Sensors and Actuators A: Physical, 2008. **142**(10): p. 361-368.

98. Susilo, E., P Valdastri, A Menciassi and P Dario, *A miniaturized wireless control platform for robotic capsular endoscopy using advanced pseudokernel approach.* Sensors and Actuators A: Physical 2009. **156**(1): p. 49-58.

99. Bellis, S.J., K Delaney and B O'Flynn, *Development of field programmable modular wireless sensor network nodes for ambient systems.* Computer Communications, 2005. **28**(13): p. 1531-1544.

100. Akyildiz, I., T. Melodia, and K.R. Chowdhury, *A survey on wireless multimedia sensor networks.* Computer Networks, 2007. **51**(4): p. 921-960.

101. *M2M White paper*. 2005. www.metrilog.at. Aug 2010

102. *Toothpick 2.1 datasheet*. www.flexipanel.com/WirelessFirmware.htm. May 2007

103. *16 Channel Spot Telemetry System Instruction Manual,* www.sensortelemetrie.de. Jun 2006

104. *Motormesstechnik_en.pdf*. www.sensortelemetrie.de. July 2007

105. Hopkins, B. and R. Antony, *Bluetooth for Java*. 2003: Apress.

106. Bray, J. and C.F. Sturman, *Bluetooth Connect Without Cables*. 2nd ed. 2002: Prentice Hall.

107. Kumar, C.B., P.J. Kline, and T.J. Thompson, *Bluetooth Application Programming with the Java APIs*. 2004: Morgan Kaufmann.

108. *Bluetooth Special Interest Group*. www.bluetooth.com. Aug 2005

109. *Wireless Antenna Products - Overview*. http://www.lairdtech.com/pages/products/Wireless-Antennas-Overview.asp. Feb 2007

110. Dixon, R.C., *Spread Spectrum Systems with Commercial Applications*. 3rd ed. 1994: Wiley.

111. *Bluetooth Enhanced Data Rate (EDR): The Wireless Evolution*. 2006, Agilent Technologies.

112. Jain, R. *Wireless Personal Area Networks (WPANs) Presentation*. http://www.cs.wustl.edu/~jain/cse574-06/ftp/j_4pan/sld010.htm. Dec 2006

113. Kammer, D., G. McNutt, B. Senese and J. Bray, *Bluetooth Application Developers Guide: The Short Range Interconnect Solution*. 2002: Syngress Publishing Inc.

114. *Digital Modulation 2*. http://www.usna.edu/Users/ee/kintzley/ee303sp09/lectures/EE303Sp09_L20_Digital%20Modulation2.pdf. Jan 2007

115. Anderson, R. and T. Kugelstadt. *Thermocouple Measurements with ΔΣ ADCs* Application Report SBAA134–June 2005, 2005, http://focus.ti.com/lit/an/sbaa134/sbaa134.pdf. Jun 2008

116. *NIST ITS-90 Thermocouple Database*. http://srdata.nist.gov/its90/main/. June 2007

117. *Automatic Temperature Control*. http://atmel.com/dyn/resources/prod_documents/controller_3_04.pdf. Jun 2008

118. *Signal Conditioning Fundamentals for PC-Based Data Acquisition Systems*. http://physweb.bgu.ac.il/COURSES/SignalNoise/signal_conditioning.pdf. Aug 2008

119. *National Institution of Standards and Technology (NIST)*. http://www.nist.gov. Jun 2007

120. *NIST type k thermocouple polynomial coefficients*. http://srdata.nist.gov/its90/type_k/kcoefficients.html. June 2007

121. *NIST type k thermocouple temperature range*. http://srdata.nist.gov/its90/type_k/0to300.html. June 2007

122. *The Thermocouple*. http://www.omega.com/temperature/Z/pdf/z021-032.pdf. Jan 2007

123. Lockhart, R.W. *Getting Started In PC-Based Data Acquisition*. http://www.dataq.com/applicat/articles/sensors.htm. Mar 2008

124. *Direction of Flux*. http://micro.magnet.fsu.edu/electromag/museum/index.html. Feb 2010

125. Scadden, B., *Electrical Installation Work*. 4th ed. 2002: Newnes.

126. *Magnetism*. http://www.electronics-tutorials.ws/electromagnetism/magnetism.html. May 2008

127. *Permanent Magnet Design Guide*. http://www.magnetsales.com/Design/DesignG.htm. May 2008

128. *BH curve image*. http://www.ndt-ed.org/EducationResources/CommunityCollege/MagParticle/Physics/HysteresisLoop.htm. Jan 2010

129. *SUPER NEODYMIUM MAGNETS*. http://www.magnetsource.com/Solutions_Pages/NEOMAIN.html. May 2008

130. Gieras, J.F. and M. Wing, *Permanent Magnet Motor Technology Design and Applications*. 2nd ed. 2002: Marcel Dekker Inc.

131. *DB101G bridge rectifier datasheet*. http://uk.farnell.com/db101g. Oct 2007

132. *MAX756 step-up converter datasheet*. www.maxim-ic.com. Aug 2008

133. *AD595 thermocouple amplifier datasheet, Rev C*. www.analog.com. Oct 2007

134. *MAX6675 thermocouple amplifier datasheet*. www.maxim-ic.com. Oct 2007

135. *Microchip PIC18LF6722 microcontroller datasheet*. www.microchip.com. 2005

136. *LinkMatik 2.0 datasheet*. www.flexipanel.com/WirelessFirmware.htm. May 2007

137. *Ezurio Bluetooth Adapter*. http://www.tdksys.com/products/highspeedusbadaptor/. Jun 2006

138. *TEAclipper/PIC datasheet*. www.flexipanel.com/TEAclipper.htm. Mar 2008

139. *MPLAB IDE user guide*. www.microchip.com. Jul 2007

140. *MPLAB C18 Compiler user guide*. www.microchip.com. Jul 2007

141. *Flexipanel Designer 1.0*. www.flexipanel.com. May 2007

142. *DARC-II datasheet*. www.flexipanel.com/WirelessFirmware.htm. Dec 2007

143. *HexWax Explorer*. www.hexwax.com/HWexplorer.aspx. Mar 2008

144. *Proteus 7.2*. http://www.labcenter.co.uk. May 2008

145. Wildi, T., *Fundamentals of Electricity, Magnetism, and Circuits*. 4th ed. 2000: Prentice Hall.

Appendix

```
#include "Toothpick.h"
#include <p18f6722.h>
#include "telemetryUI.h"              // flexipanel designer generated .h file

void main( void )
{
        unsigned long ADResult1 = 0;
        unsigned long ADResult2 = 0;
        unsigned long ADResult3 = 0;
        unsigned long ADResult4 = 0;
        unsigned char Channel = 0;
        VRefNegIsVss;                 // set power supply voltage pins
        VRefPosIsVdd;
        SetAnalogAD0toAD3;            // set analogue input channels
        ADConverterOn10bit;           // set to 10 bit ADC

        FxPCommand( FxPC_Start, 0, 0 );          // Start FlexiPanel service
        AwaitLMTComplete();                      // Service operating, no client

        // if no BlueMatik, flash red led rapidly
        while ((ToothpickSemaphores&TPSF_LMTEXISTS)==0)
        {
                LedRed = ~LedRed;
                msDelay(50);
}

// main loop
        while ( 1 )
        {
                Channel = 0;
                SetADChan( Channel );                    // select analogue channel
                CyclesDelay3p2plus3p2times( 4 );         // set acquisition delay
                StartAtoD;                               // start conversion
                AwaitAtoDComplete;                       // wait until conversion completes
                GetADResult10bit( ADResult1 );           // store conversion result in variable
                // AD595 is 10mv output per degree C
                // AD595 temerature range is 0 - 300 deg C
                // therefore, voltage range is 10mV - 3V
                ADResult1 = ADResult1 / 0.01;            // convert voltage to temperature
                SetUp_NumberT1_25( 0, &ADResult1 );      // update control value and update client control

                Channel = 1;
                SetADChan( Channel );
                CyclesDelay3p2plus3p2times( 4 );
                StartAtoD;
                AwaitAtoDComplete;
                GetADResult10bit( ADResult2 );
                ADResult2 = ADResult2 / 0.01;            // convert voltage to temperature
```

```
                SetUp_NumberT2_26( 0, &ADResult2 );

                Channel = 2;
                SetADChan( Channel );
                CyclesDelay3p2plus3p2times( 4 );
                StartAtoD;
                AwaitAtoDComplete;
                GetADResult10bit( ADResult3 );
                ADResult3 = ADResult3 / 0.01;                   // convert voltage to temperature
                SetUp_NumberT3_27( 0, &ADResult3 );

                Channel = 3;
                SetADChan( Channel );
                CyclesDelay3p2plus3p2times( 4 );
                StartAtoD;
                AwaitAtoDComplete;
                GetADResult10bit( ADResult4 );
                ADResult4 = ADResult4 / 0.01;                   // convert voltage to temperature
                SetUp_NumberT4_28( 0, &ADResult4 );
        }  // end while
} // end Main
```

Figure A1 Analogue Firmware Main Code

```
#include "Toothpick.h"
#include <p18cxxx.h>
#include "TUI_SPI.h"
#include "spi.h"

        unsigned char read_spi[2];
        unsigned char spi_H = 0;
        unsigned char spi_L = 0;
        unsigned char spi_Lval = 0;
        unsigned int spi_Hval = 0;
        unsigned char spi_H3bits = 0;
        unsigned int max6675_temp = 0;
        unsigned int TC_temp = 0;
        unsigned int ndx = 100;

        void get_spi_val();
        void get_temperature_data();
        void update_control();

        void get_spi_val() {
                while(!DataRdySPI());
                getsSPI(read_spi, 2);
        }

        void get_temperature_data() {
                spi_L = read_spi[0];
                spi_H = read_spi[1];
                spi_H3bits = (spi_H & 0x07) << 5;           // mask lower 3 bits of spi_H then shift to upper 3 bits
                spi_Lval = (spi_L >> 3) | spi_H3bits;       // shift spi_L 3 places to right then OR with spi_Hval
                spi_Hval = (spi_H >> 3) & 0x0F;             // shift spi_H 3 places to right then mask lower 4 bits
                max6675_temp = (spi_Hval << 8) | spi_Lval; // put spi_Hval in lower byte then shift to upper byte
```

```
                                                    // then OR with spi_Lval (puts spi_Lval in lower byte)
                TC_temp = max6675_temp / 4;
                ndx++;
        }


        void update_control() {
                SetUp_NumberT1_25( 0, &read_spi );
        }

void main( void )
{       //      if no BlueMatik, flash red led rapidly
        while ((ToothpickSemaphores&TPSF_LMTEXISTS)==0)
        {
                LedRed = LedRedOn;
                msDelay(50);
                LedRed = LedRedOff;
        }

        VRefNegIsVss;                           // set power supply voltage pins
        VRefPosIsVdd;
        FxPCommand( FxPC_Start, 0, 0 );         // Start FlexiPanel service
        AwaitLMTComplete();                     // Service operating, no client

// main loop
        // open SPI bus
        OpenSPI(SPI_FOSC_16, MODE_00, SMPEND);      // SPI_FOSC_64: max6675 spi timing limit of 4,3MHz
        // Enable chip select on AN11 pin
        DirAN11 = DirOutput;                        // set pin AN11 to digital output

        while(1) {
                LedRed = LedRedOn;
                AN11Pin = 0;                        // chip select signal (CS bar)
                get_spi_val();                      // read SPI bus
                AN11Pin = 1;                        // chip deselect
                LedRed = LedRedOff;
                get_temperature_data();             // convert to temperature reading
                update_control();                   // display temperature value
                msDelay(250);                       // delay 250 ms, MAX6675 220 ms update time
        } // end while

        CloseSPI();                                 // close SPI bus

} // end Main
```

Figure A2 Digital Firmware Main Code

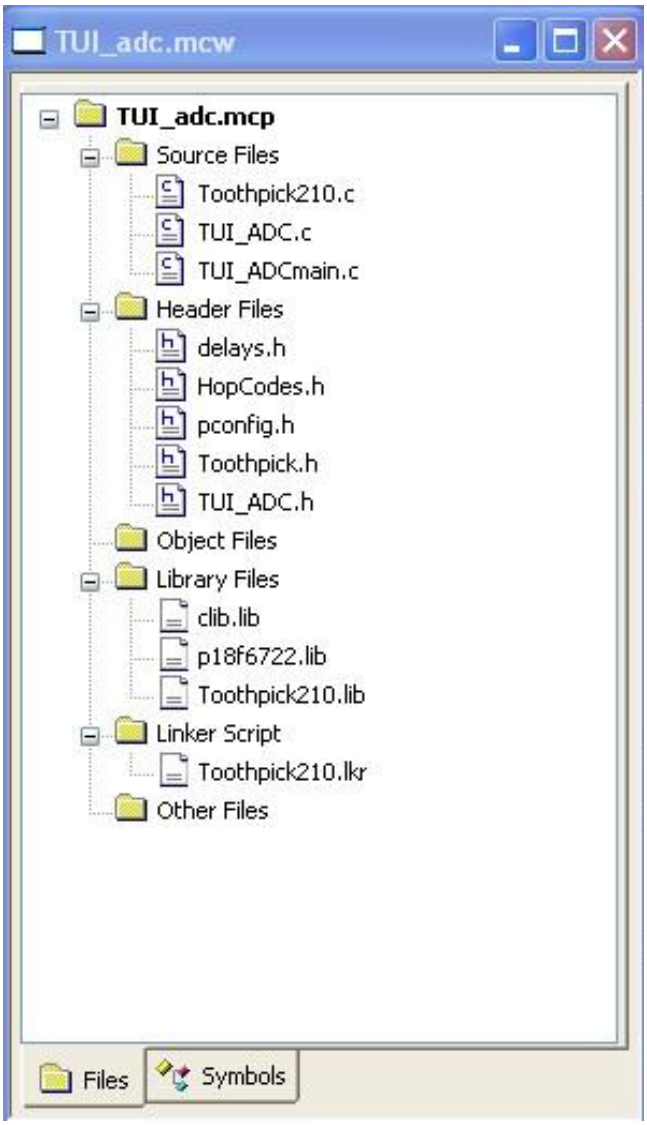

Figure A3 List of Files Included in MPLAB Project

Figure A3 shows an image of files required to be included in the firmware development project when using the Microchip IDE. Except for the renamed ‘main’ file, these project files describe the configurations for the microprocessor and the hex data file that defines the microprocessor as a DAQ device. The renamed ‘main’ file contains the user developed C code to use the microprocessor and user interface as a DAQ device.

List of Publications